

Electronic Thesis and Dissertation Repository

7-27-2017 12:00 AM

Morphodynamic Response of Spencer Creek to Large Precipitation Events and Channel Modifications: A Case Study

Emily Mae Martin, *The University of Western Ontario*

Supervisor: Dr. Andrew Binns, *The University of Western Ontario*

Joint Supervisor: Dr. Timothy Newson, *The University of Western Ontario*

A thesis submitted in partial fulfillment of the requirements for the Master of Engineering
Science degree in Civil and Environmental Engineering

© Emily Mae Martin 2017

Follow this and additional works at: <https://ir.lib.uwo.ca/etd>



Part of the [Environmental Engineering Commons](#)

Recommended Citation

Martin, Emily Mae, "Morphodynamic Response of Spencer Creek to Large Precipitation Events and Channel Modifications: A Case Study" (2017). *Electronic Thesis and Dissertation Repository*. 4870.
<https://ir.lib.uwo.ca/etd/4870>

This Dissertation/Thesis is brought to you for free and open access by Scholarship@Western. It has been accepted for inclusion in Electronic Thesis and Dissertation Repository by an authorized administrator of Scholarship@Western. For more information, please contact wlsadmin@uwo.ca.

Abstract

Severe weather events are occurring more frequently with extreme repercussions as our climate changes. Rainfall events of large magnitudes can lead to instability of river banks, riverbed erosion, and alterations in stream planform alignment. It is important to understand the hydraulic and geomorphic response of rivers and streams to storm events to predict long term morphological change, protect hydraulic structures, and manage aquatic ecosystems. The goal of this thesis is to examine the influence of precipitation events of varying magnitude on the morphodynamic processes of an urban creek. Four events are simulated: a constant averaged flow of $1.249 \text{ m}^3/\text{s}$ representative of the average flow in the creek over a 5-year period, a 5-year return period event, a 10-year return period event, and a 100-year return period event. Channel modifications are made to four cross sections at the downstream end of Spencer Creek in order to investigate the effect of planform alignment and geometry on increased flood resiliency and channel stability. The first modification widened the channel at these sections, while the second modification lengthened the channel at these sections to be representative of increased meandering (and corresponding decrease in stream bed slope) of the creek. In general, the sediment concentration changed with each event, with the largest sediment concentration in the channel occurring for the 100-year return period event. The first modification to the channel demonstrated the largest reduction in velocity, sediment concentration, and shear stress at all cross sections for all events. The second modification demonstrated little to no change in velocity and shear stress for all events. The results from this thesis provide a framework for analyzing the morphodynamic response of urban streams to storm events of varying return periods and durations and will assist river engineers and hydrologists in managing and restoring urban creeks to mitigate flooding while balancing erosion and ecological processes.

Keywords

Mathematical modeling, sediment transport, channel modification, rivers and streams, hydraulic modeling

Acknowledgments

I would like to express my extreme gratitude towards my supervisors Dr. Andrew D. Binns and Dr. Tim Newson for providing me with this opportunity. Thank you for your guidance, support, encouragement, advice, and financial support throughout my degree.

Thank you to my research group, the Binns Group, for their support and assistance throughout my degree. I would like specifically to thank Etta Gunsolus for motivating and inspiring me when times were tough. Her ability to find the silver lining in any situation helped me when life didn't go as planned.

This thesis would not have been possible without the love and support of my family and friends. Thank you to my parents, Lori and Terry, for always pushing me to do my best and for helping me look on the bright side of every situation. Thank you to my future mother- and father-in-law, Becky and Baba, for their support and care packages. I would also like to thank my girlfriends: Robyn, Julia, Amy, Michelle, and Katie for inspiring me every day.

I would especially like to thank my partner, Sam, for standing by me throughout my academic studies. His encouragement to apply to the program, his constant love and support throughout my degree, and his strong work ethic pushed me to complete this thesis. I am excited to see what the future holds for us.

Finally, a special thank you to my late grandmother, Phyllis Chapman, for her support and her contagious positivity throughout my academic studies until her final days. She was my biggest cheerleader, and I would not have reached this point without her.

Table of Contents

Abstract.....	i
Acknowledgments.....	ii
Table of Contents.....	iii
List of Tables.....	vi
List of Figures.....	viii
List of Appendices.....	xiii
List of Symbols.....	xiv
Chapter 1.....	1
1 Introduction.....	1
1.1 General.....	1
1.2 Goal and Objectives.....	3
1.3 Structure of Thesis.....	4
Chapter 2.....	6
2 Fundamentals of the Present Work.....	6
2.1 Fundamental Equations.....	6
2.1.1 Fundamental Equations of Flow.....	7
2.1.2 Fundamental Equations of Sediment Motion.....	9
2.1.3 Fundamental Equations of Shear Stress.....	12
2.1.4 Fundamental Equations of Bank Erosion.....	13
2.2 Mathematical Modeling.....	17
2.2.1 HEC-RAS.....	17
Chapter 3.....	20
3 Literature Review.....	20
3.1 Stream Restoration and Channel Design.....	20

3.2 Mathematical Modeling	23
3.3 Summary	26
Chapter 4	28
4 Study Area and Methodology	28
4.1 Flooding in Southwestern Ontario	28
4.2 Study Area	30
4.2.1 Previous Alterations to Spencer Creek	34
4.3 Methodology	36
4.3.1 Hydrographs	37
4.3.2 Channel Modifications	39
4.3.3 Simulations	40
4.3.4 Model Set-up	42
Chapter 5	44
5 Results	44
5.1 General	44
5.2 Existing Channel	45
5.3 Modification 1	49
5.4 Modification 2	52
Chapter 6	57
6 Analysis and Discussion	57
6.1 Velocity Modeling Results	57
6.2 Sediment Concentration Modeling Results	60
6.3 Hysteresis of Sediment Transport Rates	63
6.4 Aggradation and Degradation Trends	66
6.5 Shear Stress Modeling Results	68
6.6 Bank Erosion	71

6.7 Effects of Sediment Concentration on Channel Ecology	74
Chapter 7	77
7 Conclusions and Recommendations	77
7.1 Conclusions.....	77
7.1.1 Existing Channel.....	78
7.1.2 Channel Modifications.....	79
7.2 Recommendations.....	80
8 References	82
Appendix A: Event Hydrographs.....	94
Appendix B: Sediment Distribution.....	96
Appendix C: Pictures of Spencer Creek	105
Appendix D: Lag Time Showing Hysteresis Conditions.....	109
Appendix E: Cross Sectional Profiles of Spencer Creek	112
Appendix F: Simulation Summary Tables.....	121
Appendix G: Event 2 and 3 Comparison Graphs.....	136
Appendix H: HEC-RAS Equations.....	140
Meyer-Peter and Müller (1948)	140
Engelund-Hansen (1972)	141
Yang (1979)	142
Wilcock-Crowe (2003).....	143
Appendix I: Maps	145
Curriculum Vitae	149

List of Tables

Table 1: Lower Spencer Creek Watershed Land Use (Grillakis et al., 2011)	31
Table 2: Storm Events.....	40
Table 3: Summary of Simulations	44
Table 4: Aggradation and Degradation Trends in Spencer Creek (Existing Channel).....	67
Table 5: Aggradation and Degradation Trends in Spencer Creek (Modification 1).....	67
Table 6: Aggradation and Degradation Trends in Spencer Creek (Modification 2).....	68
Table 7: Increase in Sediment Load (mg/L)	76
Table 8: Complete Time to Peak and Lag Time Showing Hysteresis Conditions for the Existing Channel.....	109
Table 9: Complete Time to Peak and Lag Time Showing Hysteresis Conditions for Modification 1.....	110
Table 10: Complete Time to Peak and Lag Time Showing Hysteresis Conditions for Modification 2.....	111
Table 11: Width and Length at Each Cross Section	120
Table 12: Summary of Results for Simulation 1 (Existing Channel; Event 1).....	121
Table 13: Summary of Results for Simulation 2 (Existing Channel; Event 2).....	122
Table 14: Summary of Results for Simulation 3 (Existing Channel; Event 3).....	123
Table 15: Summary of Results for Simulation 4 (Existing Channel; Event 4).....	124
Table 16: Summary of Results for Simulation 5 (Modification 1; Event 1)	125
Table 17: Summary of Results for Simulation 6 (Modification 1; Event 2)	126

Table 18: Summary of Results for Simulation 7 (Modification 1; Event 3)	127
Table 19: Summary of Results for Simulation 8 (Modification 1; Event 4)	128
Table 20: Summary of Results for Simulation 8 (Modification 2; Event 1)	129
Table 21: Summary of Results for Simulation 10 (Modification 2; Event 2)	130
Table 22: Summary of Results for Simulation 11 (Modification 2; Event 3)	131
Table 23: Summary of Results for Simulation 12 (Modification 2; Event 4)	132
Table 24: % Difference Between Velocity and Sediment Concentration for Each Event (Existing Channel)	133
Table 25: % Difference Between Velocity and Sediment Concentration for Each Event (Modification 1)	134
Table 26: % Difference Between Velocity and Sediment Concentrations for Each Event (Modification 2)	135

List of Figures

Figure 1: Failure Circles: (a) toe circle; (b) slope circle; (c) midpoint (base) circle (Steward et al., 2010)	14
Figure 2: Bank Stability Analysis (Darby and Thorne, 1996a)	16
Figure 3: Spencer Creek in Hamilton, Ontario	31
Figure 4: Map of Spencer Creek	33
Figure 5: Bank Stabilizing Structures in Spencer Creek	35
Figure 6: Hydrographs created for simulations	42
Figure 7: Comparison of Maximum Sediment Concentrations for all Simulations in the Existing Channel	47
Figure 8: Comparison of Maximum Velocities for all Simulations in the Existing Channel.	48
Figure 9: Comparison of Maximum Shear Stresses for all Simulations in the Existing Channel	48
Figure 10: Comparison of Maximum Sediment Concentrations for all Simulations in Modification 1	51
Figure 11: Comparison of Maximum Velocities for all Simulations in Modification 1	52
Figure 12: Comparison of Maximum Shear Stresses for all Simulations in Modification 1..	52
Figure 13: Comparison of Maximum Sediment Concentrations for all Simulations in Modification 2	55
Figure 14: Comparison of Maximum Velocities for all Simulations in Modification 2	55
Figure 15: Comparison of Maximum Shear Stresses for all Simulations in Modification 2..	56

Figure 16: Comparison of Maximum Velocity at XS 15-18 for All Channel Configurations for Event 1.....	58
Figure 17: Comparison of Maximum Velocity at XS 15-18 for All Channel Configurations for Event 4.....	59
Figure 18: Comparison of Peak Sediment Concentration at XS 15-18 for all Channel Configurations for Event 1.....	61
Figure 19: Comparison of Peak Sediment Concentration at XS 15-18 for all Channel Configurations for Event 4.....	62
Figure 20: Comparison of Maximum Shear Stress at XS 15-18 for Event 1	69
Figure 21: Comparison of Maximum Shear Stress at XS 15-18 for Event 4	69
Figure 22: Spencer Creek Exposed Banks.....	72
Figure 23: Erosion Rates for Event 1	73
Figure 24: Erosion Rates for Event 4.....	73
Figure 25: Event 1 Hydrograph	94
Figure 26: Event 2 Hydrograph	94
Figure 27: Event 3 Hydrograph	95
Figure 28: Event 4 Hydrograph	95
Figure 29: Cross Section 2 Sediment % Finer	96
Figure 30: Cross Section 3 Sediment % Finer	96
Figure 31: Cross Section 4 Sediment % Finer	97
Figure 32: Cross Section 5 Sediment % Finer	97
Figure 33: Cross Section 6 Sediment % Finer	98

Figure 34: Cross Section 7 Sediment % Finer	98
Figure 35: Cross Section 8 Sediment % Finer	99
Figure 36: Cross Section 9 Sediment % Finer	99
Figure 37: Cross Section 10 Sediment % Finer	100
Figure 38: Cross Section 11 Sediment % Finer	100
Figure 39: Cross Section 12 Sediment % Finer	101
Figure 40: Cross Section 13 Sediment % Finer	101
Figure 41: Cross Section 14 Sediment % Finer	102
Figure 42: Cross Section 15 Sediment % Finer	102
Figure 43: Cross Section 16 Sediment % Finer	103
Figure 44: Cross Section 17 Sediment % Finer	103
Figure 45: Cross Section 18 Sediment % Finer	104
Figure 46: Spencer Creek downstream showing bank erosion.....	105
Figure 47: Spencer Creek Cross Section 18	105
Figure 48: Spencer Creek showing dead ash trees and bank erosion downstream.....	106
Figure 49: Spencer Creek Cross Section 2	106
Figure 50: Spencer Creek Bank Stabilization Structure	107
Figure 51: Spencer Creek Exposed Tree Roots	107
Figure 52: Spencer Creek Exposed Banks.....	108
Figure 53: XS 2 Bed Profile.....	112

Figure 54: XS 3 Bed Profile.....	112
Figure 55: XS 4 Bed Profile.....	113
Figure 56: XS 5 Bed Profile.....	113
Figure 57: XS 6 Bed Profile.....	114
Figure 58: XS 7 Bed Profile.....	114
Figure 59: XS 8 Bed Profile.....	115
Figure 60: XS 9 Bed Profile.....	115
Figure 61: XS 10 Bed Profile.....	116
Figure 62: XS 11 Bed Profile.....	116
Figure 63: XS 12 Bed Profile.....	117
Figure 64: XS 13 Bed Profile.....	117
Figure 65: XS 14 Bed Profile.....	118
Figure 66: XS 15 Bed Profile.....	118
Figure 67: XS 16 Bed Profile.....	119
Figure 68: XS 17 Bed Profile.....	119
Figure 69: XS 18 Bed Profile.....	120
Figure 70: Maximum Velocity for All Channel Configurations for Event 2	136
Figure 71: Maximum Velocity for All Channel Configurations for Event 3	136
Figure 72: Peak Sediment Concentration for all Channel Configurations for Event 2	137
Figure 73: Peak Sediment Concentration for all Channel Configurations for Event 3	137

Figure 74: Maximum Shear Stress Comparison for Event 2	138
Figure 75: Maximum Shear Stress Comparison for Event 3	138
Figure 76: Erosion Rates for Event 2.....	139
Figure 77: Erosion Rates for Event 3.....	139
Figure 78: Ward 9 of Hamilton (City of Hamilton, 2015).....	145
Figure 79: Lower Spencer Subwatershed (HCA, 2010).....	146
Figure 80: Lower Spencer Subwatershed Land Use (HCA, 2010).....	147
Figure 81: Lower Spencer Subwatershed Soil Distribution (HCA, 2010)	148

List of Appendices

Appendix A: Event Hydrographs.....	94
Appendix B: Sediment Distribution.....	96
Appendix C: Pictures of Spencer Creek	105
Appendix D: Lag Time Showing Hysteresis Conditions.....	109
Appendix E: Cross Sectional Profiles of Spencer Creek	112
Appendix F: Simulation Summary Tables.....	121
Appendix G: Event 2 and 3 Comparison Graphs.....	136
Appendix H: HEC-RAS Equations.....	140
Appendix I: Maps	145

List of Symbols

A = area

b = mean flow width

C = undrained shear strength

CN = curve number

c_a = reference concentration

D = sediment diameter

D_{gr} = dimensionless grain diameter

D^* = particle parameter

E = lateral erosion rate

F = factor used in van Rijn equation

F_s = factor of safety

F_i = infiltration

F_{gr} = mobility function

G_{gr} = dimensionless sediment transport rate

g = acceleration due to gravity

H = height

I_a = initial abstraction

k = erodibility coefficient

l = length of flowpath

N = stability number

P = total storm rainfall

Q = discharge

Q_p = peak discharge

q_b = bedload transport

q_s = sediment load transport

S = storage volume

T = transport stage parameter

T_R = time to peak of the hydrograph

t_s = time to peak of sediment

t_p = lag time

ν = kinematic viscosity

u'_* = bed shear velocity

u'_{cr} = critical bed shear velocity

X = dimensionless factor of sediment transport

y = average watershed slope

Z = suspension parameter

α = constant value

β = failure plane angle

ρ = fluid density

τ = bed shear stress

τ_c = bed shear stress

v_0 = mean water velocity

v^* = shear velocity

ω = sediment stream velocity

γ = unit weight of the soil

Chapter 1

1 Introduction

1.1 General

Rivers and streams in urban environments are increasingly challenged to satisfy hydraulic, geomorphic, and ecological functions due to numerous natural and anthropogenic effects. Urbanization, land development, and river channel modification are three of the main causes of increased flood risk in urban areas (Kait et al., 2008; Khattak et al., 2016). The frequency of riverine flooding is changed when the floodplain is modified or when hydraulic systems are altered. This frequency is increasing as a consequence of both climate change and land use changes (Khattak et al., 2016; Ashmore and Church, 2001). Heavy rainfall and floods affect channel morphology and sediment characteristics and transport, which can adversely impact the stability of the river (Ashmore and Church, 2001; Kait et al., 2008; Mandych, 2009). Furthermore, flooding events can have an effect on numerous parameters, including quality of soil (Ponnamperuma, 1984), soil erosion (Mandych, 2009), and aquatic habitat, such as the location of fauna within a river system (Rae, 1987; Blom and Voeselek, 1996; Ashmore and Church, 2001).

Flood events can greatly affect sediment transport processes in rivers. Sediment load in a river is dependent on the geomorphic and hydraulic properties of the river, the topography, and soil type (Mohammad et al., 2016). In particular, transport is dependent on many factors, such as particle size, discharge, stream bed morphology, and shear stress (Yang, 1972). Transport potential is enhanced during rainfall events due to higher flows in the channel; this affects sediment load concentrations in rivers (Mohammad et al., 2016). An increase in sediment transport rates can lead to channel enlargement, incision, and morphological planform pattern changes (Ashmore and Church, 2001; Kait et al., 2008)

Historically, channelization was a common tool used in river engineering practice to manage rivers and urban environments (Kroes and Hupp, 2010; Bukaveckas, 2007). Channelization refers to the invasive approach of modifying a river channel by re-

sectioning, re-aligning, diverting channels, or altering the flood banks (Soar and Thorne, 2001). This approach is used in river engineering to control flooding and bank stability, improve irrigation, and modify navigation routes (Brooker, 1985; Soar and Thorne, 2001; Watson et al., 1999). Although the intent of channelization efforts is often to enhance the channel, modifications can adversely impact the sedimentologic, hydrologic, and biologic properties of the channel (Bukaveckas, 2007). As outlined by Shields and Palermo (1982), environmental effects of channelization include:

1. Loss or alteration of aquatic habitat and/or aquatic habitat diversity;
2. Loss or alteration of terrestrial habitat and/or terrestrial habitat diversity;
3. Increase in sediment concentration and turbidity due to channel instability;
4. Reduction in aesthetic value of stream;
5. Increased water temperature and sediment concentration due to water quality degradation; and
6. Changes in hydraulic conditions, such as water levels and flow conditions.

Other types of channel modifications may be designed to assist with streambank instability and bank erosion (Watson et al., 1999). Modification options include the use of grade control structures or reintroducing vegetation along the streambank (Shields and Palermo, 1982; Watson et al., 1999). Bank stabilization is important because it improves water quality by reducing sediment concentration and provides protection for in-stream aquatic species (Shields and Palermo, 1982). In recent years, there has been a focus to more effectively balance hydraulic, geomorphic, and ecological functions in river engineering practice. These approaches, such as natural channel design or stream re-naturalization, are becoming critically important in urban environments where there are increasing stresses and encroachment that can prohibit the river from satisfying these functions.

Mathematical modeling tools can be used to investigate various river engineering problems, such as evaluation of stream hydraulic and geomorphic response to changes in flow regime. These models can also be used as a tool to evaluate stream restoration options in order to determine optimal stream morphological design to balance hydraulic, geomorphic, and ecological functions. Mathematical models have been created for use in applications such as floodwave propagation, aggradation-degradation in alluvial rivers,

sediment transport, and simulation of steady backwater flow (Julien, 2002). Such models have been widely used in theoretical and practical applications of flood prediction and floodwave routing in rivers and streams (Horrit and Bates, 2002).

Due to the complex nature of fluvial hydraulics and site-specific variations in hydrologic, hydraulic, and geomorphic conditions, the ability to accurately predict urban stream response to current and anticipated stresses is limited. Research is needed in this area in order to understand how urban streams respond to environmental and anthropogenic stresses in order to develop appropriate river management practices, land-use guidelines, and stream modification strategies. Effective stream restoration design requires evaluation of alternatives to determine an optimal channel design that balances hydraulic, geomorphic, and/or ecological needs of a river within an urban environment. Mathematical modeling tools, such as hydraulic models, are a proven and effective tool that can be applied to address these challenges due to their flexibility and efficiency in carrying out a wide range of simulations.

1.2 Goal and Objectives

The goal of this thesis is to examine the sediment transport and morphological performance of a small, urban creek in response to rainfall events of various intensities and durations, and to investigate the performance of various stream geomorphic modifications to improve hydraulic, geomorphic and ecological functions. This research will focus on Lower Spencer Creek, located in Hamilton, Ontario. Spencer Creek has been previously channelized to accommodate industrial and urban development (Cruikshank, 2015), resulting in a straighter channel with a steeper longitudinal slope. These historical alterations to the creek have led to increased velocity, sediment concentrations, and shear stress, and increased the risk of bank and bed erosion.

This thesis will apply the hydraulic modeling tool, HEC-RAS (Version 5.0), to investigate the morphodynamic response of the stream. In order to achieve this goal, the following objectives will be satisfied:

1. Evaluate the current stream hydraulic and geomorphic response to discharge events of varying magnitudes; and
2. Evaluate the stream hydraulic and geomorphic response to discharge events of varying magnitudes for proposed geomorphic modifications to Spencer Creek.

This research will contribute towards developing a greater understanding of the sensitivity of urban streams and their vulnerability to flooding and geomorphic instability. The methods used in the present study can be applied to similar urban systems. Results from this thesis will assist river engineers and hydrologists in designing and implementing effective river management practices, stream restoration efforts, and balancing hydraulic, geomorphic, and/or ecological needs.

1.3 Structure of Thesis

This thesis is subdivided into six chapters. Following Chapter 1 (Introduction), the chapters are organized as follows:

Chapter 2 discusses relevant fundamental equations for hydraulic and sediment transport mathematical modeling. Three methods for estimating erosion within the channel will also be discussed. The mathematical model and equations used in the present study will be presented.

Chapter 3 presents the literature review. This chapter focuses on channelization and the effects of channel modifications on rivers, and will discuss the relevant literature related to mathematical modeling of river systems.

Chapter 4 introduces the study area and presents the methodology followed in this thesis. It also includes a description of the data needed for the present study and the various methods of data collection.

Chapter 5 presents the results from the hydraulic modeling performed in the present study. This includes results for velocity, sediment transport, and shear stress for all flow events and all proposed channel morphological configurations of Spencer Creek.

Chapter 6 presents an analysis and discussion of the results obtained from the hydraulic modeling. Further analysis of the velocity, sediment concentration, and shear stress results are discussed. The chapter also investigates hysteresis conditions observed in the sediment transport rates, examines the potential for bank erosion in Spencer Creek, and examines the ecological implications of the results.

Chapter 7 presents the main conclusions resulting from this thesis and provides recommendations for future research in this area.

Chapter 2

2 Fundamentals of the Present Work

This chapter provides a comprehensive review of the theoretical fundamentals of the computational models used for the river channel modeling performed in this thesis. This includes descriptions of fundamental equations of flow, sediment transport, and bank erosion, detailed description of various computational models, and a comparison of commonly used hydraulic models.

2.1 Fundamental Equations

Flow in a river channel can be described on two orthogonal coordinate systems. The first system is the global right-hand Cartesian (x, y, z) system, where x , y , and z are the downstream direction, the lateral direction, and the vertical direction, respectively. The second coordinate system is the local cylindrical (r, θ, z) system, where r is the radius of curvature and θ is the polar angle (Julien, 2002).

Sediment in a river can be transported as bedload or suspended load by rolling and/or sliding, saltation motion, or suspended particle motion (van Rijn, 1984a). Modeling bedload transport requires the use of sediment transport equations, such as the Engelund-Fredsøe (1976), van Rijn (1984), or Meyer-Peter and Müller (1949) formulas. For horizontal flow, the bed transport direction will correspond with the direction of the bed shear stress. For sloping beds, however, gravity will affect the transport direction of bed shear stress. Suspended load is a function of the hydraulic conditions, as well as what has occurred upstream at an earlier time. Detailed modeling of suspended load in rivers requires a time-space lag in the sediment transport response to variations in hydraulic conditions. This time-space lag effect is modeled using a depth-averaged convection-dispersion model, representing the transport and distribution of suspended solids in the vertical direction. Grain size and transport formulae for bedload and/or suspended load are required as inputs in any sediment transport model. The percentage and grain size for all fractions and the initial concentration of sediment may also be required. Hydraulic

resistance in alluvial rivers can be predicted using semi-empirical models by Engelund-Hansen (1972) and Ackers and White (1973) (DHI Water and Environmental, 2004).

Equations of flow, sediment motion, and bank erosion will be discussed in the following subsections.

2.1.1 Fundamental Equations of Flow

2.1.1.1 Navier-Stokes Equations

Basic equations of conservation of mass and momentum can be used to simulate flows in open channels such as rivers and streams. The three-dimensional Cartesian coordinate system can be used to define the conservation of mass (Strum, 2001).

The Navier-Stokes equations, three equations resulting from Newton's second law, can be applied to a homogeneous, incompressible, isotropic fluid, and to viscous, turbulent flows. These equations can be applied to open channel simulations using hydraulic models (Strum, 2001).

In the x -direction the Navier-Stokes equation is expressed as:

$$\rho \frac{Du}{Dt} = -\frac{\partial p}{\partial x} + \rho g_x + \mu \left(\frac{\partial^2 u}{\partial x^2} + \frac{\partial^2 u}{\partial y^2} + \frac{\partial^2 u}{\partial z^2} \right) \quad (1)$$

where:

u = fluid velocity (m/s)

t = time (h)

g_x = acceleration due to gravity along the x -axis (m/s²)

ρ = fluid density (kg/m³)

μ = fluid dynamic viscosity (Ns/m²)

In the y -direction the Navier-Stokes equation is expressed as:

$$\rho \frac{Dv}{Dt} = -\frac{\partial p}{\partial y} + \rho g_y + \mu \left(\frac{\partial^2 v}{\partial x^2} + \frac{\partial^2 v}{\partial y^2} + \frac{\partial^2 v}{\partial z^2} \right) \quad (2)$$

where:

g_y = acceleration due to gravity along the y -axis (m/s^2)

In the z -direction the Navier-Stokes equation is expressed as:

$$\rho \frac{Dw}{Dt} = -\frac{\partial p}{\partial z} + \rho g_z + \mu \left(\frac{\partial^2 w}{\partial x^2} + \frac{\partial^2 w}{\partial y^2} + \frac{\partial^2 w}{\partial z^2} \right) \quad (3)$$

where:

g_z = acceleration due to gravity along the z -axis (m/s^2)

Turbulent flow may also be calculated using the Reynold's-averaged Navier-Stokes equations shown in Eqs. (4) and (5). This method is largely used in the prediction of transitional behavior, specifically in the coupling of fully turbulent models and in the addition of transport equations of the turbulence model equations (Walters and Cokljat, 2008).

$$\frac{\partial \bar{u}_i}{\partial \bar{x}_i} = 0 \quad (4)$$

$$\partial \bar{u}_j \frac{\partial \bar{u}_i}{\partial \bar{x}_j} + \frac{\partial \bar{u}_i}{\partial t} = -\frac{1}{\rho} \frac{\partial \bar{p}}{\partial \bar{x}_i} + \frac{\partial}{\partial \bar{x}_j} \left(\nu \frac{\partial \bar{u}_i}{\partial \bar{x}_j} - \overline{u'_i u'_j} \right) \quad (5)$$

2.1.2 Fundamental Equations of Sediment Motion

Many equations to describe sediment motion have been developed for use in mathematical models. The following sub-sections describe various sediment transport equations commonly used in mathematical models.

2.1.2.1 van Rijn (1984)

van Rijn (1984) proposed two equations dealing with sediment transport. The first equation (Eq. (6)), deals with bedload transport. The van Rijn equation for bedload is used for particles ranging from 200 – 2000 μm , and is expressed as:

$$\frac{q_b}{[(s-1)g]^{0.5} D_{50}^{1.5}} = 0.053 \frac{T^{2.1}}{D_*^{0.3}} \quad (6)$$

where:

b = mean flow width (m)

T = transport stage parameter (see Eq. (8))

D_* = particle parameter (m) (see Eq. (7))

The particle diameter is determined following:

$$D_* = D_{50} \left[\frac{(s-1)g}{\nu^2} \right] \quad (7)$$

where:

ν = kinematic viscosity (m^2/s)

The transport stage parameter, T , is calculated according to:

$$T = \frac{[u'_*]^2 - [u'_{*cr}]^2}{[u'_{*cr}]^2} \quad (8)$$

where:

u'_* = bed shear velocity (m/s)

u'_{*cr} = critical bed shear velocity (m/s)

The critical bed shear velocity is calculated following:

$$u'_* = \frac{\bar{u}}{5.75 \log\left(\frac{12d}{3D_{90}}\right)} \quad (9)$$

van Rijn (1984) presented a second equation (Eq. (10)) dealing with suspended sediment transport. This expression is appropriate for fine particles ranging from 100-500 μm and can be computed according to:

$$q_s = F\bar{u}dc_a \quad (10)$$

where:

q_s = sediment load transport (m^2/s)

F = F-factor (see Eq. (11))

c_a = reference concentration

The F-factor is calculated following:

$$F = \frac{\left[\frac{a}{d}\right]^{Z'} - \left[\frac{a}{d}\right]^{1.2}}{\left[1 - \frac{a}{d}\right]^{Z'} [1.2 - Z']} \quad (11)$$

where:

a = reference level

Z = suspension parameter

2.1.2.2 Ackers-White (1973)

Ackers and White (1973) presented a sediment transport equation dealing with total load (sum of suspended load and bedload) in a channel. According to Ackers and White (1973), fine grain soils travel in suspension and depend on the total shear stress of the bed, while the transport of coarse grain soils is largely dependent on the shear stress of the grains. Following these authors, the sediment stream velocity ω can be expressed as:

$$\omega = \rho g Q x \quad (12)$$

where:

Q = discharge (m^3/s)

X = dimensionless factor of sediment transport (see Eq. (13))

ω = sediment stream velocity (m/s)

The dimensionless factor, X , is calculated according to:

$$X = \frac{SD}{H} * \left(\frac{v_0}{v_x}\right)^n * G_{gr} \quad (13)$$

where:

D = sediment diameter (m)

S = sediment grain density to water density ratio

v_0 = mean water velocity (m/s)

n = constant value depending on D_{gr}

G_{gr} = dimensionless sediment transport rate

The dimensionless sediment transport rate G_{gr} is calculated according to:

$$G_{gr} = C \left(\frac{F_{gr}}{A} - 1 \right)^m ; D_{gr} = D \left[\frac{g(S-1)}{v^2} \right]^{1/3} \quad (14)$$

where:

A, C, n, m = constant values depending on D_{gr}

D_{gr} = dimensionless grain diameter

F_{gr} = mobility function (Eq. (15))

The mobility function, F_{gr} , is calculated with:

$$F_{gr} = \left[\frac{v_0}{\sqrt{gD(S-1)} * \sqrt{32 \log \frac{\alpha H}{D}}} \right] * \left[\frac{v_*}{v_0} \sqrt{32 \log \frac{\alpha H}{D}} \right]^n \quad (15)$$

where:

α = constant value (according to Ackers $\alpha = 12,3$)

v_* = shear velocity (m/s)

2.1.3 Fundamental Equations of Shear Stress

The DuBoys equation is a common expression used in river engineering and stream ecology to estimate the mean boundary shear stress within a channel, which can be determined according to:

$$\tau = \gamma R S \quad (16)$$

where:

τ = shear stress (kPa)

γ = specific weight of water (N/m³)

R = hydraulic radius (m)

S = slope

This equation is applicable to channels with uniform flow conditions in wide channels (width-to-depth (b/d) ratio > 20), thus resulting in the most accurate estimations in channels under high discharges where the flow is approximately uniform. Estimations of local shear stress can also be calculated based on velocity measurements. Wilberg and Smith (1991) calculated local shear stress using depth averaged velocity, and found the results to be accurate when $d/D_{84} > 1$ (Schwendel et al., 2010).

In channels where the b/d ratio is less than 20, the hydraulic radius, R , is approximately equal to depth, d . In this scenario, d may be substituted for R in Eq. (16). However, for channels with a b/d ratio greater than 20, the hydraulic radius is calculated according to:

$$R = \left[\frac{A}{2d + b} \right] \quad (17)$$

where:

R = hydraulic radius (m)

A = cross-sectional area (m²)

d = flow depth (m)

b = width (m)

2.1.4 Fundamental Equations of Bank Erosion

Soil erosion and modification of river cross section geometry is largely influenced by rainfall intensity (de Lima et al., 2003). Riverbank erosion and collapse is a fundamental

problem in fluvial geomorphology and river engineering. Tools have been created to assist river engineers in assessing the stability of cohesive and non-cohesive banks, and to investigate the effects of bank failure on fluvial processes (Julian and Torres, 2006). The following subsections discuss three methods to estimate slope stability and erosion rates.

2.1.4.1 Taylor's Charts

Classical slope stability analysis in various forms has been applied to many slope erosion problems. The most easily applied tool for analysis of a homogeneous slope is Taylor's stability chart (1937). Taylor identified three types of failure circle (Figure 1): (1) toe circles (Figure 1a); (2) slope circles (Figure 1b); and (3) midpoint (base) circles (Figure 1c) (Steward et al., 2010). Based on dimensional analysis and field observations, Taylor (1937) proposed a stability number, N , to assess critical failure circles following:

$$N = \frac{c}{F_s \gamma H} \quad (18)$$

In Eq (18), C is the undrained shear strength (kN), F_s is the factor of safety, H is the height (m), and γ is the unit weight of the soil (kN/m³).

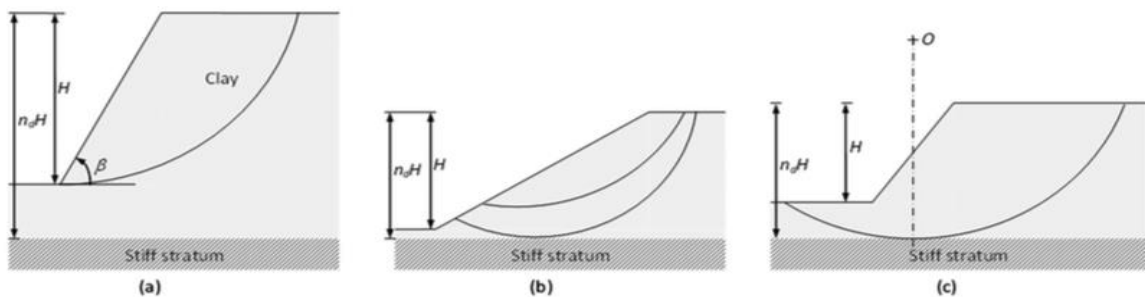


Figure 1: Failure Circles: (a) toe circle; (b) slope circle; (c) midpoint (base) circle (Steward et al., 2010)

When the failure plane angle β is greater than 53° , failure occurs along the circular arc, causing toe failure. When β is less than 53° and the depth factor, n_d , is smaller than 4, slope circles are formed. In cases where β is less than 53° and the depth factor, n_d is larger than 4, midpoint (base) circles are formed (Steward et al., 2010). This method is applied to undrained failures in cohesive slopes and has been successful for large slopes subject to normal drivers in the environment, such as material weakness, geometry, and pore pressure changes. Charts have since been developed to deal with drained soils and features, such as shrinkage cracks.

2.1.4.2 Thorne's Analysis

Although Taylor's charts have been useful for typical slope problems, their application to river bank stability has been less successful. Darby and Thorne (1996a) created a stability analysis to assist in quantifying forces acting on the incipient block failure (Figure 2). A number of assumptions were made to create the analysis. First, it was assumed that the bank is non-layered. The effects of vegetation were assumed to be accounted for in the in the bank stability and weight terms. Finally, it was assumed that the factor of safety concept could be used to model bank stability. Darby and Thorne (1996a) stated that "the resultant driving force acting on the incipient failure block is the resultant of the component of the weight of the failure block directed down the failure plane and the resultant of the hydrostatic confining pressure term directed up the failure plane" (Darby and Thorne, 1996a, pg 2). This work also identified a number of modes of failure seen in Figure 2 that do not occur for larger slopes.

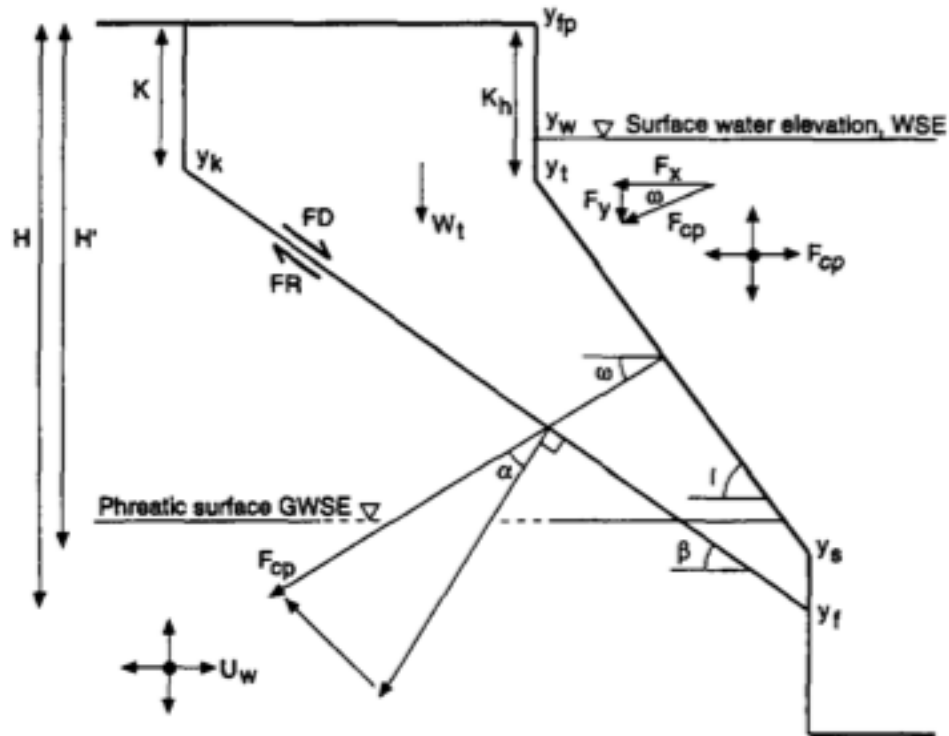


Figure 2: Bank Stability Analysis (Darby and Thorne, 1996a)

2.1.4.3 Hydraulic Erosion

Another potential process modifying the bank geometry is hydraulic erosion. The most common method used to predict hydraulic lateral erosion rates E can be expressed as:

$$E = k(\tau - \tau_c) \quad (19)$$

In Eq. (19), E is the lateral erosion rate, k is the erodibility coefficient, τ is the applied shear stress by flow, and τ_c is the critical shear stress. Channel banks with silt-clay ratios higher than 40% are thought to have negligible erosion from hydraulic shear. In these cases, the erosion of the banks is most likely governed by subaerial processes. Silt-clay ratios of 20-40% have both subaerial and hydraulic processes that lead to bank erosion. Hydraulic processes are the main cause of bank erosion in channel banks with less than 20% silt-clay ratios (Julian and Torres, 2006).

2.2 Mathematical Modeling

Computational models are often used as a cost-effective tool in research and design within the fields of hydraulic engineering and river restoration design (Fischer-Antze et al., 2001; Doyle et al., 2007; Jai and Wang, 1999). Computational models are used to assist in understanding river channel dynamics, such as channel morphology, flow, and sediment transport (Lane et al., 1998). Advancements in computational tools have led to numerous one-dimensional models (Han, 1980; Chang, 1982; Thomas, 1982; Holly and Rahuel, 1990; Wu and Vieira, 2002) used to calculate long-term channel erosion and deposition for quasi-steady and unsteady flows (Wu, 2004).

One-dimensional computational models are widely used in theoretical and practical applications of flood-wave routing and flood prediction (Horrit and Bates, 2002). Simplicity of computer codes, reduced computation times, and economic feasibility make one-dimensional computational models an ideal tool for analyzing flood extent and channel and floodplain sensitivity (Wu et al., 2004; Leandro et al., 2009; Sholtes and Doyle, 2011). Small scale, one-dimensional computational models can provide a more realistic output than two-dimensional computational models. Flows contained within a channel can be appropriately approximated with a one-dimensional computational model. However, once flows exceed the banks a two-dimensional computational model is required (Leandro et al., 2009)

2.2.1 HEC-RAS

The Hydraulic Engineering Center River Analysis System (HEC-RAS) is an integrated system of software designed by the U.S. Department of Defense, Army Corps of Engineers to manage rivers and other types of channels. The first version of HEC-RAS was released in July 1995, with the most recent version, Version 5.0, being released February 2016.

HEC-RAS is a steady and unsteady flow model with one-dimensional and two-dimensional modeling capabilities. Sediment transport and movable boundary computations, as well as water quality analysis can also be modeled. Water surface profiles for steady, gradually varied flow can be modeled for a network of channels, a dendritic system, or a single river

reach. Subcritical, supercritical, and mixed flow regimes may be considered, as well as effects of obstructions, such as bridges, culverts, and other structures. These are computed based on the solution of a one-dimensional energy equation, expressed in Appendix H. The model makes use of the equations presented in Sections 2.1.1 and 2.1.2 (Brunner & CEIWR-HEC, 2016).

One-dimensional unsteady flow through a network of open channels can be simulated using HEC-RAS, using Eq. (20), below. Initially, unsteady flow could only be simulated for subcritical flow regimes. The ability for users to simulate mixed flow regimes has recently been added. Effects of obstructions in the steady flow module have been included in the unsteady flow module. Two-dimensional unsteady flow modeling is now capable with the most recent version of HEC-RAS Version 5.0, as well as combined one-dimensional and two-dimensional routing.

$$Z_2 + Y_2 + \frac{a_2 V_2^2}{2g} = Z_1 + Y_1 + \frac{a_1 V_1^2}{2g} + h_e \quad (20)$$

In Eq. (20) Z_1 and Z_2 are the elevations of the main channel invert, Y_1 and Y_2 are the depth of the water at each cross section, V_1 and V_2 are the average velocities, a_1 and a_2 are the velocity weighing coefficients, g is the gravitational acceleration, and h_e is the energy head loss.

The sediment transport component of HEC-RAS was designed to model long-term trends in scour and deposition using a variety of equations, see Section 2.1.2 and Appendix H.

These equations include:

- Ackers and White (1973);
- Engelund and Hansen (1972);
- Meyer-Peter and Müller (1949);
- Toffaleti (1969);
- Yang (1979); and
- Wilcock and Crowe (2003).

HEC-RAS can model a network of streams, channel dredging, and numerous levee and encroachment alternatives. Deposition in reservoirs, maximum scour during large flood events estimates, and sedimentation in fixed channels can be evaluated using this component. Version 5.0 allows users to incorporate a bank stability and toe erosion model (BSTEM) with HEC-RAS to model channel stability.

HEC-RAS can also perform riverine water quality analyses. This includes a detailed temperature analysis, and transport of a confined number of water quality constituents. Transport of numerous water quality constituents are planned to be included in further versions of the model.

Although the recent update of HEC-RAS has added many features, there are still limitations within two-dimensional flow area component of the model. It cannot simulate unsteady flow with sediment transport erosion/deposition or water quality modeling. Pump stations cannot be added, and bridge modeling capabilities are not applicable within a two-dimensional flow area (Brunner & CEIWR-HEC, 2016).

Chapter 3

3 Literature Review

This chapter provides a comprehensive review of channel design and mathematical modeling of rivers and streams. The aim of this literature review is to discuss channel restoration and design techniques, and to review mathematical modeling techniques for hydraulic, sediment transport, and erosion processes in rivers and streams.

3.1 Stream Restoration and Channel Design

Soar and Thorne (2001) outlined four main applications for channel restoration projects: (1) urban projects; (2) restoring straightened channels; (3) river diversions; and (4) restoration following diversion. Restoration projects are required for various reasons including channel instability, low ecological diversity, and unsustainable maintenance (Soar and Thorne, 2001). Changes in the sediment regime upstream and geomorphic controls downstream may also cause instability in river channels (Doyle et al., 2007).

Stability of a river channel can be determined by continuity of sediment, continuity of flow, and flow resistance (Byars and Kelly, 2001). Adjustment to a river channel to improve stability include alterations to geometry, cross sections, bed configuration, and slope (Byars and Kelly, 2001). A fundamental aspect of restoration projects is altering the width and depth of a river channel to ensure stability (Shields et al., 2003).

Designing a channel to convey channel forming discharge will assist in reducing future sedimentation and erosion issues (Byars and Kelly, 2001; Doyle et al., 2007). The channel forming discharge concept is based on the idea that there is a single discharge that will produce channel dimensions, which coincide with those shaped by a natural, long-term hydrograph. This concept is determined by three parameters: (1) bankfull discharge; (2) effective discharge; and (3) design flood peak frequency. Bankfull discharge is defined as the full discharge the channel can convey, while effective discharge is defined as the discharge rate carrying the most sediment over time (Copeland et al., 2005; Doyle et al., 2007; Watson et al., 1999).

Doyle et al. (2007) employed the channel forming discharge concept to Carson River, Teton River, and two sites at Lincoln Creek. Carson River was re-channelized in the 1960s and 1990s, which triggered incising within the river. The two sites at Lincoln Creek had become incised upstream while remaining relatively stable downstream. Teton River has limited influence by humans, and was found to be geomorphically stable. The results from this study were found to be consistent with previous studies in the area (e.g., Soar and Throne, 2001). However, it was stated that channel designers employing this method on incised or disturbed systems should do so cautiously, and designs should be based on general physical principles as oppose to an empirically defined equilibrium state (Doyle et al., 2007; Wilcock, 1997).

Channel design and rehabilitation often focuses on erosion control, streambank protection and stability, and flood mitigation. Designing a channel aims to provide a geomorphically stable system, which has more opportunity for instream habitat. Although sediment supply greatly impacts equilibrium of a channel, sediment transport, geometry of the channel, and habitat sustainability are often overlooked when designing a stable channel in equilibrium (Byers and Kelly, 2001; Watson et al., 1999).

Streambank failure can occur for many reason, such as erosion of soil on the bank, of the upper bank or river bottom due to wave attenuation, and loss of protective vegetation (Henderson, 1986; Watson et al., 1999). Streambank protection structures can be implemented, often in combination with other engineering projects, to protect land, prevent failure due to eroding banks, and maintain channel alignment. Protection structures, however, can alter the amount of vegetation bordering a stream, which may be valuable for existing habitat within and surrounding a stream (Henderson, 1986). Natural and anthropogenic factors contribute to bed aggradation and degradation by disturbing balance between water discharge, sediment flow, and channel geometry (Bhallamini and Chaudhry, 1991). Bed degradation can lead to channel incision and instability, mass failure, and channel widening (Wu et al., 2004; Julien, 2002).

Frequency and magnitude of large flood events affect river morphology (Ashmore and Church, 2001; Kait et al., 2008). Urbanization has become a main cause for flooding in

urban areas, therefore it is important to estimate damages associated with large flood events and evaluate flood control policies (Kait et al, 2008; Boyle et al, 1998). Hydraulic models have been developed in conjunction with Geographic Information System (GIS) software to evaluate water elevation, sediment deposition, and stream velocity, and create flood forecasting tools (Boyle et al., 1998; Khattak et al., 2016).

Byers and Kelly (2001) used restoration design of Fort Branch of Boggy Creek in Austin Texas to demonstrate challenges associated with sediment supply in restoration projects. Urbanization in this area has led to downcutting, bank erosion, and higher peak flows. Rehabilitation efforts aim to stabilize the banks and prevent further downcutting, while providing habitat features such as riffles and vegetation. Comparing the design channel reach to historical channel profiles, the channel bed had shown an increase in width and a lowered elevation. Sediment transport computations showed rates more than 200% of the design reach capacity for the entire channel upstream of the design reach, while the channelized reach immediately upstream showed sediment transport rates 150% higher than the design reach capacity. The results from this study indicate that sensitivity to sediment transport can be achieved using equilibrium methods (Byers and Kelly, 2001).

Römken et al. (2002) conducted multiple studies examining the effects of rainstorm intensity, surface roughness, and slope steepness on soil loss. This included examining how sediment yield and the topographic gradient field are affected by prolonged rainfall and drainage network development in soil beds, and assessing the role of subsurface soil pressures on detachment of soil and sediment concentration. Results suggest that drainage network development is influenced by surface roughness, sediment yield is influenced by gradient, and soil loss is influenced by intensity of the storm event. Storms with initial high intensities were more likely to develop rills. Rough surfaces showed an increase in drainage density, while initially smooth surfaces showed a decrease in drainage density and less soil loss than initially rough surfaces (Römken et al., 2002).

3.2 Mathematical Modeling

River engineering often focuses on controlling and predicting river behavior, as well as investigating the effect of changes in morphology on stream response (i.e., bed shape, geometry, and cross sections) (Haghiani and Zaredehdasht, 2012). Physical models are often used to assist in river engineering projects (Julien, 2002). Julien (2002) outlined three main purposes of physical models: (1) laboratory duplication of flow in a river; (2) performance of hydraulic structures; and (3) investigation of different hydraulic and sediment conditions.

Although physical models are important in the field of river engineering, developments in computer science and mathematical modeling have reduced the need for physical models, and created an increase in the use of mathematical models in geomorphological and river engineering studies (Haghiani and Zaredehdasht, 2012). One-dimensional mathematical models are used in open channel flow hydraulics simulations as a cost-effective alternative to physical modeling, and can be applied in various engineering applications (Garcia-Navarro et al., 1992; Wu et al., 2004). Numerous one-dimensional models have been applied to a variety of applications, including: (1) simulation of steady backwater flow; (2) unsteady wave propagation; (3) advection-dispersion of sediment contamination; and (4) aggradation-degradation in alluvial rivers (Julien, 2002).

An area of one-dimensional modeling that has had extensive development is mathematical modeling of sediment transport. One approach to modeling sediment transport is a non-equilibrium sediment transport model. This approach determines the sediment transport rate using mass transport equations, which is ideal for sediment transport in natural rivers in non-equilibrium state (Wu et al., 2004). Wu et al. (2004) defines an equilibrium transport model as one where the sediment transport capacity and the bed change at each cross section is calculated using the sediment continuity equation. The non-equilibrium transport model makes use of mass transport equations to determine the sediment transport rate, which is more suitable for determining sediment transport in a natural channel.

Wu et al. (2004) applied a one-dimensional model to simulate unsteady flow and non-equilibrium sediment transport in the Goodwin Creek watershed in Mississippi and in the Pa-Chang River in Taiwan. The model created was used to simulate alterations within the channel from 1978 to 1995 for Goodwin Creek, and between 1995 to 1998 for Pa-Chang River. The model accurately predicted flow discharges and determined sediment transport and morphological changes within the designated channel networks (Wu et al., 2004).

Kait et al. (2008) used the one-dimensional model FLUVIAL-12 to evaluate channel changes and sediment transport causing problems on river bank and bank stability in Kulim River in Malaysia. The model simulation was run for 42 years, with two major floods occurring within this period. Calculated results showed that sediment delivery will decrease with time, and that the river was stable at most locations following major flood events. The predicted results and measured data were found to be in good agreement when looking at water levels and bed profiles, demonstrating that FLUVIAL-12 is a useful tool to simulate sediment transport and flooding (Kait et al., 2008).

The one-dimensional model HEC-RAS was applied by Shelley et al. (2016) to evaluate the effectiveness of modifying Tuttle Creek Lake reservoir, located in the United States of America, to decrease sediment trapping efficiency. Simulations were performed on the reservoir using the new integration of sediment transport simulations with unsteady flow calculations. Time-steps had to be reduced to achieve stability in the sediment transport computations, however, once stable, the model was able to successfully perform sedimentation analysis (Shelley et al., 2016).

Zhou and Lin (1998) used a one-dimensional mathematical model for natural rivers to compute suspended sediment deposition for the Three Gorges Project in China. Results from the one-dimensional mathematical model compared well with physical model results and two-dimensional computations. The mathematical model presented shows the capability of using a one-dimensional model as opposed to a two-dimensional model, which is often more time consuming, to assess erosion and deposition processes (Zhou and Lin, 1998).

Bhallamini and Chaudhry (1991) applied a one-dimensional model to three scenarios: (1) aggradation due to sediment overloading; (2) development of longitudinal profiles; and (3) bed level changes associated to knickpoint migration. Knickpoint refers to a sharp change in slope, which migrates due to erosion of bedrock. The first case looked at an alluvial channel with constant discharge and uniform depth. Results from this case showed that the one-dimensional model will give stable results without performing many iterations. The second case computed degradation due to base-level lowering. Although degradation was higher in the measured results as oppose to the computed results, it was found that the computed results compared well with the measured results, and the model was able to effectively predict degradation. The final case looked at knickpoint migration and its impact on bed level changes. Deposition was found to be greater in the measured results, and the downstream bed profiles in measured results were higher than model prediction. Despite the differences between computed and measured results, Bhallamini and Chaudhry (1991) stated the overall results correlated well.

Two one-dimensional models, MIKE 11 and HEC-RAS, were used by Haghiani and Zaredhendasht (2012) to simulate bed changes in the Karun River in Iran. A five-year simulation with each model showed significant sedimentation in the river, likely due to the decrease in longitudinal slope and increase in Manning's n value. When comparing the two models, depth of sedimentation was found to be lower using the HEC-RAS model at most discharge levels. These differences can be related to removal of some of the Saint-Venant terms in the HEC-RAS model (Haghiani and Zaredhendasht, 2012).

Hicks and Peacock (2005) assessed the HEC-RAS model to evaluate its suitability for flood routing and water level forecasting applications. To assess this, Peace River, located in Alberta, Canada, was modeled. Simulation results were compared to measured water level and discharge data, as well as water level and discharge hydrographs obtained from Alberta Environment using two other one-dimensional models. Results showed that the magnitude of the wave peak and water levels were comparable to observed data and hydrographs. When looking at wave speed, however, the HEC-RAS results produced slower speeds than other model outputs. There was a slight lag in the timing of the peak water levels, and the peak water levels were overestimated in comparison to observed data. Overall, HEC-RAS

was found to be a suitable one-dimensional model for investigating flood routing and water level forecasting (Hicks & Peacock, 2005).

Sholtes and Doyle (2011) applied the one-dimensional model HEC-RAS to model synthetic and field-based stream reaches for impaired and restored channels. The study focused on three main components of flood wave attenuation: (1) is it enhanced by channel restoration; (2) the response of various flood scales to restoration; and (3) critical elements of channel restoration. Results for the synthetic reach simulations for all flood frequencies showed minimal increase in flood wave attenuation. The restored reach showed an increase in attenuation to peak discharge by 1.2%, and a 50% reduction in celerity (i.e., wave speed). The first channel showed no significant change in flood attenuation for the largest flood event. Peak discharge was reduced 1% with a medium overbank flood, and reduced 5% for a bankfull flood. The second channel showed no increase in flood attenuation when examining the restored reach. This study provides guidance on how restoration can be utilized to increase the potential for attenuation. It shows that, in an ideal scenario, attenuation can be achieved in channel restoration, and is best utilized when applied to larger scales (Sholtes and Doyle, 2011).

Khattak et al. (2016) used HEC-RAS in combination with ArcGIS to develop floodplain maps for Kubal River. Six return periods were simulated, as well as a flood that occurred in 2010. Flood inundation maps were produced for the 2010 flood, and were found to be representative of satellite images from this event. This study showed the suitability of the HEC-RAS model in simulating open channel flows, and it pairs well with ArcGIS to produce realistic flood maps (Kattack et al., 2016).

3.3 Summary

The articles outlined in this literature review discuss various areas of channel restoration and design that have been previously examined. Byers and Kelly (2001) and Römken et al. (2002) studied the effects of channel design on streambank and streambed stability, bed and bank failure, and sediment transport. Wu et al. (2004), Kait et al. (2008), Zhou and Lin (1998), and Shelley et al. (2016) used mathematical models in predicting channel

behavior due to flooding, sediment transport in the channel, and bed and bank stability. Hicks and Peacock (2005), Sholtes and Doyle (2001), and Khattak et al. (2016) used mathematical models to determine the effects of flooding on a channel and to create floodplain maps.

The literature discussed in the preceding section discusses many aspects of channel design, mathematical modeling, and effects of flooding. However, there is a lack of literature focusing on the use of mathematical models to analyze the effects of flood events on various channel design options. This type of investigation and the development of an appropriate methodology would prove useful to river engineers in order to design effective stream modifications to mitigate flooding, while also ensuring other geomorphic and ecological functions of the stream are preserved.

Chapter 4

4 Study Area and Methodology

This chapter will discuss the area of study used for this thesis, including details on the location, land use, and previous alterations to the area. This chapter will also include the methodology followed for the present research.

4.1 Flooding in Hamilton, Ontario

The city of Hamilton in Southwestern Ontario, Canada is known for being susceptible to flooding due to rainfall events and snowmelt, with 17 storm events resulting in flooding between 2004 and 2012. Of these 17 storms, 16 occurred between May 25 and September 10, with one occurring in December. At least five of these storms were found to be either a 50-year storm or a 100-year storm, and one storm was classified as a plus 100-year storm. All large storm events occurred between the months of June and August (Citizens at City Hall, 2012).

Certain areas within the City of Hamilton have experienced flooding due to heavy rainfall more frequently than others. The Red Hill Valley Parkway, for example, has been a location of severe flooding for many years. In 2009 and 2010 sections of the Red Hill Valley Parkway between the Queen Elizabeth Way exit and the Barton Street exit were closed due to flooding. The area between these exits crosses a creek several times, which contributed to flooding of the parkway (van Dongen, 2013).

Ward 9 of Hamilton (see Figure 78 in Appendix I) is another location that has experienced a significant amount of flooding (van Dongen, 2013). In July 2012, over 130 homes in proximity to Ward 9 experienced major flooding (van Dongen, 2012; van Dongen, 2013). Storm intensity and storm localization are considered contributing factors to flooding in this area. Similar events have occurred between the Stoney Creek area and the Mount Hope and Winona areas, where 160 homes reported flooding following a storm in 2013 (van Dongen, 2013).

Large rainfall events are a common cause of flooding. A well-known example of this is Hurricane Hazel, occurring on October 15 and 16, 1954 in Southern Ontario; this hurricane affected many municipalities in the region, including Hamilton. Within 24 hours, 200 mm of rain fell, and wind speeds reached 124 km/h. This event resulted in 81 deaths, left 1900 civilians homeless, and caused between \$25 and \$100 million in damages; this is equivalent to approximately \$1 billion in 2016 dollars. The fast occurrence of flooding during this hurricane was believed to come from the recent deforestation of the Humber River drainage basin. This deforestation resulted in water flowing quickly into the river, surpassing the floodplain. A total of 40 bridges were damaged or destroyed, 40 highways and roads were flooded, and passenger trains were taken from tracks (Marsh, 2012).

Flooding in Hamilton, Ontario has experienced catastrophic flooding events in recent years. A storm event on July 26, 2009 produced 110 mm of rain in three hours. This storm was classified as a plus 100-year event; a storm of this magnitude had yet to be experienced by the Woodward Avenue Treatment. A peak flow was recorded to be 1067 Megalitres per day (ML/d) at the storm's peak. This flow surpassed the treatment plant's average daily flows rating of 409 ML/d, and 614 ML/d for wet weather. Damages caused by this event lead to \$300 million in insured losses, and damaged 7000 homes. Flooding occurred in homes and on streets between Mount Hope and the Stoney Creek area (Scheckenberger, 2010; Citizens at City Hall, 2012).

July 22, 2012 brought another storm event leading to flooding in the Greater Binbrook area, located just outside of Hamilton, Ontario. Within 24 hours, gauges at Highland Road and Valley Park Community Centre recorded 140 mm and 116 mm of rain, respectively. Gauges directly outside the city recorded rainfall levels up to 250 mm. A storm of this magnitude, which extrapolated to a 1-in-1000-year event, had yet to be experienced on record in this area. Flooding throughout the city was thought to occur due to the intensity of the storm overwhelming the sanitation and storm infrastructure (Gainham, 2013; van Dongen, 2013).

Burlington, Ontario experienced a flash flood event on August 4, 2014. Within one day, up to 150 mm of rain fell; this is equivalent to two months of rainfall in this region.

Although no injuries were reported, many homes were flooded, vehicles were submerged, sewer systems were backed up, and mudslides occurred (Williams, 2014). The intensity of this event lead to many roads becoming flooded, with some closed completely due to excess water. Highway 407 was closed in both directions between Highway 403 to Appleby Line. On the Queen Elizabeth Way, eastbound lanes were closed at Guelph Line, while westbound lines were flooded West of Appleby Line (News Staff, 2014).

It is predicted that heavy storm events and flooding will continue to occur in Hamilton, Ontario. According to van Dongen (2013) in an article in *The Hamilton Spectator* (July 10, 2013), “Climate change is delivering severe wet weather events that are more dramatic and more intense than we’ve ever seen, and our systems are not designed for those types of events” (van Dongen, 2013).

The City of Hamilton is creating a digital map of the flooding hot spots within the city. This map will include 900 flooding hot spots, which are mainly inlets/outlets that are prone to flooding due to heavy rainfall. Two areas with many drainage issues within the city are Dundas, with 161 flooding hot spots, Ancaster, with 114 flooding hot spots, and Red Hill Valley Parkway, with 78 flooding hot spots. Dundas and Ancaster areas of concern are due to the older areas being built without storm sewers (van Dongen, 2012).

4.2 Study Area

Spencer Creek (shown in Figure 3), located in the Lower Spencer subwatershed (see Figure 79 in Appendix I) in Hamilton, Ontario, Canada, was the site selected for this project. Spencer Creek is currently under evaluation for restoration by the Hamilton Conservation Authority (HCA). Hamilton has an area of 113.11 km² (HCA, 2010), a population of 519,950, and population density of 465.4/km² (Statistics Canada, 2011).

Land use refers to the use of land which occurs on land or within structures on the land (Barnegat Bay Partnership, 2010). The Lower Spencer Creek watershed can be divided into seven land uses, shown in Table 1 below (Grillakis et al., 2011). See Figure 80 in Appendix I for a land use map for the Lower Spencer Creek watershed.



Figure 3: Spencer Creek in Hamilton, Ontario

Table 1: Lower Spencer Creek Watershed Land Use (Grillakis et al., 2011)

Land Use	Percentage of Land
Agriculture land	46.8%
Urban and paved areas	21.7%
Forested areas	15%
Wetlands	14.9%
Water surface	0.9%
Bare fields	0.7%

Spencer Creek is 7 km in length, however, this the present research only examined the lower 4.25 km of the creek between King Street and Cootes Drive, as shown in Figure 4. The area of the creek being re-channelized is at the most downstream section between Thorpe Street and Cootes Drive. Figure 4, below, shows the entire study area, with the 4.25 km of Spencer Creek used for this thesis lined in blue and each cross section labelled.

Six soil types are present within the Spencer Creek watershed. These soil types are mostly well drained, and have varying ranges for erosion potential, from very low to high. The soil type with the lowest erosion potential is Chinguacousy Loam; this soil type is imperfectly drained. The soil type with the highest erosion potential is Oneida Loam; this soil type is well drained. The remaining four soil types have moderate erosion potential and are well drained. These soil types are as follows: Farmington Loam, Grimsby Loam, Springvale Sandy Loam, and Ancaster Silt Loam (HCA, 2010). See Figure 81 in Appendix I for Soil Type map.

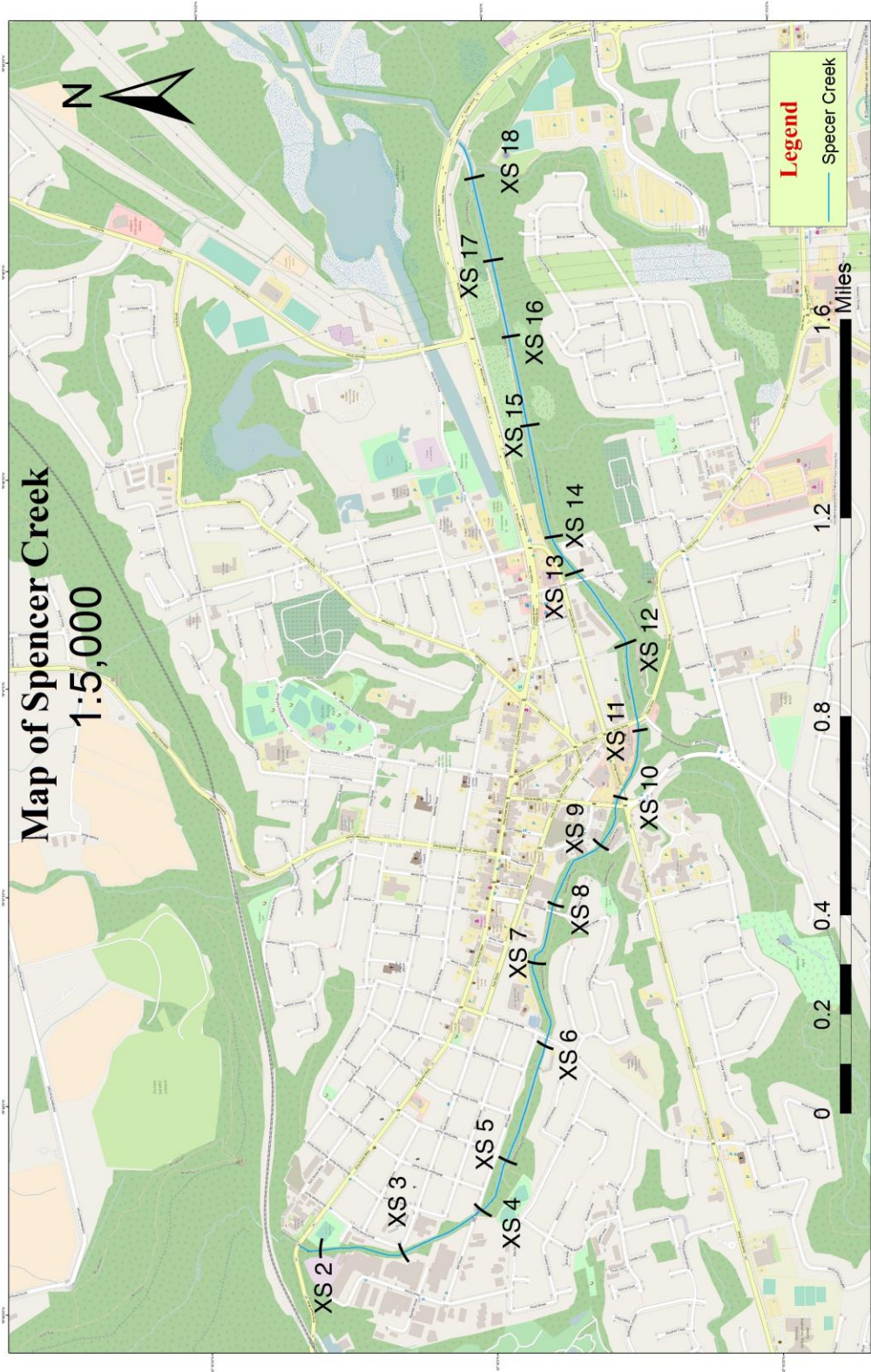


Figure 4: Map of Lower Spencer Creek Watershed Within Hamilton

4.2.1 Previous Alterations to Spencer Creek

As the former town of Dundas, Ontario, now a community within the city of Hamilton, began to develop, Spencer Creek underwent modifications to accommodate industrial and urban development within the town (Cruikshank, 2015). Modifications to Spencer Creek led to straightening of the channel, resulting in a decrease in the total length of the channel, as well as an increase in the slope of the channel. Due to these alterations, there were increases in flow velocities, shear stress, and potential/kinetic energy. There was also an increase in bed and bank erosion due to the ability of flow to carry larger sizes and volumes of sediment.

The bed and banks of Lower Spencer Creek were stabilized with concrete, stone, and gabion baskets to reduce erosion and prevent lateral migration of the creek at various locations, see Figure 5. Additionally, grade control structures, such as concrete drops, were incorporated to decrease the channel slope and to assist in reducing flow velocities and reduce the severity of erosion. Additional photographs of the banks of Spencer Creek are shown in the Appendix C.

The overall health of Spencer Creek and the quality of the ecology, specifically the fish habitat, within the creek have been affected as a result of the addition of grade control structures and hardening of the bed and banks. Channel modifications of Lower Spencer Creek have been considered barriers of fish migration by various agencies, and restoration of the area has been considered of high priority. To assist in alleviating the issues, the Hamilton Conservation Authority (HCA) began removing the grade control structures in 2011. This resulted in active spawning of salmon in the creek (JTB Environmental Systems Inc., 2012).

With climate change expected to increase the intensity and frequency of rainfall events (Teegavarapu, 2012), it is anticipated that populated areas of Southern Ontario, such as Hamilton, will be more vulnerable in the occurrence of a heavy rainfall event. Similarly,

changes in land use are expected to cause changes in runoff and erosion, thereby affecting small urban streams, such as Spencer Creek (Ashmore and Church, 2011).

Spencer Creek is presently under investigation by the Hamilton Conservation Authority (HCA) to return the channel to a more natural channel pattern. The channel design will aim to reduce flooding within the channel by reducing the channel velocity. It will also aim to control erosion within the channel, aid in reducing flooding, and create a stable stream for the ecology of the channel to thrive (JTB Environmental Systems Inc., 2012).



Figure 5: Bank Stabilizing Structures in Spencer Creek

The channelized stretch of Spencer Creek between Thorpe Street and Cootes Drive has a plan in place to restore it to a natural, meandering form of the channel. The plan proposes a relocation of the existing Spencer Creek Trail near Cootes Drive, replacement of dead ash trees, and removal of invasive grasses. See Appendix C for pictures showing this reach of Spencer Creek. These transformations will attempt to balance sediment transport, flood prevention, and ecology. By creating nesting areas, the plan has potential to protect the existing turtle population in the Spencer Creek area. The initial phase will focus on 300 m of Spencer Creek closest to Cootes Drive, with future restoration moving upstream towards Thorpe Street (Leitner, 2014).

4.3 Methodology

The Hamilton Conservation Authority (HCA) provided a variety of information to assist in the analysis of Spencer Creek. Flow data from the Market Street flow gauge was provided, with discharge data available dating back to 1984. Profile measurements of each cross section were given, which included chainages and elevation of each section. Figures in Appendix E display the cross-section profiles for each cross section, see Figure 4 for the location of each cross section. A Wolman pebble count for each cross section was also provided by HCA. The water surface elevation, stage, discharge, velocity, flow area, wetted perimeter, and top width were provided throughout the channel by HCA. Finally, the HEC-RAS 4.1 files used to perform a one-dimensional steady state simulation were provided; these files included geometric data, including cross-sectional data and Manning's n values, as well as steady flow data, and were used as the geometric input for the present work. These files were used to perform steady flow simulation in the model to ensure the model was calibrated.

For information that was not provided by the Hamilton Conservation Authority, field measurements were collected by the author. Field measurements, including bankfull widths, cross-sectional depths, and sediment samples were collected at Cross Sections 15, 16, 17, and 18 of Spencer Creek. A bank-to-bank width was measured using a measuring tape at each section, and recordings of depth at five locations across each section using a depth rod were measured. Sediment samples at each location of depth measurement were collected to use for further analysis. Five (5) samples were taken at each cross section for use in analysis.

Hydrometer tests were performed according to ASTM D422 on the collected sediment samples to determine the grain size analysis for the sediment passing through the No. 200 sieve. This data was used to adjust the one-dimensional model provided by HCA to include more accurate sediment data at the cross sections downstream (XS 15, 16, 17, and 18). See Appendix B for sediment distribution graphs for each cross section.

4.3.1 Hydrographs

Hydrographs were created for various storm durations and intensities to be simulated in the hydraulic modeling. Three events having occurred in Hamilton, Ontario within the past 100 years were chosen to be simulated. Included in these events was Hurricane Hazel, discussed in Section (4.1), which caused significant damage to Hamilton and surrounding areas. Events of this magnitude are likely to occur again and it is therefore important to study the effects these events have on the morphology and ecology within the creek. Intensity-duration-frequency (IDF) curves provided by the Ontario Ministry of Transportation were used to classify storm events and to create hydrographs corresponding to these events. The recent version of the IDF Curves Finder, version 3.0, was released in September 2016. The IDF curve used was at the Market Street gauge (coordinates 43.262500,-79.962500), located on Spencer Creek (Ministry of Transportation, 2013).

Hydrographs were created using the Soil Conservation Service (SCS) Method; Soil Conservation Service has changed its title to National Resources Conservation Services (NRCS). This method uses a dimensionless unit hydrograph to develop a hydrograph. Peak flow (ft^3/s), Q_p , for the hydrograph is calculated according to Eq. (21) (where A is the area of the watershed (mi^2), Q is the direct runoff (in), and T_R is the time to peak of the hydrograph from the start of the rainfall excess (hr)). T_R is calculated following Eq. (22) and the lag time t_p (hr), which represents the time from the centroid of the rainfall excess to the peak of the hydrograph, is calculated following Eq. (23) (where D is the rainfall duration (hr)).

$$Q_p = \frac{484AQ}{T_R} \quad (21)$$

$$T_R = \frac{D}{2} + t_p \quad (22)$$

$$t_p = \frac{l^{0.8}(S + 1)^{0.7}}{1900y^{0.5}} \quad (23)$$

In Eq. (23) l refers to the length of the flow path (ft), y refers to the average watershed slope (in percent), and S is the storage volume (in), calculated according to Eq. (20).

$$S = \frac{1000}{CN} - 10 \quad (24)$$

The average runoff curve number, CN , for the watershed was calculated using values defined for soil and land use characteristics (Bedient et al., 2008). The CN value for Spencer Creek was calculated to be 72.8.

Runoff estimation for SCS hydrographs assumes that there is a relationship between the total storm rainfall P (in), direct runoff Q (in), and infiltration F (in) plus initial abstraction I_a (in) (i.e., $F + I_a$). The relationship to determine direct runoff Q , as expressed in Bedient et al. (2008), is shown in Eq. (25).

$$Q = \frac{(P - 0.2S)^2}{P + 0.8S} \quad (25)$$

For each event, an averaged flow of 1.25 m³/s was applied for five hours prior to the storm event. The averaged flow value was calculated by assessing the average of the peak flows for Spencer Creek over a 5-year period. A constant discharge of 1.25 m³/s was used as a “base” event to assess the current condition of Spencer Creek as well as the response of Spencer Creek to channel modifications. Hydrographs were then created for a 24-hour period. The peak flows for the 5-year, 10-year, and 100-year events were determined to be 6.144 m³/s, 9.361 m³/s, and 12.231 m³/s, respectively.

4.3.2 Channel Modifications

The present study will investigate two potential modifications for Lower Spencer Creek. Modification 1 will look into widening sections downstream in Spencer Creek, with the aim to reduce velocity and sediment transport in the channel. Modification 2 will aim to return Spencer Creek a more natural, pre-channelization condition.

Modifications of Lower Spencer Creek were made to sections between Thorpe Street and Cootes Drive, Cross Sections 15, 16, 17, and 18, using the Channel Modification extension in HEC-RAS. The goal of the modifications was to evaluate the degree of improvement in flood control, excess sediment transport and channel stability in these sections, as described in Chapter 1. These sections were selected for proposed modifications due to the high risk of flooding and stream instability in this reach.

The first modification, hereafter referred to as Modification 1, included a widening of cross sections 15, 16, 17, and 18 by 15%. The second modification, hereafter referred to as Modification 2, included a lengthening of the distance between these cross sections by 10%, thereby reducing the slope by 10% and simulated the creation of a more sinuous channel, returning it to a more natural channel pattern. These modifications aim to reduce velocity within the creek, thereby decreasing its sediment transport capacity; this will result in less sediment erosion (Watson et al., 1999). Sediment data for the modified simulations remained consistent with the existing channel simulations.

Simulations were performed for all four rainfall events: (1) averaged flow; (2) 5-year return period; (3) 10-year return period; and (4) 100-year return period. These results were individually compared with the results from the simulation for the existing channel conditions. Equations for transport and fall velocity functions for the modified simulations remained consistent with the existing channel simulations.

4.3.3 Simulations

Sediment transport simulations were performed using the one-dimensional model, HEC-RAS Version 5.0 (see Section 2.2.1). Quasi-unsteady flow with sediment transport simulations were then performed for this thesis.

The geometry input of the channel was provided by the Hamilton Conservation Authority. This input included station elevation and chainage at each cross section. To increase stability, sections were interpolated at 75 m intervals and placed between the 17 cross sections used for the present study. Main channel banks were defined for the main channel, with the remainder being the overbank area. Manning's n values provided by HCA were 0.055, 0.030, and 0.055 for the left overbank, channel, and right overbank, respectively. These values were consistent throughout the entire channel.

Four events with varying return periods and durations were simulated in this study, see Table 2 below. The first storm was a constant flow run for a 24-hour period. This simulation was performed to observe the existing conditions of the channel during a constant flow, and was used as a comparative event for the remainder of the events. The second event had a 5-year return period, with a storm duration of 12 hours. The third event has a 10-year return period, with a storm duration of 6 hours. The final event has a return period of 100-years, with a duration of 24 hours. These events were determined based on events having occurred in Hamilton. As summary of each event is outlined in Table 2.

Table 2: Storm Events

Event Number	Storm Event Return Period	Intensity (mm/hr)	Duration (hr)
Event 1	Averaged flow	n/a	24
Event 2	5 year	5.2	12
Event 3	10 year	9.7	6
Event 4	100 year	5.3	24

All events had 5 hours of averaged flow conditions applied before the event began and were run for a 24-hour period to allow for the storm to reach its peak flow and begin to return to base flow conditions. The parameters of the present study did not permit simulations longer than 24 hours. Therefore, while Event 4 began to approach the averaged flow, it was not able to fully reach the averaged flow due to the 5-hour averaged flow at the beginning of the event. Figure 6 illustrates the four event hydrographs. Individual hydrographs are shown in Appendix A.

Sediment data was input into the model for each cross section according to the field measurements of substrate conditions described above. Sediment data was interpolated for the interpolated sections input between cross sections. Sediment sizes ranged from gravel to clay. Cross Sections 15-18 had mostly sand, silt, and clay, while Cross Sections 2-14 had larger sediment such as gravel and medium coarse sand.

The transport function selected was Ackers-White (1973) due to its ability to allow for multiple grain sizes. This equation allows for particles sized between 0.04 mm to 0.4 mm. The fall velocity method selected was the van Rijn (1984) due to its accuracy in calculating fall velocity for a large range of grain sizes. These equations allow for particles between 200-2000 μm and 100-500 μm for bed load and suspended load, respectively. The majority of stream bed within the creek, specifically at the modified downstream sections, is composed of sediment which falls within these ranges. A description of these equations was provided in Chapter 2.

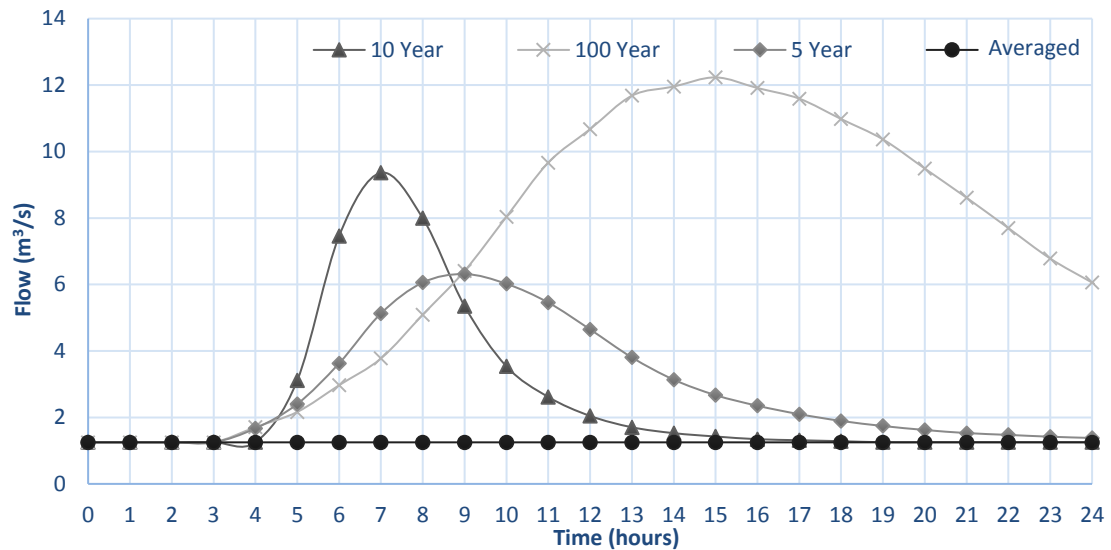


Figure 6: Hydrographs created for simulations

4.3.4 Model Set-up

Sediment transport computations performed in HEC-RAS require the use of the Quasi-Unsteady Flow or Unsteady Flow options. For the purpose of this thesis, the Quasi-Unsteady Flow option was utilized. The Quasi-Unsteady Flow option simulates a flow series for a sequence of steady flow computations using steady flow backwater equations. The model then estimates a flow hydrograph for a series of steady flow profiles with corresponding flow durations.

A Flow Series is the only option for the upstream boundary condition. The downstream boundary condition has three options, however, only one can be chosen. These include a stage time series, a rating curve, or normal depth. Finally, optional internal boundary conditions are available, including lateral flow series, uniform lateral flow series, and time series gate operations. The present study utilized the normal depth option for the downstream boundary condition.

Due to the sensitive nature of sediment transport models to load boundary conditions, sediment transport models often require calibration and validation to ensure accurate and reliable results. When using the HEC-RAS Sediment Transport option, it is important to

test the model over a range of flows using the Steady Flow Analysis option, calibrate the n -values, identify any ineffective flow areas, and assess cross section spacing (Brunner & CEIWR-HEC, 2016). For the current study, steady flow simulations were performed to work out errors within the model.

Chapter 5

5 Results

This chapter presents and discusses the results for the mathematical modeling conducted for this thesis. The general results subsection will be discussed in two parts: the results for the existing channel and the results for the modified channels. Cross sections will be further referred to as XS for this chapter.

5.1 General

This section presents and discusses the velocity, sediment concentration, and shear stress results at each cross section from the HEC-RAS hydraulic modeling. These parameters are discussed due to their influence on channel stability, erosion potential, and ecological health. Four events were used to examine the effect of precipitation events of varying magnitude on Lower Spencer Creek for three channel configurations (existing channel configuration, and two proposed channel modifications), as described in Chapter 4. A total of 12 simulations were performed, as summarized in Table 3.

Table 3: Summary of Simulations

Simulation	Channel	Event	Duration (hr)	Simulation	Channel	Event	Duration (hr)
1	Existing	Averaged	24	7	Modification 1	10-year	6
2	Existing	5-year	12	8	Modification 1	100-year	24
3	Existing	10-year	6	9	Modification 2	Averaged	24
4	Existing	100-year	24	10	Modification 2	5-year	12
5	Modification 1	Averaged	24	11	Modification 2	10-year	6
6	Modification 1	5-year	12	12	Modification 2	100-year	24

5.2 Existing Channel

For Simulation 1 (using the existing channel configuration), the peak sediment concentration occurred at later times (i.e., $t = 16$ hr) in the simulation for all cross sections, except XS 4, where it occurred at $t = 6$ hr of the simulation. The mean and maximum velocities for this event were equal at most cross sections. At the cross sections where the mean and maximum velocities differed, there was only a slight change. This trend is likely due to Event 1 being the averaged event where the discharge remains constant for the duration of the entire simulation.

For Simulation 2, upstream cross sections (e.g., XS 3 through XS 9) showed the peak sediment concentration occurring between $t = 10$ hr and $t = 11$ hr. At XS 10 the peak sediment concentration occurred later in the simulation at $t = 19$ hr. This time remains consistent for the majority of the downstream sections, demonstrating hysteresis conditions in the sediment transport rates in the stream in response to this event. The maximum velocity occurred at the same time as the peak discharge of the hydrograph. The sections farthest downstream, XS 15, 16, 17, and 18, showed maximum velocities much lower than the remainder of the channel. This trend likely occurs at these sections because of the milder slope at these sections.

During Simulation 3, the majority of the upstream cross sections showed the peak sediment concentration occurring at the same time as the peak flow of the hydrograph. Hysteresis conditions began to occur at downstream cross sections, especially at XS 15, 16, 17, and 18. These sections also showed a large decrease in velocity when compared to the cross sections upstream. Similar to the results for Simulation 2, this trend is likely occurred due to the milder slope at these sections.

Simulation 4 showed peak sediment concentrations occurring towards the end of the event for all cross sections, except XS 16, 17, and 18. At these sections the peak sediment concentration occurred at $t = 4$ hr, showing hysteresis conditions. Similar to previous simulations, the maximum velocity was relatively lower at XS 15, 16, and 18. This is likely due to the milder slope at these sections.

A complete summary of the results for each simulation are found in Tables 10, 11, 12, and 13 in Appendix F. The sections with the greatest change in peak sediment concentration between events (i.e., between simulations) were XS 15, 16, 17, and 18. As the return period increased, sediment concentrations at these sections increased by 0.42-1% from Event 1 to Event 2 and by 0-1% from Event 1 to Event 3. Event 4 (the hydrograph with the largest return period), however, only had an increase in sediment concentration at XS 15 (increase of 14%), while sediment concentrations decreased at XS 16, 17, and 18 by 3% from Event 1. The increase in sediment concentration can be associated to the increase in velocity at these sections for the larger flow events. Refer to Table 22 in Appendix F for changes in maximum velocity and sediment concentration for the existing channel.

As the return period of events increased, the maximum velocity in the stream increased accordingly. The greatest increases in velocity were at the downstream section of the channel, namely XS 15, 16, 17, and 18, with the greatest change occurring at XS 18 where the velocities increased from Event 1 (averaged flow) by 128%, 146%, and 156% for Events 2, 3, and 4, respectively. XS 3 and 9 also had significant changes in velocity. XS 3 increased from Event 1 by 104%, 121%, and 135% for Events 2, 3, and 4, respectively. XS 9 increased from Event 1 by 102%, 120%, and 132% for Events 2, 3, and 4, respectively.

Figure 7 displays the maximum sediment concentration for each event at each cross section for the simulations performed in the existing channel. The high sediment concentrations at the inlet of the model (i.e., XS 2), followed by the quick decline in sediment concentration starting at XS 3, indicates that there is an influx of sediment as the model begins. The simulated sediment concentration at this section is likely an inaccurate representation of the actual sediment concentration at this cross section. The sediment concentration is highest for Event 4; this was expected as Event 4 is the largest event. This event, however, had a decrease in sediment concentration at XS 16, 17, and 18. This trend will be discussed further in Chapter 6.

Figure 8 displays the maximum velocity for each event at each cross section for simulations performed on the existing channel. A large decrease in the maximum velocity compared

to other sections is observed at XS 3, 9, 15, 16, 17, and 18. The peak in velocity at the inlet of the channel is consistent with the sediment concentration results.

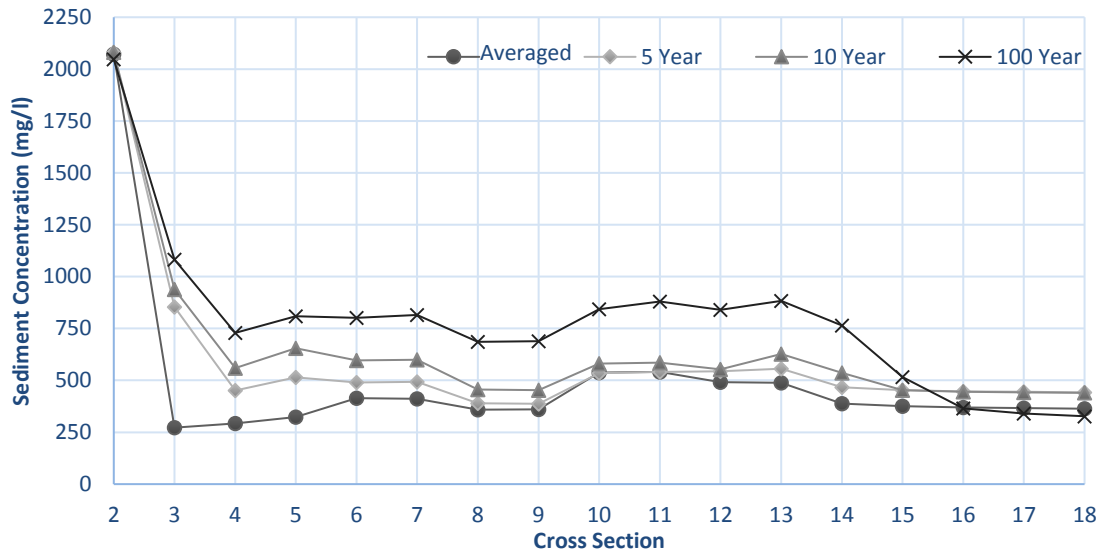


Figure 7: Comparison of Maximum Sediment Concentrations for all Simulations in the Existing Channel

Figure 9 presents a comparison in the maximum shear stress for each event at each cross section for the simulations performed in the existing channel. As can be shown from Figure 9, the shear stress is highly variable throughout the channel. The results show relatively high shear stress at XS 2, followed by a sudden decrease in shear stress at XS 3; this trend is consistent with the sediment concentration and velocity results. The pattern for the remainder of the cross sections closely resembles trend shown in the velocity results, showing that the lowest shear stress values occurred at XS 3, 9, 15, 16, 17, and 18. The reduction in velocity at these sections is likely due to the reduction in width of the channel at these sections. The reduction in velocity, sediment concentration, and shear stress at these sections will affect the erosion in the channel, as well as the ecology of the channel.

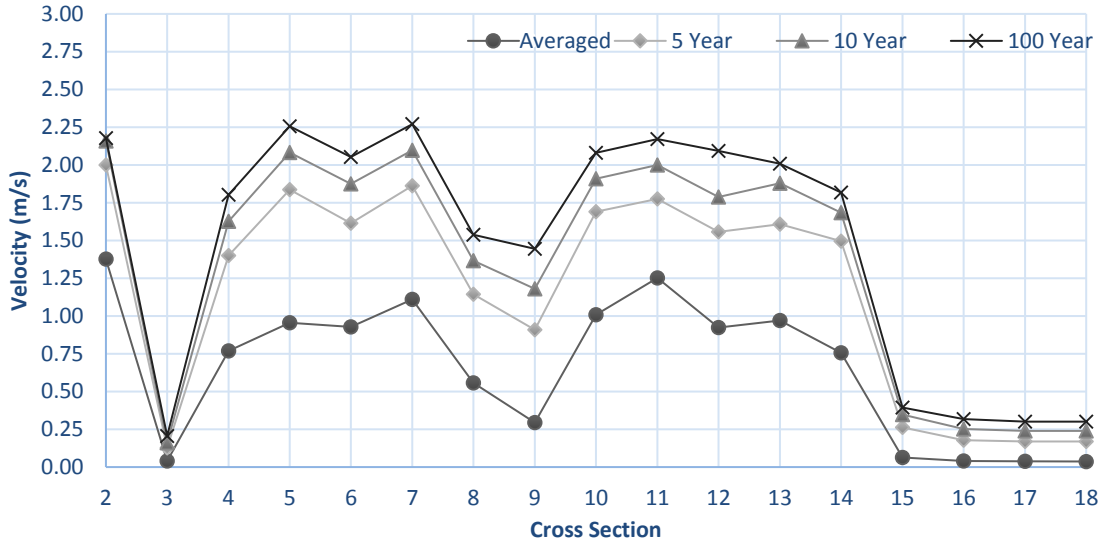


Figure 8: Comparison of Maximum Velocities for all Simulations in the Existing Channel

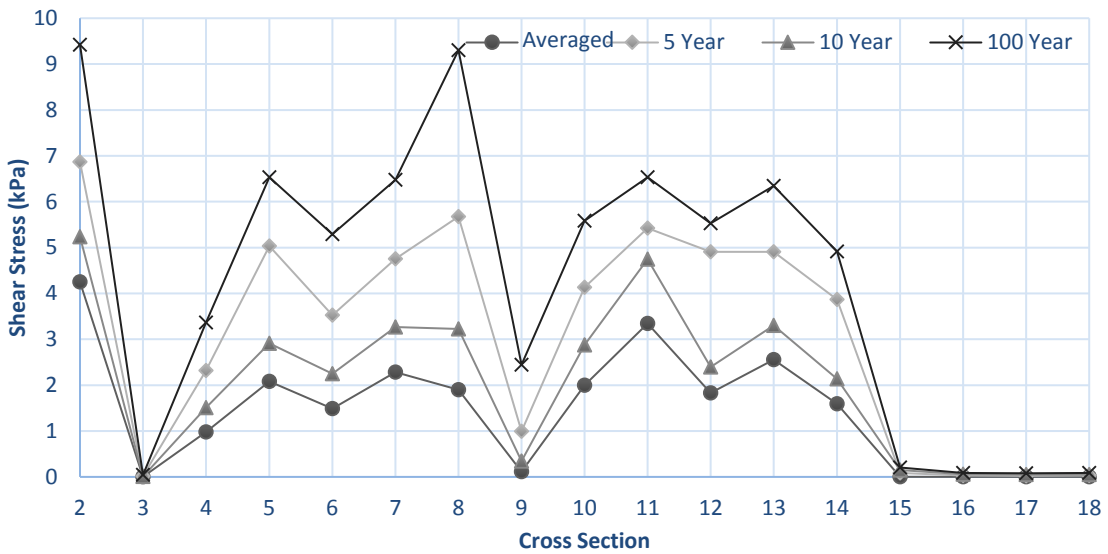


Figure 9: Comparison of Maximum Shear Stresses for all Simulations in the Existing Channel

5.3 Modification 1

The first modification widened the final four cross sections of the model (e.g., cross sections 15, 16, 17, and 18), by 15%. Refer to Table 10 in Appendix E for the original and modified widths at each cross section.

Similar to the results for the existing channel, the peak sediment concentration occurred at later times in the simulation for all cross sections, except XS 4, where it occurred at $t = 6$ hr of Simulation 5. The mean and maximum velocities for this event were equal at most cross sections. At the cross sections where the mean and maximum velocities differed, there was only a slight change. As mentioned in the previous section, this trend likely occurs due to Event 1 being the averaged event with a constant discharge.

At upstream cross sections (e.g., XS 3 through XS 9) the peak sediment concentration occurred between $t = 10$ hr and $t = 11$ hr for Simulation 6. At XS 10 the peak sediment concentration occurred later in the simulation at $t = 19$ hr; this remains consistent for the majority of the downstream sections. This trend demonstrates hysteresis conditions in the sediment transport rates in response to the event. The maximum velocity occurred at the same time as the peak discharge of the hydrograph. The sections farthest downstream (XS 15, 16, 17, and 18) demonstrated maximum velocities much lower compared to those observed in the remainder of the channel. These sections also showed a decrease in maximum velocity when compared to the existing channel. As previously mentioned, the large decrease in velocity at these sections likely occurred due to the milder slope in these locations.

Results from Simulation 7 indicated that the peak sediment concentration occurred at the same time as the peak flow of the hydrograph for the majority of upstream cross sections. Hysteresis conditions began to occur later downstream, especially at XS 15, 16, 17, and 18. These sections also showed a large decrease in velocity when compared to the cross sections upstream. This trend likely occurred due to the milder slope at these sections. These sections also showed a decrease in sediment concentration and maximum velocity in comparison to the results from the simulations in the existing channel.

Simulation 8 revealed peak sediment concentrations occurring towards the end of the simulation for all cross sections, except XS 16, 17, and 18. At these sections the peak sediment concentration occurred at $t = 4$ hr, showing hysteresis conditions. Similar to previous simulations, the maximum velocity was relatively lower at XS 15, 16, and 18. This was likely due to the milder slope present in these locations. These sections showed a decrease in the maximum velocity in comparison to the results from the simulations in the existing channel. A complete summary of the results for each simulation can be found in Tables 14, 15, 16, and 17 in Appendix F.

Peak sediment concentrations for the channel conditions of Modification 1 at XS 15, 16, 17, and 18 increased by 0.5%, 1%, 1%, and 2% from Event 1 to Event 2. Peak sediment concentrations from Event 1 to Event 3 increased by 0.4%, 0.8%, 0.9%, and 1% at XS 15, 16, 17 and 18, respectively. Similar to the existing channel, Modification 1 resulted in an increase in a peak sediment concentration at XS 15 by 9%, and a decrease in peak sediment concentration at XS 16, 17, and 18 by 3% from Event 1 to Event 4. Refer to Table 23 in Appendix F for changes in maximum sediment concentration for Modification 1.

The conditions created by Modification 1 (widening the channel at XS 15, 16, 17, and 18), resulted in greater increases in velocity between events at each cross section compared to the results from the existing channel simulations. This modification produced the largest increase in velocity at XS 18, with an increase of 160% from Event 1 to Event 4. The velocity increase with this modification may be due to Event 4 being the largest event, and XS 18 being the section farthest downstream, therefore it may be receiving sediment carrying over from upstream reaches of the creek.

Figure 10 displays the maximum sediment concentration at each cross section for each event in the simulations for Modification 1. The high sediment concentrations at the inlet of the model (i.e., XS 2), followed by the sharp decline in sediment concentration starting at XS 3, indicates that there is an influx of sediment as the model begins. As previously mentioned, the simulated sediment concentration at this section is likely an inaccurate representation of the actual sediment concentration at this cross section.

Figure 11 displays the maximum velocity at each cross section for each event of the simulations for Modification 1. XS 3, 9, 15, 16, 17, and 18 show a large decrease in the maximum velocity compared to other sections. The peak in velocity at the inlet of the channel is consistent with the sediment concentration results.

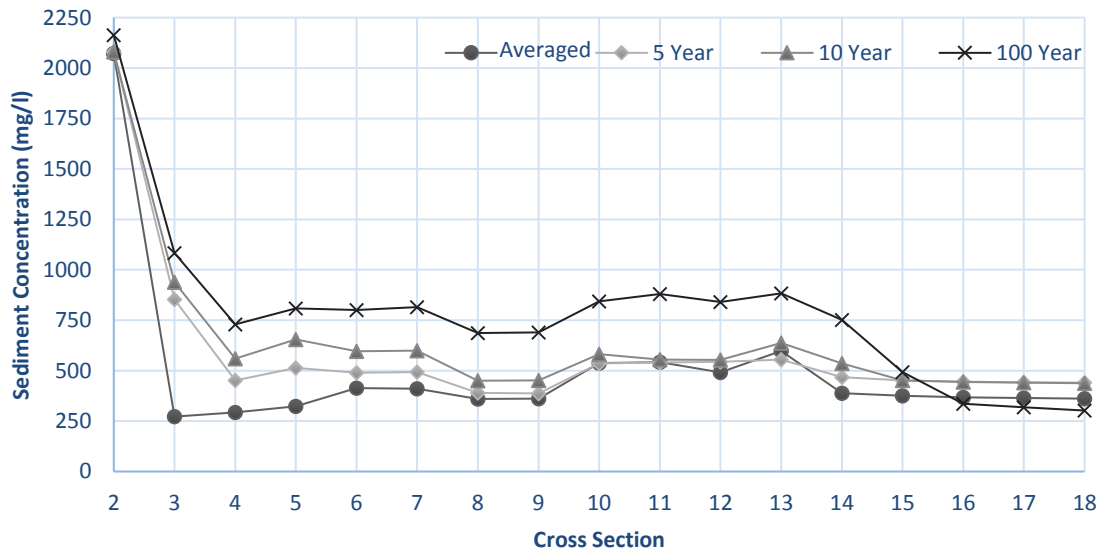


Figure 10: Comparison of Maximum Sediment Concentrations for all Simulations in Modification 1

Figure 12 shows a comparison in the maximum shear stress at each cross section for each event in the simulations for Modification 1. As can be shown from Figure 12, the shear stress is variable throughout the channel. The results show relatively high shear stress at XS 2, followed by a decrease at XS 3; this trend is consistent with the sediment concentration results and velocity results. The pattern for the remainder of the cross sections closely resembles the trend observed in the velocity results, showing that the lowest shear stress occurred at XS 3, 9, 15, 16, 17, and 18.



Figure 11: Comparison of Maximum Velocities for all Simulations in Modification 1

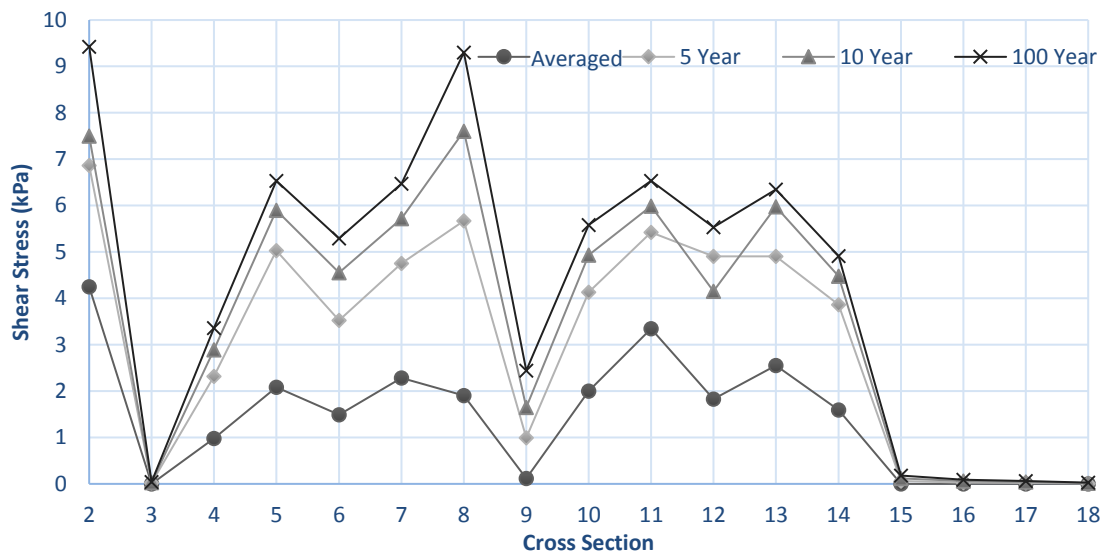


Figure 12: Comparison of Maximum Shear Stresses for all Simulations in Modification 1

5.4 Modification 2

The second modification (Modification 2) increased the distance between cross sections 15 and 16, 16 and 17, and 17 and 18, by 10%, thereby reducing the slope of the channel. Refer to Table 10 in Appendix E for original and modified lengths between cross sections.

The peak sediment concentration occurred at later times in the simulation for all cross sections, except XS 4, where it occurred at $t = 6$ hr of Simulation 9. The mean and maximum velocities for this event were equal at most cross sections. At the cross sections where the mean and maximum velocities differed, there was only a slight change. As mentioned previously, this trend likely occurred due to Event 1 being the averaged event with a constant discharge.

At the upstream cross sections the peak sediment concentration occurred between $t = 10$ hr and $t = 11$ hr for Simulation 10. At XS 10 the peak sediment concentration occurred later in the simulation at $t = 19$ hr; this remained consistent for the majority of the downstream cross sections. This trend demonstrated hysteresis conditions of the sediment transport rates in the stream in response to the event. The maximum velocity occurred at the same time as the peak discharge of the hydrograph. The sections farthest downstream (XS 15, 16, 17, and 18) showed maximum velocities much lower than the remainder of the channel. As previously mentioned, the large decrease in velocity at these sections likely occurred because of the milder slope in these locations.

Simulation 11 indicated that the majority of upstream cross sections showed the peak sediment concentration occurring at the same time as the peak flow of the hydrograph. Hysteresis conditions began to occur later downstream, especially at XS 15, 16, 17, and 18. These sections also showed a large decrease in velocity when compared to the upstream cross sections. This trend likely resulted from the milder slope at these sections. These sections also showed an increase in sediment concentration in comparison to the results observed in the existing channel.

Simulation 12 revealed that the peak sediment concentrations occurred towards the end of the simulation for the majority of cross sections, with the exception of XS 16, 17, and 18. At these cross sections the peak sediment concentration occurred at $t = 4$ hr, demonstrating hysteresis conditions. Similar to previous simulations, the maximum velocity was relatively lower at XS 15, 16, 17 and 18. This was likely due to the milder slope in these locations. A complete summary of the results for each simulation can be found in Tables 18, 19, 20, and 21 in Appendix F.

The largest increase in sediment concentration for simulations in Modification 2 was observed to occur between Event 1 and Event 2, with increases of 3-4% for XS 15, 16, 17, and 18. Between Events 1 and Event 3 there was an increase in sediment concentration between 0.8-3% for XS 15, 16, 17, and 18. The change in sediment concentration for Event 4 from Event 1 showed an increase at XS 15 of 9%, and a decrease of 3% in sediment concentration at XS 16, 17, and 18. The conditions created by Modification 2 responded similarly to the existing channel. All cross sections produced an increase in velocity for larger return periods, with XS 18 resulting in the largest increase of 156% from Event 1 to Event 4. Refer to Table 24 in Appendix F for changes in maximum and sediment concentration for Modification 2.

Figure 13 displays the maximum sediment concentration at each cross section for each event in the simulations for Modification 2. The relatively higher sediment concentrations at the inlet of the model (i.e., XS 2), followed by a sharp decline in sediment concentration starting at XS 3, indicated that there was an influx of sediment as the model begins. As previously mentioned, the simulated sediment concentration at this section was likely an inaccurate representation of the actual sediment concentration at this cross section.

Figure 14 displays the maximum velocity at each cross section for each event in the simulations for Modification 2. A large decrease in the maximum velocity compared to other cross sections was observed at XS 3, 9, 15, 16, 17, and 18. The peak in velocity at the inlet of the channel is consistent with the observed sediment concentration results.

Figure 15 shows a comparison in the maximum shear stress at each cross section for each event in the simulations for Modification 2. As observed in Figure 15, the shear stress is inconsistent throughout the channel. The results reveal high shear stress at XS 2, followed by a sharp decrease at XS 3; this trend is consistent with the sediment concentration results and velocity results. The pattern for the remainder of the cross sections closely resembles the trend observed in the velocity results, showing that the lowest shear stress occurring at XS 3, 9, 15, 16, 17, and 18.

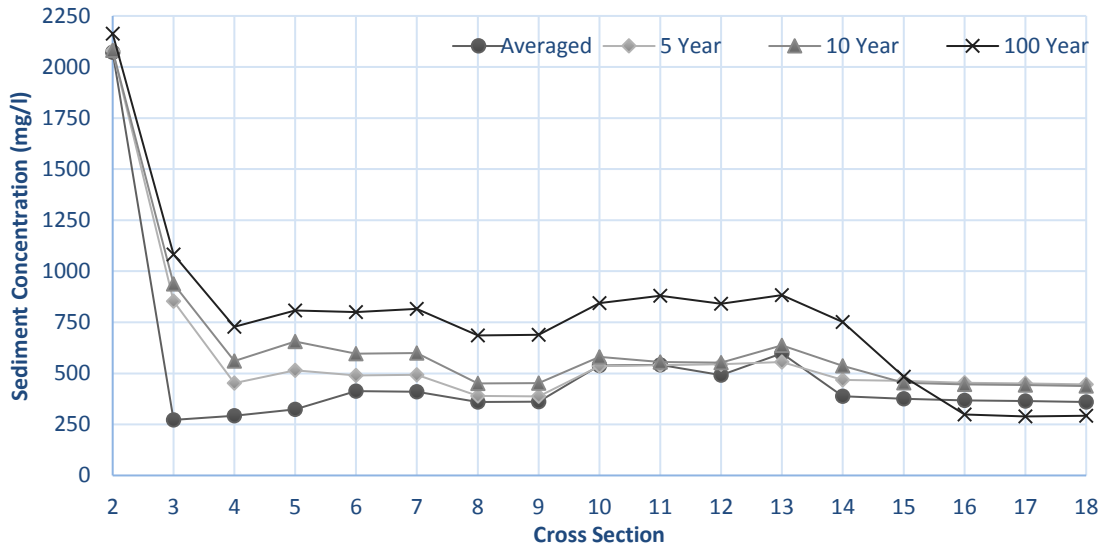


Figure 13: Comparison of Maximum Sediment Concentrations for all Simulations in Modification 2



Figure 14: Comparison of Maximum Velocities for all Simulations in Modification 2

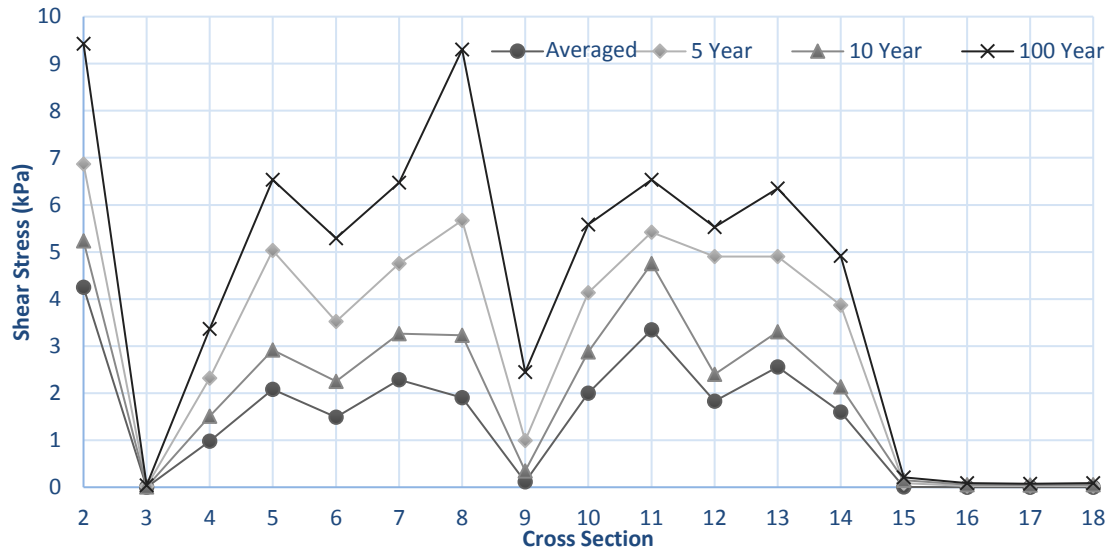


Figure 15: Comparison of Maximum Shear Stresses for all Simulations in Modification 2

Chapter 6

6 Analysis and Discussion

This chapter discusses and analyzes the hydraulic modeling results obtained from modifying Cross Sections 15, 16, 17, and 18 of Spencer Creek. It discusses hysteresis trends in sediment concentrations for each channel modification and the implications of the resulting type of hysteresis observed. It will also discuss the potential for erosion to occur in the channel and ecological considerations.

6.1 Velocity Modeling Results

For all channel configurations, the change in velocity increased as the return period increased (i.e., the lowest velocities were observed in the averaged flow event, and the largest velocities were observed in the 100-year event). As anticipated, the majority of the modified cross sections showed a decrease in maximum velocity for both Modification 1 and Modification 2. Maximum velocities increased with increasing event intensities, with the greatest velocity observed at XS 15 for Event 4 (100-year event) for all channel configurations. The largest change in velocity between channel configurations was for Event 1 (averaged event), while the smallest change, though still significant, was for Event 4 (100-year event) for all channel configurations. Modification 1 resulted in a decrease in maximum velocity for all cross sections for all events. This is to be expected, as the wider the river channel, the lower the stream velocity. Modification 2 had a narrower width and had a milder slope than Modification 1, therefore the velocity in the channel would have to compensate accordingly to accommodate the same discharge through the channel.

As shown in Figure 16, Event 1 showed an overall decrease in maximum velocity following the application of Modification 1. The greatest change occurred at XS 18, with a 51% decrease in maximum velocity from the existing channel. Maximum velocities at XS 15, 16, and 17 decreased by 38%, 13%, and 11%, respectively, with Modification 1. For Modification 2, a 1.6% reduction in maximum velocity was observed at XS 15, while no change was observed at XS 16, 17, or 18. The results for Event 1 imply that for the averaged flow conditions, implementing Modification 1 would result in a significant

decrease in velocity when compared to the existing channel conditions. This is ideal as it will, in theory, reduce the sediment concentration in the channel, and reduce the risk of channel instability issues.

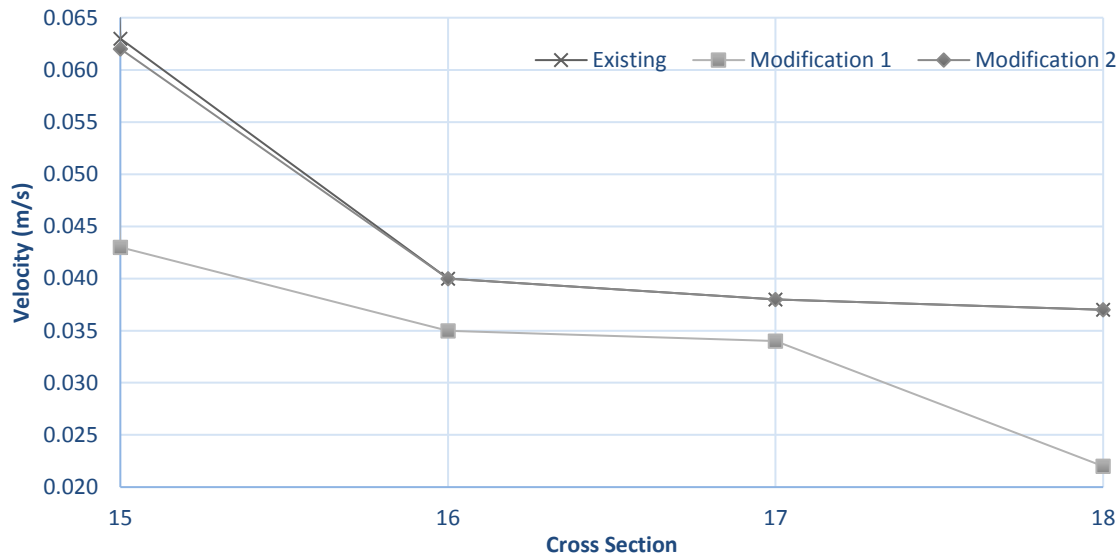


Figure 16: Comparison of Maximum Velocity at XS 15-18 for All Channel Configurations for Event 1

Event 4 resulted in an increase in velocity by 4.2% at XS 15 for Modification 2. From there, the velocity decreased from 0.95-0.33% below the existing channel velocity at XS 16-18, as shown in Figure 17. Modification 1 resulted in a decrease in velocity for all cross sections, with the largest decrease of 40% occurring at XS 18. Similar to Events 1, 2, and 3, the results for Event 4 imply that implementing Modification 1 will provide a decrease in velocity compared to the existing channel. Event 2 had the same decreasing trend as Event 1 for the application of Modification 1. The overall velocity was decreased, with the largest change was at XS 18 (44%). However, applying Modification 2 resulted in an increase in velocity by 0.4% at XS 15, and no change at XS 16, 17, and 18, as shown in Figure 45 in Appendix G. Event 3 had a reduction in velocity for both modification options at all cross sections, see Figure 46 in Appendix G. The greatest velocity change was at XS 18 with a 42% reduction in velocity when applying Modification 1. The changes between the existing channel and Modification 2 were found to be infinitesimal, with only a 0.28 – 0.42% reduction. The results for Event 2 and 3 imply that employing Modification 1 will

significantly decrease the velocity in the channel when compared to the existing channel. The decrease in velocity for these event is ideal as it will assist in reducing the sediment concentration in the channel.

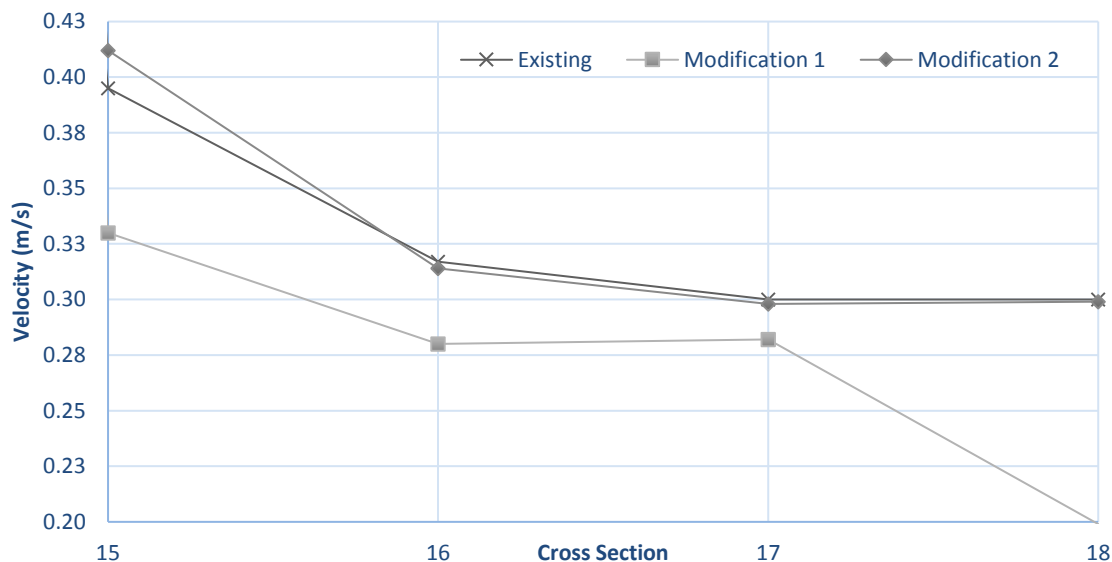


Figure 17: Comparison of Maximum Velocity at XS 15-18 for All Channel Configurations for Event 4

As described above for each event, the greatest change in velocity occurs when applying Modification 1 (channel widening) to Spencer Creek. This option provides the greatest velocity change farthest downstream at XS 18, and the least amount of change at XS 16 and 17. Applying Modification 2 to XS 15, 16, 17, and 18 of Spencer Creek resulted in a slight change in velocity. This indicates that a greater reduction in slope (i.e., increased meandering of the stream) may be required to produce a greater change in velocity. These results suggest that Modification 1 would be a practical option for Spencer Creek to reduce velocity, thereby reducing the sediment concentration and shear stress in the channel. These reductions will likely lead to a more stable channel.

Each cross section responded differently to the modifications as the return period increased. At XS 15, for example, an 18-38% decrease in velocity was observed when Modification 1 was implemented. When implementing Modification 2, Events 1 and 3 resulted in a decrease in velocity of 1.6% and 0.3%, respectively. For this modification, Events 2 and

4 produced an increase in velocity of 0.4% and 4.2%, respectively. XS 15 was the only cross section to demonstrate changes in velocity for Modification 2 for Events 1 and 2. XS 16 showed minimal to no change in velocity after employing Modification 2. Events 1 and 2 showed no change in velocity, and Events 3 and 4 had a 0.4% and 0.95% decrease, respectively, when applying Modification 2. Modification 1 had between a 12-13% decrease in velocity for each event at XS 16. No change in velocity with Modification 2 for Events 1 and 2 was observed at XS 17. Events 3 and 4 showed a slight decrease in velocity by 0.42% and 0.67%, respectively. Modification 1 influenced the velocity least at XS 17, changing it between 6-11%. The velocity at XS 18 was influenced most by Modification 1, decreasing the velocity by 40-50%. Events 3 and 4 for Modification 2 had minimal change, only decreasing 0.3% and 0.4%, respectively. Events 1 and 2 had no change. Analysis of the results at individual cross sections show that Modification 1 resulted in the greatest reduction in velocity, with the greatest reduction occurring at XS 18. These results imply that implementing Modification 1 would be an ideal channel configuration for these sections, as it will likely result in a reduction in sediment concentration at these sections due to the reduction in velocity.

6.2 Sediment Concentration Modeling Results

For all channel configurations, the sediment concentrations increased at XS 10 and 11 for Event 2, XS 7 for Event 3, and XS 16, 17, and 18 for Event 4 when compared to Event 1 (averaged flow conditions). The remainder of the cross sections experienced a decrease in sediment concentration for each event, when compared to Event 1, as expected. Modification 1 resulted in a decrease in sediment concentration at all cross sections for all events when compared to the existing channel. This is likely due to the decrease in velocity at these cross sections, as discussed above. The sediment concentration decreased at most cross sections when implementing Modification 2.

The peak sediment concentration for Event 1 for XS 15, 16, 17, and 18 was observed after five hours of simulation for all channel configurations (i.e., after $t = 5$ hr). Both modification options resulted in a decrease in sediment concentration, as shown in Figure 18, with the largest reduction in sediment concentration being observed at XS 15 when

applying Modification 2 (1.7% reduction). Figure 18 shows only a slight reduction in sediment concentration at XS 15 for Modification 1, then a larger reduction in subsequent cross sections, dipping below sediment concentration results from Modification 2. These results indicate that an increase in width does not influence XS 15, however, a decrease in slope will have a significant impact on this section. With XS 16 being the narrowest section, it is reasonable to assume that this section would be largely influenced by the application of Modification 1. Increasing the width of the channel decreased the velocity in the channel, thereby decreasing the sediment concentration. This trend continued for the remainder of the channel, likely due to the decrease in available sediment for transport.

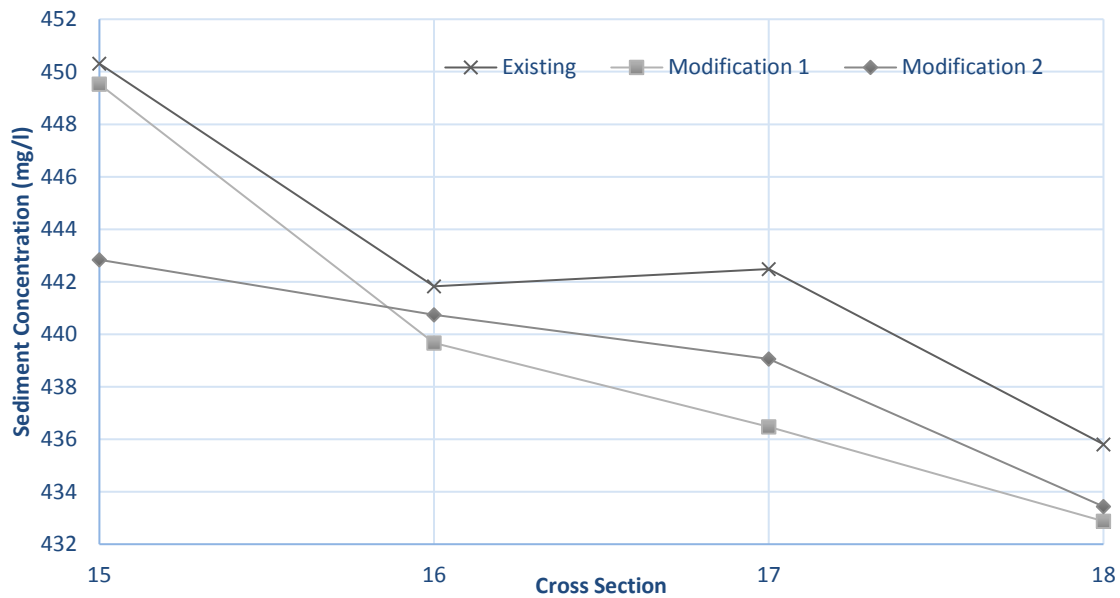


Figure 18: Comparison of Peak Sediment Concentration at XS 15-18 for all Channel Configurations for Event 1

Modifications 1 and 2 resulted in a decrease in peak sediment concentrations for all cross sections during Event 4, as shown in Figure 19. The application of Modification 1 decreased the sediment concentration by 4.7%, 0.4%, 0.5%, and 0.6% for XS 15, 16, 17, and 18, respectively. The largest decrease was at XS 15 for Modification 2, where peak sediment concentration was observed to decrease by 7%. XS 17 and 18 resulted in decreases in peak sediment concentration of 0.08% and 0.62%, respectively, and an increase in sediment concentration of 0.09% at XS 16 for Modification 2. XS 16, 17 and

18 had a large decrease in sediment concentration for Event 4 for all channel configurations. Results for this event are consistent with the reduction in velocity at these cross sections for this event, implying that Modification 2 may provide a suitable channel configuration for events of this magnitude.

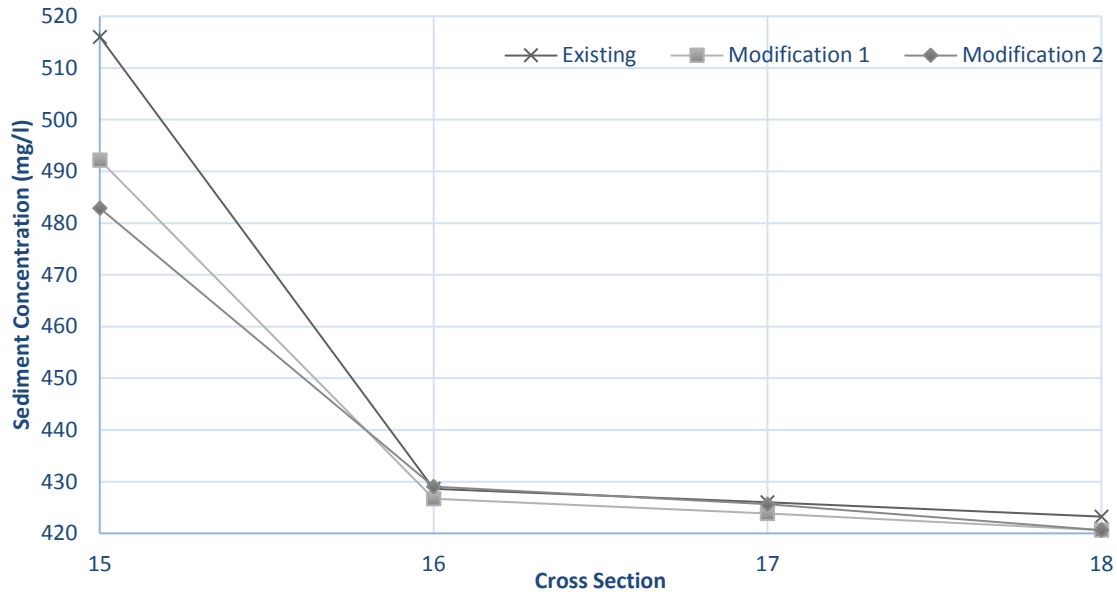


Figure 19: Comparison of Peak Sediment Concentration at XS 15-18 for all Channel Configurations for Event 4

Modification 1 resulted in a decrease in peak sediment concentration at each cross section, with the largest decrease being observed at XS 18 (0.43%) for Event 2. Modification 2, however, produced an increase in peak sediment concentration at all cross sections, with the largest increase occurring at XS 15 (2.2%), see Figure 47 in Appendix G. The increase in peak sediment concentration for this event may be caused by the sediment load at XS 14 carrying over to XS 15, leading to an excess sediment concentration at subsequent cross sections (XS 16, 17, and 18). For Event 3, Modification 1 resulted in a slight decrease in peak sediment concentration for each cross section, see Figure 48 in Appendix G. Modification 2 resulted in a slight decrease at XS 18, but had an increase for XS 15, 16, and 17, respectively. These results for Event 3 suggest that implementing Modification 2 may not be optimal to ensure stream stability for events of this magnitude. The increase in peak sediment concentration at XS 16, 17, and 18 is not ideal for the channel. Modification

1, however, showed a decrease at all cross sections, implying that this channel configuration would be a more appropriate strategy to ensure stream stability for an event of this magnitude.

All channel modifications resulted in a decrease in peak sediment concentration for Event 1 and an increase in peak sediment concentration for Event 2 when applying Modification 2. The remainder of the change in peak sediment concentration for each event varied with cross section. XS 15 had a decrease in peak sediment concentration between 0.7-5% for all events for Modification 1. Modification 2, however, only produced a decrease in sediment concentration for Events 1 and 4, with decreases of 2% and 7%, respectively. Events 2 and 3 produced an increase in peak sediment concentration of 2% and 0.4%, respectively. At XS 16, peak sediment concentration for Event 1 for Modification 1 and Modification 2 decreased by 0.5% and 0.2%, respectively. Modification 1 resulted in a decrease in peak sediment concentration for the remainder of the events between 0.3-0.5%. Modification 2 produced an increased peak sediment concentration for the remainder of events between 0.1-2%. With Modification 1 XS 17 showed an overall decrease between 0.4-1.3% in peak sediment concentration for all events. Events 1 and 4 decreased by 1% and 0.1% for Modification 2, respectively. Events 2 and 3 produced an increase in peak sediment concentration of 1.5% and 0.02%, respectively, for Modification 2. Similar to all cross sections, Modification 1 produced a decrease in peak sediment concentration at XS 18; this concentration decreased between 0.4-0.7%. Event 2 was the only event to have an increase in peak sediment concentration at XS 18, with an increase of 1% when applying Modification 2. The remainder of the events resulted in a decrease in peak sediment concentration between 0.5-1%. These results suggest that implementing Modification 1 would be the most appropriate channel configuration for these sections due to the reduction in sediment concentration, which may lead to a reduction in erosion of the channel.

6.3 Hysteresis of Sediment Transport Rates

The hysteresis observed with the sediment transport rates were analyzed in the present study. This section will discuss the types of hysteresis occurring in Spencer Creek for Events 2, 3, and 4.

Sediment transport hysteresis has been observed in many studies (Ahanger et al., 2009, Klein, 1984). Hysteresis refers to situations where flow depth or sediment concentration have varying values on the rising and falling limb of a discharge hydrograph. This may indicate that an event cannot be described as a single value function, but more accurately described as a loop (Brownlie, 1981). Sediment transport hysteresis can be caused by many factors, such as bed structure, development of bed forms, and transport of sediment (Ahanger et al., 2009).

Williams (1989) classified five types of hysteresis behavior:

1. Clockwise loop;
2. Counter-clockwise loop;
3. Single value line;
4. Single value line with a loop; and
5. Figure eight loop.

The clockwise loop and the counter-clockwise loop are the two most common forms of hysteresis, and have been observed in the modeling results of the present work. A clockwise loop occurs when the sediment peak occurs prior to the discharge peak; this type of hysteresis is observed most often in literature. A counter-clockwise loop has the opposite occurrence, where the sediment peak occurs after the discharge peak (Williams, 1989).

Hysteresis trends can be used as an indicator of changes in sediment availability within a channel. Clockwise hysteresis occurs when there is sediment depletion in a channel. Counterclockwise hysteresis, however, is an indicator of excess sediment in a channel. Excess sediment can be caused by bank collapse (which would result in an influx of sediment being available for transport), or by a sediment source originating from an upstream location (Bača, 2008).

Tables A, B, and C in Appendix D show the time lag between the time to peak of the event hydrograph (T_r) and time to peak of sediment concentration (t_s) for the existing channel, Modification 1, and Modification 2, respectively. Lag time (t_p) is calculated according to:

$$t_p = T_r - t_s \quad (26)$$

Event 2 produced a positive time lag (i.e., clockwise hysteresis) for XS 3, 4, 5, and 13 for all channel configurations, suggesting a lack of sediment supply conditions from the upstream reaches (Hassan et al., 2006). A negative time lag (i.e., counter-clockwise hysteresis) was produced at XS 2, 10, 11, 12, 14, 15, 16, 17, and 18, suggesting excess sediment supply conditions (Hassan et al., 2006). The time to peak of the event hydrograph and the time to peak of the sediment concentration were equal at XS 6, 7, 8, and 9 (i.e., no hysteresis).

For all channel configurations, Event 3 produced clockwise hysteresis at XS 13, and demonstrated counter-clockwise hysteresis at XS 2, 8, 9, 10, 12, 15, 16, 17, and 18. XS 3, 4, 5, 6, 7, 11, and 14 had equivalent time to peak for the event hydrograph and sediment concentration. These results suggest that this event produces excess sediment supply conditions at a majority of the cross sections. As will be further discussed in the following section (Section 6.4), this event resulted in aggradation at the majority of cross sections.

In the existing channel, Event 4 demonstrated clockwise hysteresis at XS 2, 14, 15, 16, 17, and 18, suggesting a lack of sediment supply conditions at these sections (Hassan et al., 2006). Counter-clockwise hysteresis was observed at XS 3, 8, and 9, and time to peak of the event hydrographs was equivalent to the time to peak of sediment concentration at XS 3, 4, 5, 6, 10, 11, 12, and 13.

As previously mentioned, results from the existing channel demonstrated counter-clockwise hysteresis for XS 15, 16, 17, and 18 for Event 2 and Event 3. The time lag for these events was 8 hours for Event 2 and 7 hours for Event 3. Event 4 showed clockwise hysteresis at XS 15, 16, 17, and 18. However, the time lag for XS 15 was only 1 hr, while the time lag for XS 16, 17, and 17 was 12 hr.

Modification 1 produced counter-clockwise hysteresis for XS 15, 16, 17, and 18 for Event 2 and Event 3. The time lag for these events was 8 hours for Event 2 and 7 hours for Event 3. Event 4 produced clockwise hysteresis at XS 16, 17, and 18, with a time lag for 12

hours. XS 15 demonstrated the same time to peak for the event hydrograph and time to peak of sediment concentration.

Modification 2 produced counter-clockwise hysteresis for XS 15, 16, 17, and 18 for Event 2 and Event 3. The time lag for these events was 8 hours for Event 2 and 7 hours for Event 3. Event 4 showed clockwise hysteresis at XS 16, 17, and 18, with a time lag for 12 hours. XS 15 had the same time to peak for the event hydrograph and time to peak of sediment concentration.

The clockwise trend at XS 16, 17, and 18 for Event 4 of all channel configurations demonstrates a potential lack of sediment supply at these cross sections (Hassan et al., 2006). This trend is demonstrated by the decrease in sediment concentration at these cross sections. This trend may also indicate that there is a breakage of an armor layer (Kuhnle, 1992), or may be an indication bed restructuring, leading to lower sediment mobility and sediment transport rate (Mao, 2012).

The counter-clockwise trend shown at XS 15, 16, 17, and 18 for Events 2 and 3 for all channel configurations suggest an increase in sediment supply after a discharge peak has been reached. This trend may also be due to armour or bedform breakage occurring after the peak water discharge (Kuhnle, 1992; Lee et al., 2004). Complete detailed results presenting the time to peak of the hydrograph (t_r), time to peak of the sediment (t_s), and lag time (t_l) are found in Appendix D.

6.4 Aggradation and Degradation Trends

Tables 4, 5, and 6 display which sections are experiencing aggradation (a) or degradation (d) for each event for the existing channel, Modification 1, and Modification 2, respectively. An uppercase notation indicates a change in sediment concentration of 25 mg/l or more of aggradation (A) or degradation (D) is occurring. All channel configurations resulted in the majority of aggradation is occurring at the downstream sections of the channel, at XS 14 through 18. Modification 1 increased the amount of

aggradation occurring for all events, which is to be expected due to the decrease in velocity resulting from this modification. Cross sections experiencing aggradation (i.e., XS 14-18) are largely made up of fine sediments, namely the sections examined for the proposed stream modifications (XS 15, 16, 17, and 18). As a result of aggradation, these sections may be at risk of harming the fish habitat in the channel, as well as the vegetation on the bed and banks of the channel, in addition to impacting stream stability and increasing the potential for erosion.

Table 4: Aggradation and Degradation Trends in Spencer Creek (Existing Channel)

	Cross section (XS)																	
	2	3	4	5	6	7	8	9	10	11	12	13	14	15	16	17	18	
Event 2	a	A	A	A	A	A	d	d	d	d	a	D	a	a	a	a	a	
Event 3	a	A	A	A	A	A	A	A	A	d	A	D	A	a	a	a	a	
Event 4	d	A	A	A	A	A	A	A	A	A	A	A	A	A	d	d	d	

Table 5: Aggradation and Degradation Trends in Spencer Creek (Modification 1)

	Cross section (XS)																	
	2	3	4	5	6	7	8	9	10	11	12	13	14	15	16	17	18	
Event 2	a	A	A	A	A	A	d	d	d	d	a	D	a	a	a	a	a	
Event 3	a	A	A	A	A	A	A	A	A	d	A	D	A	a	a	a	a	
Event 4	A	A	A	A	A	A	A	A	A	A	A	A	A	A	d	d	d	

Table 6: Aggradation and Degradation Trends in Spencer Creek (Modification 2)

	Cross section (XS)																
	2	3	4	5	6	7	8	9	10	11	12	13	14	15	16	17	18
Event 2	a	A	A	A	A	A	d	d	d	d	a	D	a	a	a	a	a
Event 3	a	A	A	A	A	A	A	A	A	d	A	D	A	a	a	a	a
Event 4	A	A	A	A	A	A	A	A	A	A	A	A	A	A	d	d	d

6.5 Shear Stress Modeling Results

All cross sections for all events have an increase in shear stress as the event return period increased. The greatest increases were observed at XS 3, 9, 15, 16, 17, and 18. This trend also occurred with each applied channel modification. These sections have a milder slope than the remainder of the channels, which may be the cause of this trend. The existing channel had the lowest shear stresses at XS 17 and 18 for Event 1. Events 2, 3, and 4, however, had the lowest shear stress at XS 17.

No change in shear stresses for XS 15, 16, 17, and 18 were observed between the existing channel and Modification 2 (see Figure 20) for Event 1. Applying Modification 1, however, resulted in a decrease in shear stresses at XS 15, 17, and 18 of 46%, 33%, and 113%, respectively. The shear stress increased by 7% at XS 16. These results imply that the shear stress is largely influenced by the width and depth ratio of the flow in the channel.

Event 4 was the only event to have changes in shear stress at all cross sections for Modification 2. XS 15 increased by 4%, and XS 16, 17, and 18 decreased between 1-3%. This may be due to the increase in velocity at this section caused by this modification. Applying Modification 1 resulted in a decrease in shear stress at XS 15, 17, and 18, while XS 16 increased by 4% (see Figure 21), likely as a result of the narrowness of this section.

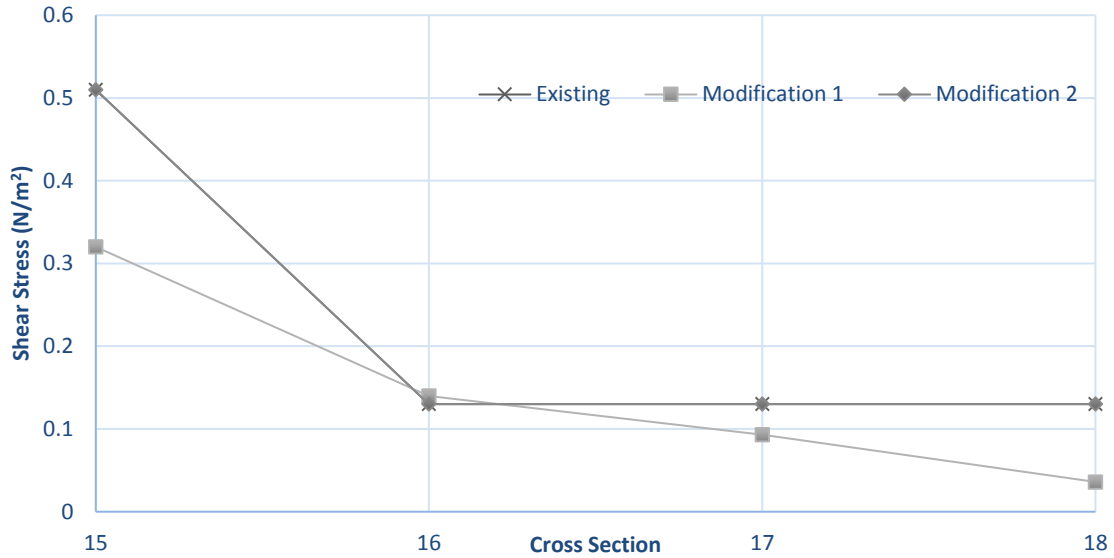


Figure 20: Comparison of Maximum Shear Stress at XS 15-18 for Event 1

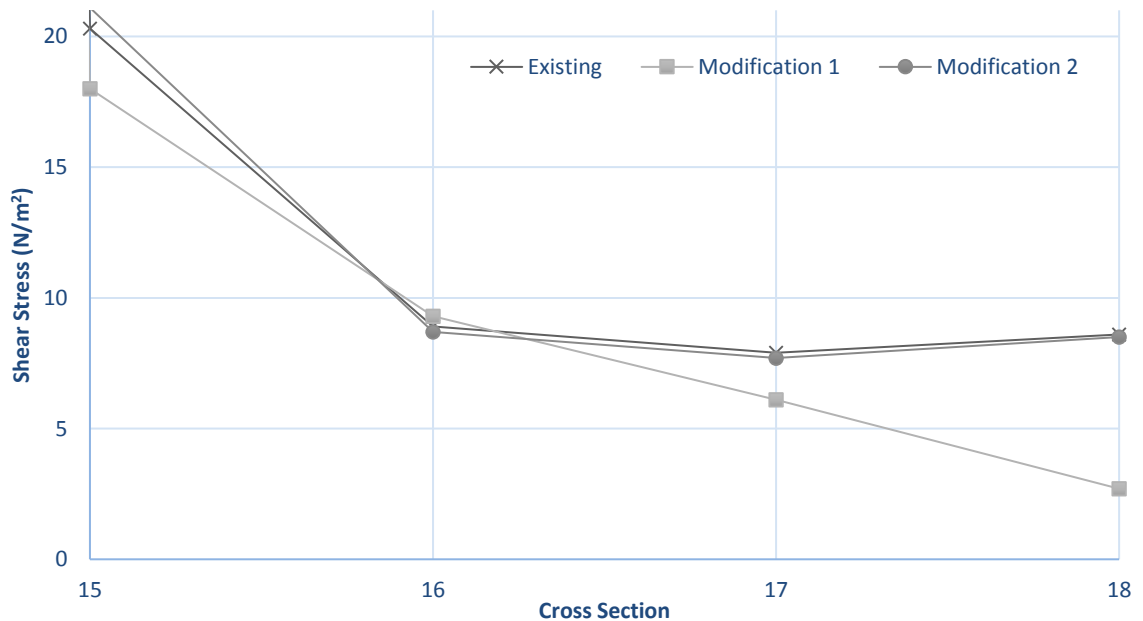


Figure 21: Comparison of Maximum Shear Stress at XS 15-18 for Event 4

As in Event 1, Modification 2 produced no change in shear stress (see Figure 74 in Appendix G) for Event 2. Modification 1 produced an increase in shear stress at XS 16 by 4%. XS 15, 17, and 18 produced decreases in shear stress by 35%, 27%, and 109%, respectively. Modification 2 began to show a change in shear stress from the existing

channel with Event 3. There was no change for XS 18, however, XS 15, 16, and 17 decreased by 1%, 2%, and 2%, respectively. Similar to Event 1 and Event 2, XS 16 had an increased shear stress by 5%. XS 15, 17, and 18 decreased by 27%, 25%, and 104%, respectively (see Figure 75 in Appendix G) when applying Modification 1. Results for this event show the same trends as Events 1 and 2. The reduction in shear stress for these events after applying Modification 1 may be due to the increase in width.

Applying Modification 1 decreased the shear stress at XS 15 for all events between 12-46% compared to the existing channel. Similar to the explanation above, this increase may be due to the increase in width created by this modification. The largest change in shear stress for Modification 1 occurred for Event 1, with a 46% change from the existing channel. Modification 2 did have an influence on XS 15 for Events 1 and 2. Event 3 had a slight decrease in shear stress (1%). Event 4 was the only event to have an increase in shear stress, increasing by 4% when applying Modification 2. Minimal change in shear stress for both modifications was observed in XS 16. Similar to XS 15, XS16 had no change for Events 1 and 2 when applying Modification 2. Modification 2 conditions produced a decrease in shear stress at XS 16 for Events 3 and 4 by 1.8% and 2%, respectively. Modification 1 produced an increase in shear stress between 4-7% for all events at this cross section. The increase under Modification 1 may be influenced by the smaller width of XS 16. For Modification 2, Events 1 and 2 resulted in no change in shear stress and produced a decrease in shear stress by 2% and 3% for Events 3 and 4, respectively. Similar to XS 15, XS 17 produced a decrease in shear stress for all events under the conditions of Modification 1. Event 1 had the largest decrease in shear stress when applying Modification 1, with a decrease of 33%. The largest changes in shear stress was observed at XS 18 when applying Modification 1. This may be due changes at previous sections carrying over the sediment supply to this section. The decreases for Events 1, 2, 3, and 4 were 113%, 109%, 104%, and 104%, respectively. Modification 2, however, had little influence at XS 18. Events 1, 2, and 3 had no change in shear stress, and Event 4 had a small decrease of 1% at this section.

6.6 Bank Erosion

Riverbank erosion is likely to occur in Spencer Creek during high discharge events. Due to the range of sediment sizes present on the stream bed and banks, hydraulic erosion, discussed in Section 2.1.3.3, is likely to occur within the channel. Figure 22 is an example of the exposed banks present in Spencer Creek. See Appendix C for further photographic examples of bank erosion occurring in Spencer Creek.

Sediment in Spencer Creek is largely made up of gravel, sand, silt, and clay. The downstream sections, which were the focus of present research, were mostly made up of sand, silt, and clay. The silt and clay content of XS 15 and 16 are 6% silt and 1% clay. Sand and gravel make up the remainder of the sediment in at these sections, with a 17% sand content and 76% gravel. XS 17 is made up of 1% clay, 31% silt, and the remainder 68% of the sediment is sand. XS 18 is similar to XS 17; however, it has a lesser silt content. The clay content at this section is 1%, silt is 23%, and the remainder 76% of the sediment is sand. XS 15 and 16, which each have silt-clay contents of 7%, will have erosion caused mainly by hydraulic processes. XS 17 and 18, with a silt-clay content of 32% and 24%, respectively, will have erosion caused by hydraulic process and by subaerial processes.



Figure 22: Spencer Creek Exposed Banks

Erosion rates for each event for all channel configurations were calculated using Eq. (19). Event 1 showed negative (-) values for erosion rate of the banks, indicating deposition is occurring at these sections under averaged flow conditions. As can be expected, erosion rates are high during Event 4 due to the large return period of this event. XS 15 has the largest erosion rate during Event 4, which may indicate instability at this section during large events. The erosion rate at XS 15, 16, 17, and 18 for Events 1 and 4 are displayed below in Figures 23 and 24, respectively. Events 2 and 3 are shown in Figures 76 and 77, respectively, in Appendix G.

The erosion rate is decreased with Modification 1 at XS 15, 17, and 18 for all events when compared to the existing channel. Alternatively, an increase in erosion rate when applying this modification for all events was observed at XS 16. The trend in increased erosion rates at XS 16 is consistent with the shear stress results in the channel. Modification 2 showed no change in erosion rates at all cross sections for Events 1 and 2 when compared to the existing channel. Events 3 resulted in a slight decrease in the erosion rate at XS 15, but no

change at XS 16, 17, and 18. All cross sections presented a decrease in erosion rate for Event 4. The trends in erosion rates for Modification 2 are the same as the trends shown in the shear stress results.

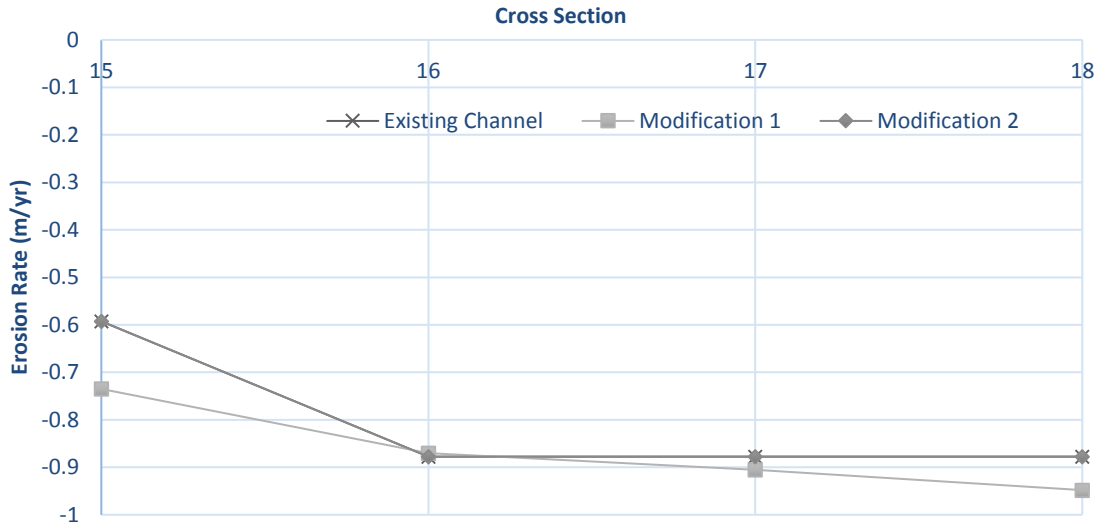


Figure 23: Erosion Rates for Event 1

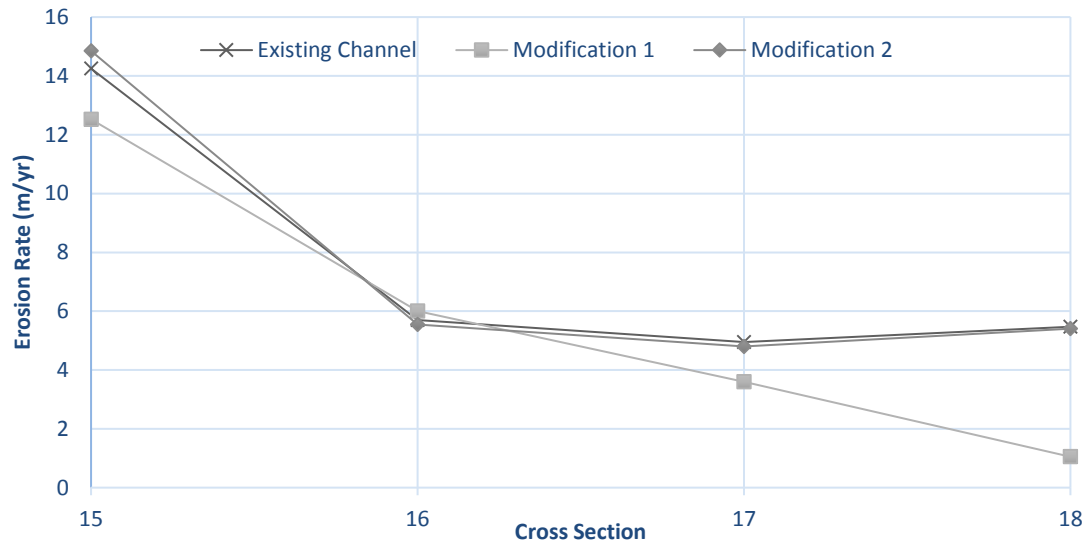


Figure 24: Erosion Rates for Event 4

6.7 Effects of Sediment Concentration on Channel Ecology

Aquatic ecosystems are highly dependent on sediment within a channel for nutrients and the creation of benthic habitats and spawning areas. Without the presence of sediment transport and deposition, new habitats cannot be formed, submerged vegetation cannot thrive, and species native to the area cannot survive due to a lack of nutrients. The effects of sediment deposition and sediment transport concentrations, both ecological and physical, have become more serious as a result of human activities close to river channels. The impact of sedimentation processes in a channel can completely alter the morphology and/or ecology of the channel, if extended over several months or years (Wood and Armitage, 1997; Fondreist Environmental Inc., 2014).

An excess amount of sediment transport and deposition in a channel is considered to be one of the main causes of habitat degradation. Algal blooms, alluvial fans, and deltas can be formed as a result of excess sediment transport and deposition, leading to disruptions in aquatic migrations and cause a buildup of sediment in channel plugs and levees.

While excess sediment transport and deposition can be harmful to a channel, too little sediment transport and deposition can have detrimental effects as well. Nutrient depletion in floodplains and marshes occurring due to a lack of sediment in the channel can diminish vegetation growth. It may also lead to erosion of the banks, causing land loss and destruction of nearshore habitat (Wood and Armitage, 1997; Fondreist Environmental Inc., 2014).

The deposition of fine sediments affects the fish, benthic organisms, and faunal diversity. An increased volume of fine sediment has been shown to cause a reduction in light penetrating the water surface, resulting in a reduction in food available to fish. This has been shown to reduce egg survival and an increase in the number of premature alevins (Reiser and White, 1990). Fine sediments have been shown to smother eggs and affect other benthic organisms in a channel by reducing the available habitat (Wood and Armitage, 1997; Fondreist Environmental Inc., 2014).

Tables 4 through 6 in Section 6.4 display the aggradation/degradation occurring in the channel at each cross section for each modeled event. These tables show large amounts of aggradation occurring along Spencer Creek, namely at the upstream cross sections. The largest amount of aggradation occurs during Event 4 (100-year event) for all channel configurations, indicating that, when exposed to an event of this magnitude, there is potential for the ecology of the channel to be damaged.

Previous research has sought to investigate the effect of sediment concentrations on aquatic ecosystems in rivers and streams (see, e.g., Newcombe and Macdonald 1991; Newcombe and Jensen 1996, Birtwell 1999). Birtwell (1999) estimated that an increase in sediment load of 100 mg/L would present a moderate risk to the aquatic systems, while an increase in sediment load greater than 200 mg/L would result in high risk to aquatic ecosystems. Table 7, below, displays the increase in sediment load from Event 4 (100-year event) to Event 1 (averaged flow event) at XS 15,16, 17, and 18 of Spencer Creek for all modeled channel configurations. In all channel configurations, Event 4 presents an increase in sediment load greater than 100 mg/L at XS 15; an increase which presents a moderate risk to aquatic ecosystems in Spencer Creek according to Birtwell (1999).

A more conservative guideline has been suggested by the Canadian Environmental Quality Guidelines (2002), which suggests that a short-term increase in sediment concentration of 25 mg/L over background levels could have adverse impacts to aquatic ecosystems. Based on this guideline, adverse impacts to aquatic ecosystems could occur at all cross-sections displayed in Table 7 for the 100-year event (Event 4).

In order to protect aquatic ecosystems from these adverse impacts, further meandering of the stream (i.e., a greater reduction in the slope), or a combination of Modification 1 and Modification 2, at these sections of Spencer Creek could reduce the increase in sediment load.

Table 7: Increase in Sediment Load (mg/L)

XS	Existing channel			Modification 1			Modification 2		
	Event 1	Event 4	Increase	Event 1	Event 4	Increase	Event 1	Event 4	Increase
15	376	516	140	375	492	117	376	483	107
16	369	429	60	367	426	59	368	429	61
17	367	426	59	364	424	60	365	426	61
18	364	423	59	361	421	60	360	421	61

Chapter 7

7 Conclusions and Recommendations

7.1 Conclusions

The results of this thesis examined the sediment transport and morphological performance of Lower Spencer Creek in response to rainfall events of various intensities using the mathematical hydraulic model HEC-RAS. Channel modifications were then made to investigate the effect of the various stream geomorphic modifications on hydraulic, geomorphic and ecological functions.

Based on trends and climate change models, climate change is expected to cause an increase in the intensity and frequency of extreme precipitation events for some regions (Teegavarapu, 2012). Populated areas of Southern Canada, including Southern Ontario, where Spencer Creek is located, are vulnerable to these effects of climate change. There is expected to be a shift in rainfall dominated flows leading to increased flood flows, which will affect river hydraulics and morphology. Changes in climate are expected to lead to changes in the magnitude of flooding, thereby affecting streamflow.

Furthermore, the effects of land-use changes are expected to result in changes to runoff and erosion processes within a drainage basin. Small basins will be affected by high-intensity storms, while larger basins will be greatly affected by snowmelt and tropical cyclonic events. With the increased rate of urbanization, small urban streams become more vulnerable to flooding which will affect the surrounding land (Ashmore and Church, 2001).

Models predicting how small, urban streams respond to various rainfall durations and intensities can be useful for future land use planning and river management. When considering alterations to a channel, it is important to consider how the sediment in the channel will be affected, how the flow is altered, and how it will affect erosion of the bed and banks. It is important to understand how the floodplain is affected by rainfall durations and intensities when considering any future construction. Event 4 (100-year event) showed relatively high flow velocities and sediment concentrations in all channel configurations.

Events of large magnitudes, such as this event, are predicted to occur more frequently in the future. Therefore, it is important to understand the channel response to these events to accurately plan for the future (Takemura and Fukoma, 2014).

Results from this thesis provide a framework for analyzing the response of river channel modification options to storm events with varying return periods and durations. This research aids in furthering the understanding of the response of small, urban streams to modifications of the width, length, and slope of the channel, and provides a basis for further research within this field of study.

The present study can assist river engineers and hydrologists in modifying Spencer Creek and other similar urban channels to mitigate flooding and balance erosion and ecological processes. The modeling approach used in this research can aid in modifying upstream reaches that are at risk of flooding due to urbanization and past channelization. Future work can expand this approach to deal with bank erosion, floodplain analysis, and the effect of vegetation on the channel.

7.1.1 Existing Channel

Four events were modeled using the existing channel configuration. Event 1 was a averaged flow event and was used as a benchmark for the remainder of the events. Event 2 had a return period of 5 years and a storm duration of 12 hours. This event showed an increase in velocity, thereby increasing the sediment concentration in the channel. The sediment concentration for this event showed counter-clockwise hysteresis at the majority of cross sections.

Event 3 had a return period of 10 years and a storm duration of 6 hours. Similar to Event 2, this event produced an increase in velocity. The sediment concentration in the channel was increased at most cross sections for this event, however it did not change at Cross Section 17. The majority of cross sections experienced counter-clockwise hysteresis for Event 3.

Event 4 was the longest event (24 hours) and had a return period of 100 years, making this the largest storm event to occur on the creek for the purpose of this research. As with previous events, Event 4 had an increase in velocity. The sediment concentration, however, did not respond as expected. The cross sections farthest downstream (cross sections 16, 17, and 18), experienced an increase in sediment concentration, while the remainder of cross sections had a decrease in sediment concentration. The majority of cross sections had a time to peak of sediment equal to the time to peak for flow, however, three cross sections with a reduction in sediment concentration experienced clockwise hysteresis.

The increase in velocity with increasing return periods suggest that water velocity is largely influenced by the return period of the event. A trend in sediment concentration is not as easily detected. Events 2 and 3 experienced an increase in sediment concentration as the velocity increased, as expected. Event 4, however, produced a reduction in sediment concentration at the downstream end of the channel. These results suggest that event length may be an important factor when determining the effect of large rainfall events on sediment concentration.

7.1.2 Channel Modifications

Two modifications were made to the existing channel to look at how the channel will respond to modifications for the four events simulated on the existing channel. Modification 1 widened the channel by 15%. As expected, this modification decreased the velocity and sediment concentration at cross sections for all four events. The largest change in velocity was observed at Cross Section 18 for all events. This may be due to Cross Section 18 being the widest cross section in the existing channel, therefore it had the largest change in width.

Modification 2 looked at increasing the length of the channel between each cross section by 10%, thereby decreasing the slope of the channel. The velocity decreased for Events 1 and 2 at Cross Section 15, but had no change was observed at the remaining cross sections. As expected, Event 3 had a decrease in velocity at all cross sections. Event 4, however, had a decrease in velocity at Cross Section 16, 17, and 18, but had an increase at Cross Section 15. The sediment concentration changes were not consistent with the velocity changes.

Events 1 and 4 had a decrease in sediment concentration at all cross sections, while Event 2 had an increase in sediment concentration at all cross sections. Event 3 decreased in sediment concentration at Cross Section 18, but increased at Cross Section 15, 16, and 17.

As the event return period increases, the change in velocity between events decreases. The largest change was observed with Event 1, the averaged event, while the smallest change occurred during Event 4, the largest event. These results suggest that with a widened channel (Modification 1), the overall change in velocity becomes less significant as the event increases. As with the existing channel results, no clear trend was observed when looking at the changes in sediment concentration.

The results of the two modification options suggest that Modification 1, widening the channel, would be overall more successful in reducing the velocity and sediment transport within the channel, which can further benefit the ecology of the channel, and reduce the risk of flooding. However, a combination of the two modifications may better reduce the sediment concentration in the channel. Further analysis, however, is recommended as this thesis only looked at three storm events. Recommendations for further research are outlined in the following section.

7.2 Recommendations

It is recommended that future analysis of Spencer Creek look at more event durations and return periods. Only three return periods were simulated for this thesis, however, it would be beneficial to simulate more events, such as a 25-year return period and a 50-year return period, as well as regional storm events (e.g., Hurricane Hazel) to have a better understanding of how the channel responds to these events.

It is also recommended that additional channel designs for Spencer Creek be considered. Two designs were created for this thesis; however, it would be beneficial to look at various widths of the channel, various lengthening options, and various slopes. It is also recommended that a larger section be modified in future studies. This thesis focused on the four sections farthest downstream, however it would be useful incorporate a larger

number cross sections upstream to assess further the changes in velocity and sediment concentration.

Additionally, it is recommended that the effects of vegetation within the channel be analyzed. The present work did not include this component, however, the effects of vegetation on velocity and sediment transport in the channel would be an integral component in finding an appropriate channel modification option for Spencer Creek.

Finally, it is recommended that greater analysis of bank and bed erosion be completed. Due to the one-dimensional hydraulic modeling completed in this study, this could not be accounted for. Use of the two-dimensional component of HEC-RAS (or a similar model) would allow for this type of analysis. An analysis of bed and bank erosion could be performed with the newly added BSTEM tool in the HEC-RAS model.

8 References

- Ackers, P., & White, W. R. (1973). Sediment transport: new approach and analysis. *Journal of the Hydraulics Division*, 99(hy11).
- Ahanger, M. A., Asawa, G. L., & Lone, M. A. (2008). Experimental study of sediment transport hysteresis. *Journal of Hydraulic Research*, 46(5), 628-635.
- Anderson, N. H., & Lehmkuhl, D. M. (1968). Catastrophic drift of insects in a woodland stream. *Ecology*, 49(2), 198-206.
- Ashmore, P., & Church, M. (2001). The Impact of Climate Change on Rivers and River Processes in Canada. Geological Survey of Canada Bulletin 555. *Ottawa, Ontario: Natural Resources Canada*.
- ASTM D422-63. 2007. Standard Test Method for Particle-Size Analysis of Soils, ASTM International, West Conshohocken, PA, 2007.
- Bača, P. (2008). Hysteresis effect in suspended sediment concentration in the Rybárik basin, Slovakia/Effet d'hystérèse dans la concentration des sédiments en suspension dans le bassin versant de Rybárik (Slovaquie). *Hydrological Sciences Journal*, 53(1), 224-235.
- Barnegat Bay Partnership. (2010). Watershed Land Use. Retrieved from: <http://bbp.ocean.edu/pages/147.asp>.
- Bedient, P.B., Huber, W.C., Vieux, B.E. (2008). Hydraulic Analysis. In *Hydrology and Floodplain Analysis* (133-141). Upper Saddle River, NJ: Prentice Hall.

- Bhalla, S. M., Chaudhry, M.H. (1991). Numerical Modeling of Aggradation and Degradation in Alluvial Channels. *Journal of Hydraulic Engineering*, 117(9), 1145-1164.
- Blom, C.W.P.M., and Voesenek, L.A.C.J. 1996. Flooding: The Survival Strategy of Plants. *Trends in Ecology and Evolution*. 11(7): 290-5. DOI: 10.1016/0169-5347(96)10034-3.
- Boyle, S.J., Tsanis, I.K., Kanaroglou, P.S. (1998). Developing geographic information systems for land use impact assessment in flooding conditions. *Journal of Water Resources Planning and Management*, 124(2), 89-98.
- Birtwell, I. K. (1999). *The effects of sediment on fish and their habitat*. Fisheries and Oceans Canada.
- Brunner, G., CEIWR-HEC. 2016. HEC-RAS River Analysis System User's Manual, 5.0 (February).
- Brooker, M.P. (1985). The ecological effects of channelization. *The Geographical Journal*, 151(1), 63-69.
- Brownlie, William R. (1981) Prediction of flow depth and sediment discharge in open channels. W. M. Keck Laboratory of Hydraulics and Water Resources Report, 43A. California Institute of Technology, Pasadena, CA. Brunner, G., CEIWR-HEC. 2016. HEC-RAS River Analysis System User's Manual, 5.0 (February).
- Bukaveckas, P.A. (2007). Effects of Channel Restoration on Water Velocity, Transient Storage, and Nutrient Uptake in a Channelized Stream. *Environmental Science & Technology*, 41(5), 1570-1576.

- Byars, M.S., Kelly, M. (2001). Sediment Transport in Urban Stream Restoration Design. *Wetlands Engineering and River Restoration*.
- Citizens at City Hall. (2012). The Floods of Hamilton (part one). Retrieved from http://www.hamiltoncatch.org/view_article.php?id=1072.
- Citizens at City Hall. (2012). The Floods of Hamilton (part two). Retrieved from http://www.hamiltoncatch.org/view_article.php?id=1073.
- City of Hamilton. June 1, 2015. City of Hamilton Ward Profiles: Ward 9. Retrieved from: <https://www.hamilton.ca/sites/default/files/media/browser/2015-06-01/ward-profiles-2011-ward-9.pdf>
- Copeland, R.R., McComas, D.N., Throne, C.R., Soar, P.J., Jonas, M.M. (2001). *Hydraulic Design of Stream Restoration Projects* (No. ERDC/CHL-TR-01-28). Engineering Research and Development Center Vicksburg MS Coastal and Hydraulics Lab.
- Cruikshank, K. (2009). Retrieved from: <http://www.thecanadianencyclopedia.ca/en/article/dundas/>.
- Darby, S.E., Thorne, C.R. (1996a). Development and testing of riverbank-stability analysis. *Journal of Hydraulic Engineering* 122(8), 443-454.
- de Lima, J.L., Singh, V.P., de Lima, M.I.P. (2003). The influence of storm movement on water erosion: storm direction and velocity effects. *Catena*, 52(1), 39-56.
- DHI Water and Environment. (2004). MIKE21C RIVER MORPHOLOGY: A Short Description.

- Doyle, M.W., Shields, D., Boyd, K.F., Skidmore, P.B., and Dominick, D. (2007). Channel Forming Discharge Selection in River Restoration Design. *Journal of Hydraulic Engineering*, 133(7): 851-857.
- Engelund, F., and Fredsøe, J. (1976). A Sediment Transport Model for Straight Alluvial Channels. *Nordic Hydrology*, 7: 293-306.
- Engelund, F., and Hansen, E. (1972). *A Monograph on Sediment Transport in Alluvial Streams*. Teknisk.
- Fischer-Antze, T., Stoesser, T., Bates, P., and Olsen, N.B.R. (2001). 3D Numerical Modelling of Open Channel Flow with Submerged Vegetation. *Journal of Hydraulic Research*, 39(3): 303-310. DOI: 10.1080/00221680109499833.
- Fondriest Environmental, Inc. (2014, December 5). "Sediment Transport and Deposition". Fundamentals of Environmental Measurements. Retrieved from <http://www.fondriest.com/environmental-measurements/parameters/hydrology/sediment-transport-deposition/>.
- Gainham, C. (2013, April 2). Binbrook Sanitary and Stormwater System Performance (PED12182(a)/PW13016) (Ward 11) (Outstanding Business List Item). Retrieved from http://www2.hamilton.ca/NR/rdonlyres/1880A339-2534-401D-B971-C1DBF03A6359/0/Apr02_7_1_PED12182a_PW13016.pdf.
- Garcia-Navarro, P., Alcrudo, F., Saviron, J.M. (1992). 1-D Open-Channel Flow Simulation Using TVD-McCormack Scheme. *Journal of Hydraulic Engineering*, 118(10): 1359-1372.
- Ghanem, A.M., Steffler, P., Hicks, F, and Katopodis, C. (1996). Two-dimensional hydraulic simulation of physical habitat conditions in flowing streams. *Regulated*

Rivers Research & Management, 12: 185-200. DOI: 10.1002/(sici)1099-1646(199603)12:2/33.0.CO;2-4.

Grillakis, M.G., Koutroulis, A.G., and Tsanis, I.K. (2011). Climate Change Impact on the Hydrology of Spencer Creek Watershed in Southern Ontario, Canada. *Journal of Hydrology*, 409: 1-19.

Haghiabi, A.H., Zaredehdasht. (2012). Evaluation of HEC-RAS Ability in Erosion and Sediment Transport Forecasting. *World Applied Sciences Journal*, 17(11): 1490-1497.

Hamilton Conservation Authority (HCA). (2010). Lower Spencer Creek Watershed Stewardship Action Plan 2010.

Han, Q. (1980). A study on the non-equilibrium transportation of suspended load. In *Proceedings of the International Symposium on River Sedimentation, Beijing, China* (pp. 793-802).

Hassan, M.A., E. Roey, and G. Parker. (2006). Experiments on the effect of hydrograph characteristics on vertical grain sortin gin gravel bed rivers. *Water Resour. Res.* , 42, W09408, DOI: 10.1029/2005WR004707.

Henderson, J.E. (1986). Environmental designs for streambank protection projects. *JAWRA Journal of the American Water Resources Association*, 22(4), 549-558.

Hicks, F.E., and Peacock, T. (2005). Suitability of HEC-RAS for Flood Forecasting. *Canadian Water Resources Journal*, 30(2), 159-174.

Horritt, M., and Bates, P. D. (2002). Evaluation of 1D and 2D numerical models for predicting river flood inundation. *Journal of Hydrology*, 268: 87–99.

- Hunter, N.M., Bates, P.D., Neelz, S., Pender, G., Villanueva, I., Wright, N.G., Liand, D., Falconer, R.A., Lin, B., Waller, S., Crosley, A.J., Masson, D. (2008). Benchmarking 2D hydraulic models for urban flood simulations. *Proceedings of the Institution of Civil Engineers: Water Management*. 161(1). 13-30. ISSN: 1741-7589.
- Hynes, H.B.N. (1968). Further Studies on the Invertebrate Fauna of a Welsh Mountain Stream. *Arch. Hydrobiol*, 65: 360-379.
- Jai, Y., and Wang, S.S.Y. (1999). Numerical Modeling for Channel Flow and Morphological Change Studies. *Journal of Hydraulic Engineering*, 125(9): 924-933.
- Julian, J.P., Torres, R. (2006). Hydraulic erosion of cohesive riverbanks. *Geomorphology*, 76(1), 193-206.
- Julien, P.Y. (2002). *River Mechanics*. Cambridge, United Kingdom: Cambridge University Press.
- JTB Environmental Systems Inc. (2012). Final Report. Fluvial Geomorphic Assessment, Lower Spencer Creek. Cambridge, ON: Beeb, J.
- Kait, C.C., Ghani, Ab., Abdullah, R., Zakaria, N.A. (2008). Sediment Transport Modeling for Kulim River – A Case Study. *Journal of Hydroenvironment Research*, 2(1), 47-59.
- Khattak, M.S., Anwar, F., Saeed, T.U., Sharif, M., Sheraz, K., Ahmed, A. (2016). Floodplain mapping using HEC-RAS and ArcGIS: A case study of Kabul River. *Arabian Journal for Science and Engineering*, 41(4), 1375-1390.

- Klein, M. (1984). Anti clockwise hysteresis in suspended sediment concentration during individual storms. *CATENA*, 11(1): 251-257.
- Kroes, D.E., Hupp, C.R. (2010). The Effects of Channelization on Floodplain Sediment Deposition and Subsidence Along the Pokomoke River, Matyland1. *JAWRA Journal of the American Water Resources Association*, 46(4), 686-699.
- Kuhnle, R.A. (1992). Bed load transport during rising and falling stages on two small streams. *Earth Surface Processes and Landforms*, 17: 191-197. DOI: 10.1002/esp.3290170206.
- Leandro, J., Chen, A. S., Djordjević, S., & Savić, D. A. (2009). Comparison of 1D/1D and 1D/2D coupled (sewer/surface) hydraulic models for urban flood simulation. *Journal of hydraulic engineering*, 135(6), 495-504.
- Lee, K.T., Liu, Y-L., Cheng, K-H. (2004). Experimental investigation of bedload transport processes under unsteady flow conditions. *Hydrological Processes*, 18: 2439-2454. DOI: 10.1002/hyp.1473.
- Leinter, R. (2014, October 10). \$1M Plan to Respire Spence Creek Could Help Protect Turtle Population. *Hamilton Spectator*. Retrieved from <http://www.thespec.com/news-story/4908520--1m-plan-to-restore-spencer-creek-could-help-protect-turtle-population/>.
- Maitland, P.S., and Penney, M.M. (1967). The Ecology of the Sumuliidae in a Scottish River. *The Journal of Animal Ecology*, 36: 179-206.
- Mandych, A.F. (2009). Floods and Soil Erosion. In M.C. Donoso *Water Interactions with Energy, Environment, Food and Agriculture – Volume II*. Oxford, United Kingdom: Eolss Publishers Co Ltd.

- Mao, L. (2012). The effects of hydrographs on bed load transport and bed sediment spatial arrangements. *Journal of Geophysical Research – Earth Surfaces*, 117: F03024. DOI: 10.1029/2012JF002428.
- Marsh, J.H. (2012, August 20). Hurricane Hazel. Retrieved from <http://www.thecanadianencyclopedia.ca/en/article/hurricane-hazel/>.
- Meyer-Peter, E., and Müller, R. (1948). Formulas for Bedload Transport. *Association for Hydraulic Research, Second Congress (Stockholm)*: 39-65.
- Ministry of Transportation. (2013). IDF Curve Look Up. Retrieved from http://www.mto.gov.on.ca/IDF_Curves/results_out.shtml?coords=43.265181,-79.964061.
- Mohammad, M.E., Al-Ansari, N., Issa, I.A., Knutsson, S. (2016). Sediment in Mosul Dam Reservoir Using the HEC-RAS Model. *Lakes and Reservoirs: Research and Management*, 21: 235-244.
- Molles, M.C. (1980). Recovery of Stream Invertebrates from Disturbance Resulting from a Flash Flood. *Bull Ecol Soc Am*, 61: 96.
- Newcombe, C. P., & Jensen, J. O. (1996). Channel suspended sediment and fisheries: a synthesis for quantitative assessment of risk and impact. *North American Journal of Fisheries Management*, 16(4), 693-727.
- Newcombe, C. P., & MacDonald, D. D. (1991). Effects of suspended sediments on aquatic ecosystems. *North American journal of fisheries management*, 11(1), 72-82.

- News Staff. (2014). Flooding Closes 407 at Appleby Line and QEW at Guelph Line. Retrieved from <http://www.680news.com/2014/08/04/flooding-closes-wb-407-at-appleby-line-qew-at-guelph-line/>.
- Ponnamperuma, F.N. (1984). Chapter 2: Effects of Flooding on Soils. In T.T. Kozlowski (Ed.), *Flooding and Plant Growth* (pp. 10-44). Orlando, FL: Academic Press.
- Rae, J.G. (1987). The Effects of Flooding and Sediments on Structure of a Stream Midge Assemblage. *Hydrobiologica*, 144: 3-10.
- Römken, M.J., Helming, K., Prasad, S.N. (2002). Soil erosion under different rainfall intensities, surface roughness, and soil water regimes. *Catena*, 46(2), 103-123.
- Scheckenberger, R. (2010). The Day the Rains Came. Retrieved from <http://www.canadianconsultingengineer.com/features/the-day-the-rains-came/>.
- Schwendel, A.C., Death, R.G., Fuller, I.C. 2010. The Assessment of Sear Stress and Bed Stability in Stream Ecology. *Freshwater Biology*, 55, 261-281. DOI: 10.1111/j.1365-2427.2009.02293.x
- Shelley, J., Gibson, S., Williams, A. (2016). Unsteady Flow and Sediment Modeling in a Large Reservoir Using HEC-RAS 5.0.
- Shields Jr, F.D., Copeland, R.R., Klingeman, P.C., Doyle, M.W., Simon, A. (2003). Design for Stream Restoration. *Journal of Hydraulic Engineering*, 129(8), 575-584.
- Shields Jr, F.D., Palermo, M.R. (1982). *Assessment of Environmental Considerations in the Design and Construction of Waterway Projects* (No. WES/TR/E-82-8). Army Engineer Waterways Experiment Station Vicksburg Ms Environmental Lab.

- Sholtes, J.S., Doyle, M.W. (2011). Effects of Channel Restoration on Flood Wave Attenuation. *Journal of Hydraulic Engineering*. 137 (2): 196-208
- Soar, P.J., Throne, C.R. (2001). *Channel Restoration for meandering rivers* (No. ERDC/CHL-CR-01-1). Engineer Research And Development Center Vicksburg Ms Coastal And Hydraulics Lab, 2001.
- Statistics Canada. (2011). Census Metropolitain Area of Hamilton, Ontario. Retrieved from <https://www12.statcan.gc.ca/census-recensement/2011/as-sa/fogs-spg/Facts-cma-eng.cfm?LANG=Eng&GK=CMA&GC=537>
- Steward, T., Sivakugan, N., Shukla, S.K., Das, B.M. (2010). Taylor's slope stability charts revised. *International Journal of Geomatics*, 11(4), 348-352.
- Strum, T.W. (2001). *Open Channel Hydraulics*. Boston, MA: McGraw-Hill.
- Takemura, Y., Fukuoka, S. (2014). Effects of channel shape on propagation characteristics of flood flows through a valley. *Journal of Flood Risk Development*, 7: 152-158. DOI: 10.1111/jfr3.12035.
- Taylor, D.W. (1937). *Stability of Earth Slopes* (pp. 1925-1940). Boston: Boston Society of Civil Engineers.
- Teegavarapu, R.S. (2012). *Floods in a changing climate: extreme precipitation*. Cambridge University Press.
- Toffaletti, F.B. (1969). Definitive Computations of Sand Discharge in River. *A.S.C.E., Hydraulics Division Journal*, 95(HY1): 225-246.
- van Rijn, L.C. (1984a, October). Part I: Bed Load Transport. *Journal of Hydraulic Engineering*, 110: 10.

- van Rijn, L.C. (1984b, November). Part II: Suspended Load Transport. *Journal of Hydraulic Engineering*, 110: 11.
- van Dongen, M. (2012). City to map flooding hotspots. Retrieved from <http://www.thespec.com/news-story/2210089-city-to-map-flooding-hot-spots/>.
- van Dongen, M. (2013). Why Storm Flooding is Inevitable in Hamilton. Retrieved from <http://www.thespec.com/news-story/3885049-why-storm-flooding-is-inevitable-in-hamilton/>.
- Waters, T.F. (1972). The Drift of Stream Insects. *Annual Review of Entomology*, 17: 253-272.
- Watson, C.C., Biedenharn, D.S., Scott, S.H. (1999). *Channel rehabilitation: Processes, design and implementation*. Army Engineer Waterways Experiment Station Vicksburg MS Hydraulics Lab.
- Walters, K.D., Cokljat, D. (2008). A Three-Equation Eddy-Viscosity Model for Reynolds-Averaged Navier-Stokes Simulations of Transitional Flow. *Journal of Fluids Engineering*, 130.
- Wiberg, P.L., and Smith, J.D. (1991). Velocity Distribution and Bed Roughness in High-Gradient Streams. *Water Resources Research*, 27, 825-838.
- Wilcock, P.R., and Crowe, J.C. (2003). Surface-based Transport Model for Mixed-Size Sediment. *Journal of Hydraulic Engineering*, 129: 120-128. DOI: 10.1061/(ASCE)0733-9429(2003)129:2(120).
- Williams, G.P. (1989). Sediment concentration versus water discharge during single hydraulic events in rivers. *Journal of Hydrology*, 111(1-4), 89-106.

- Williams, R. (2014). FLASH FLOOD: Months of rain flood Burlington in mere hours. Retrieved from <http://www.thespec.com/news-story/4733800-flash-flood-months-of-rain-flood-burlington-in-mere-hours/>.
- Wood, P.J., Armitage, P.D. (1997). Biological Effects of Fine Sediment in the Lotic Environment. *Environmental Management*, 21 (2): 203-217.
- Wu, W., Vieira, D.A., and Wang, S.S.Y. (2004). One-dimensional numerical model for nonuniform sediment transport under unsteady flows in channel networks. *Journal of Hydraulic Engineering*. 130(9): 914-923. Doi: 10.1061/(ASCE)0733-9429(2004), 130: 9(914).
- Yang, C.T. (1972). Unit Stream Power and Sediment Transport. *Journal of Hydraulic Engineering*, ASCE, 98(HY10): 1805-1826.
- Zhou, J., Lin, B. (1998). One-dimensional mathematical model for suspended sediment by lateral integration. *Journal of Hydraulic Engineering*, 124(7), 712-717.

Appendix A: Event Hydrographs

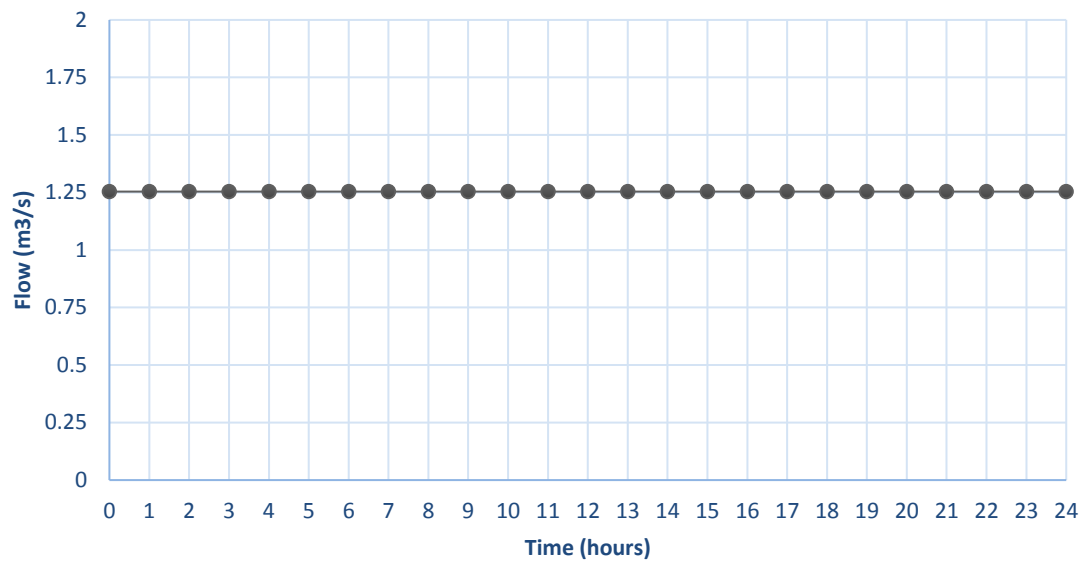


Figure 25: Event 1 Hydrograph

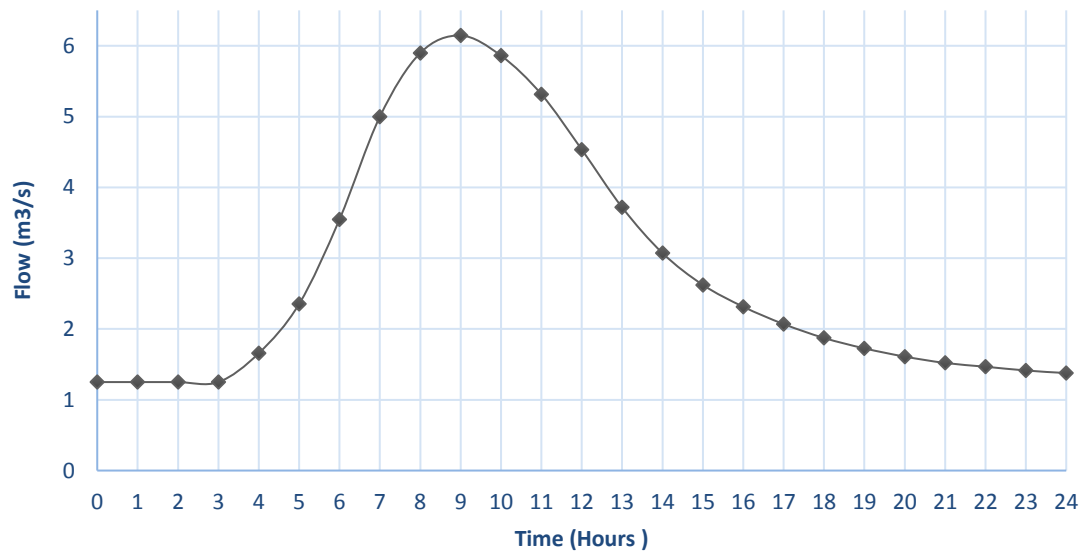


Figure 26: Event 2 Hydrograph

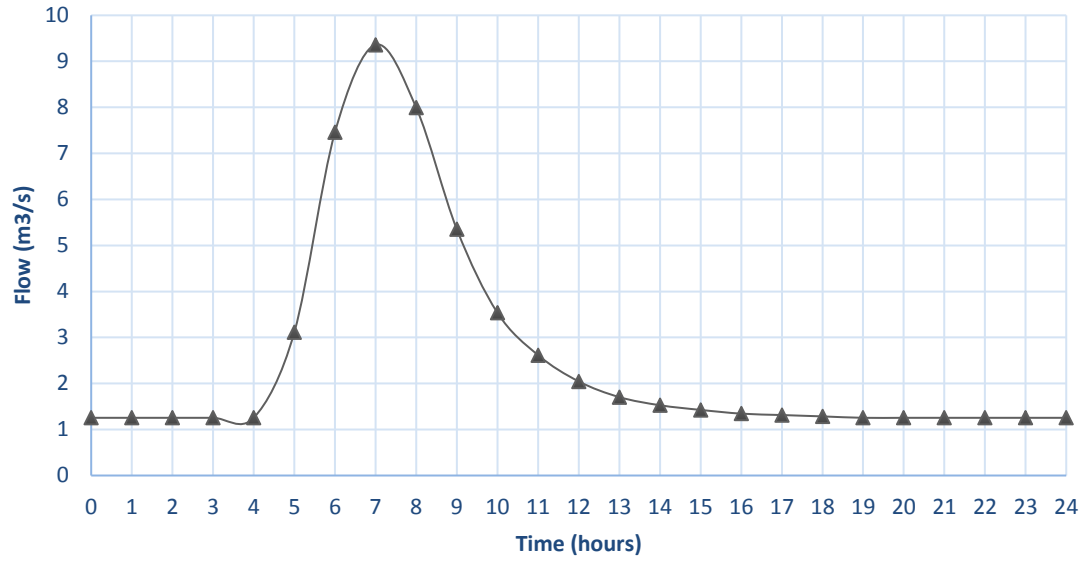


Figure 27: Event 3 Hydrograph

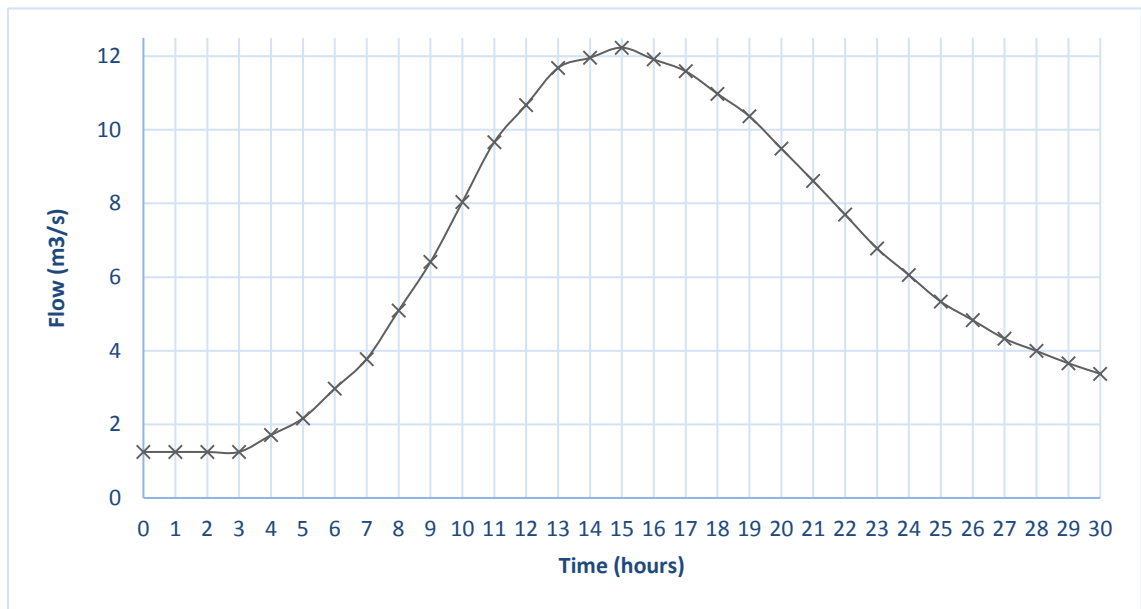


Figure 28: Event 4 Hydrograph

Appendix B: Sediment Distribution

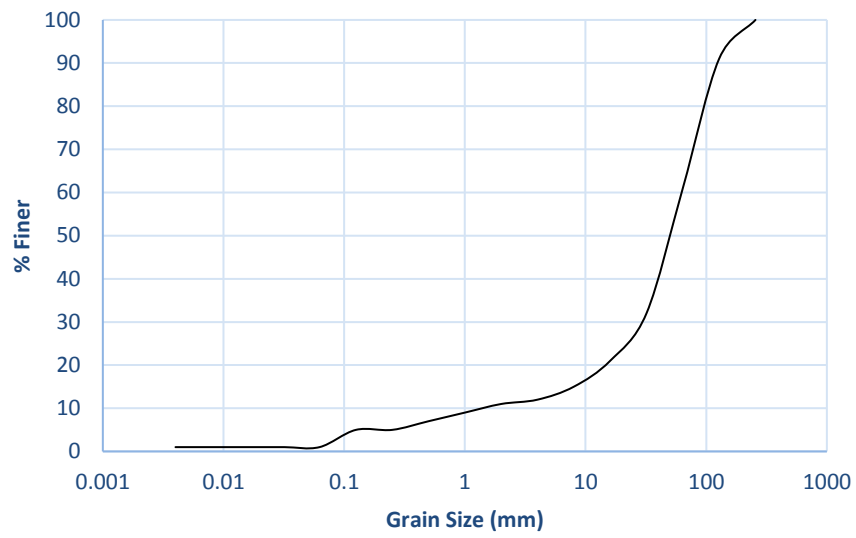


Figure 29: Cross Section 2 Sediment % Finer

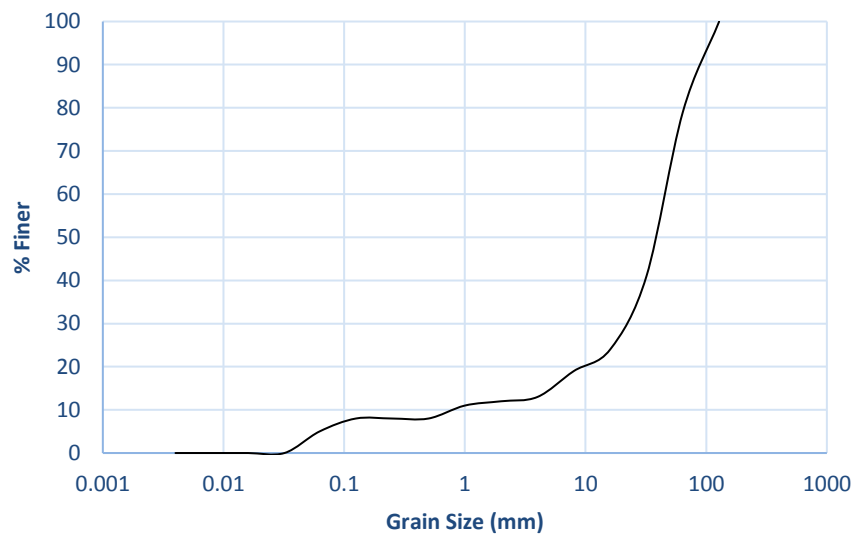


Figure 30: Cross Section 3 Sediment % Finer

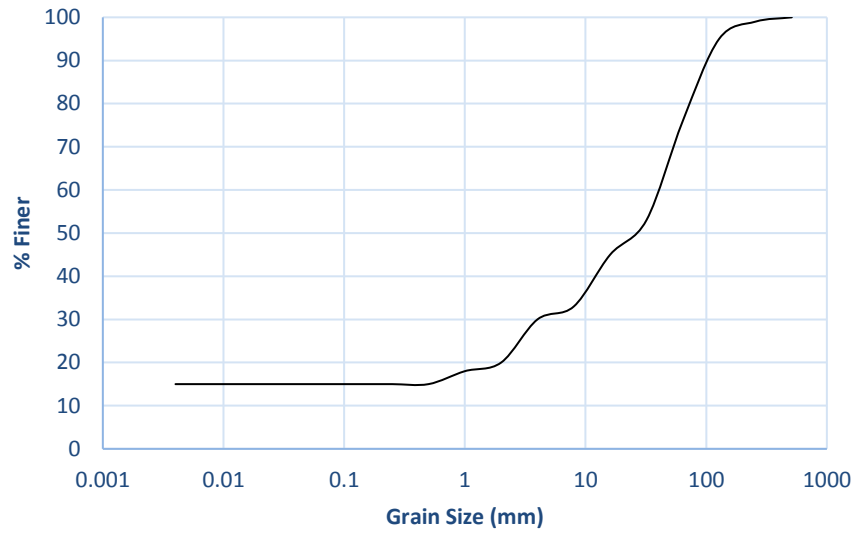


Figure 31: Cross Section 4 Sediment % Finer

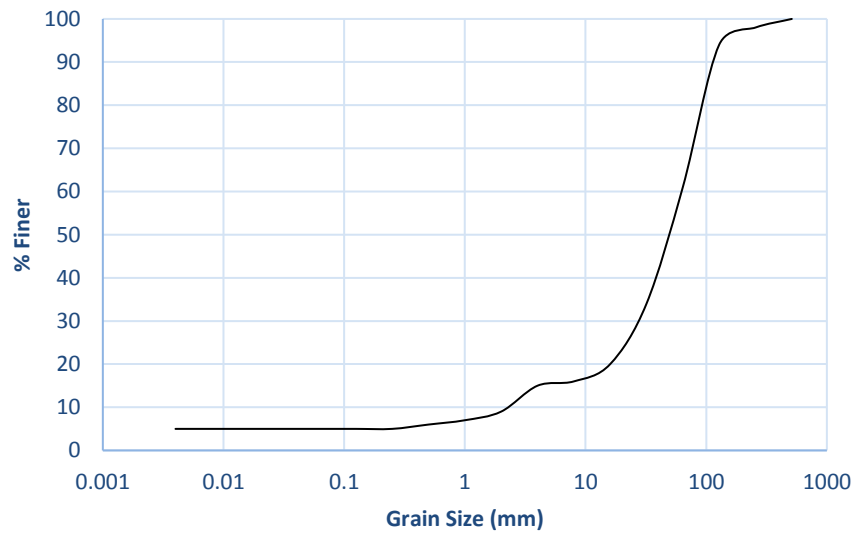


Figure 32: Cross Section 5 Sediment % Finer

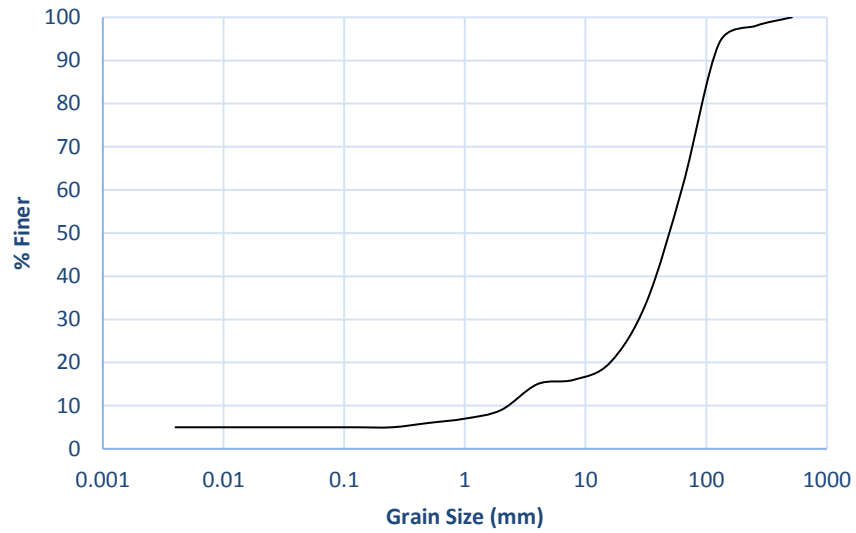


Figure 33: Cross Section 6 Sediment % Finer

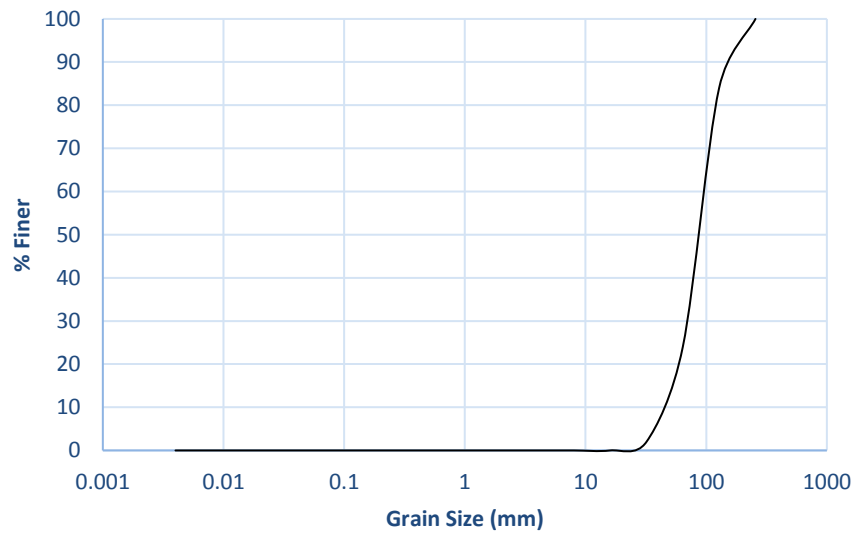


Figure 34: Cross Section 7 Sediment % Finer

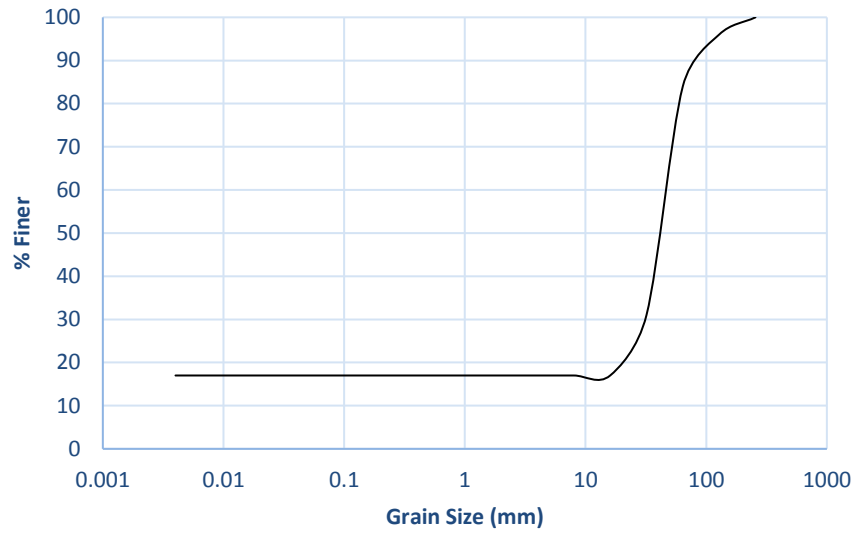


Figure 35: Cross Section 8 Sediment % Finer

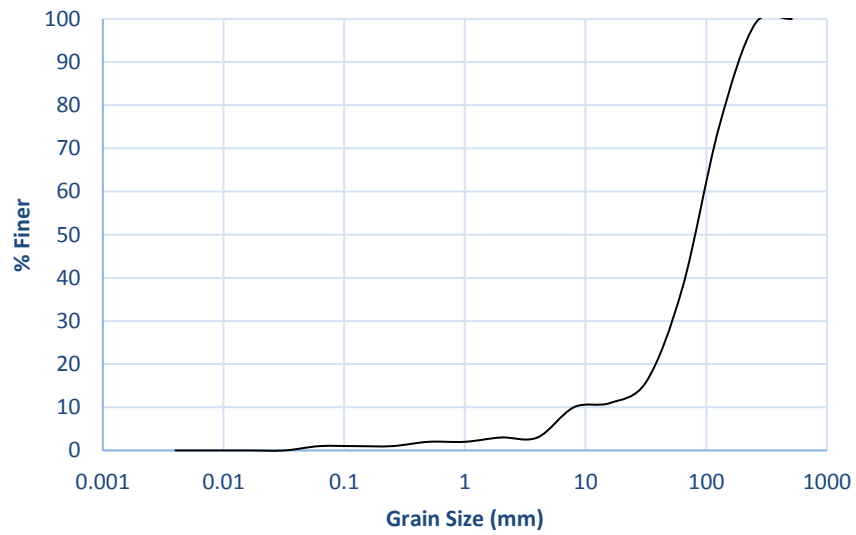


Figure 36: Cross Section 9 Sediment % Finer

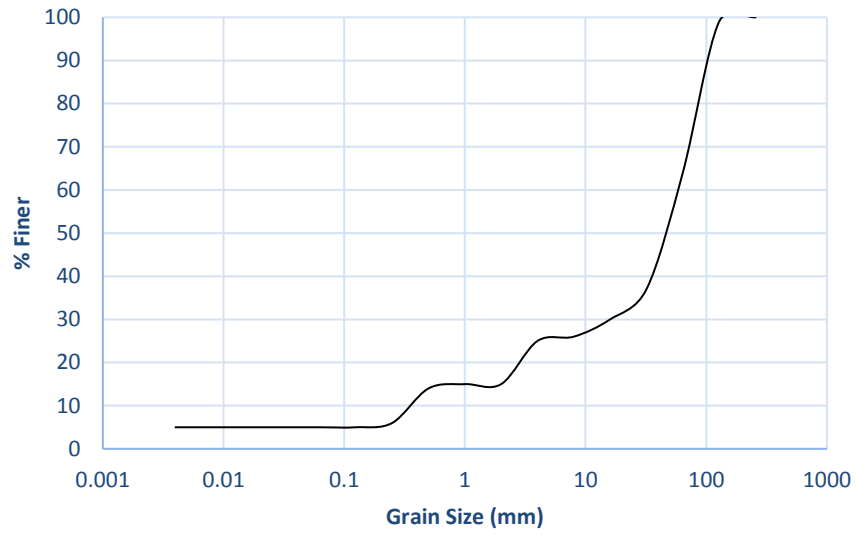


Figure 37: Cross Section 10 Sediment % Finer

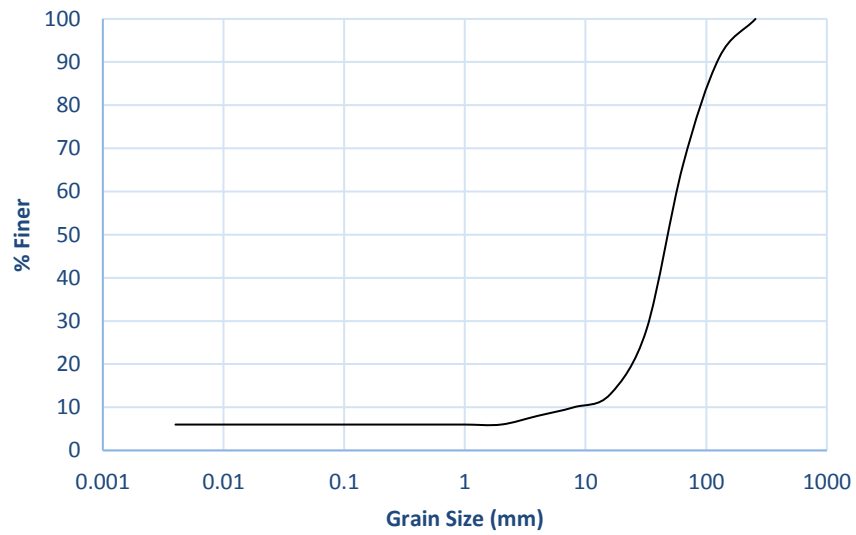


Figure 38: Cross Section 11 Sediment % Finer

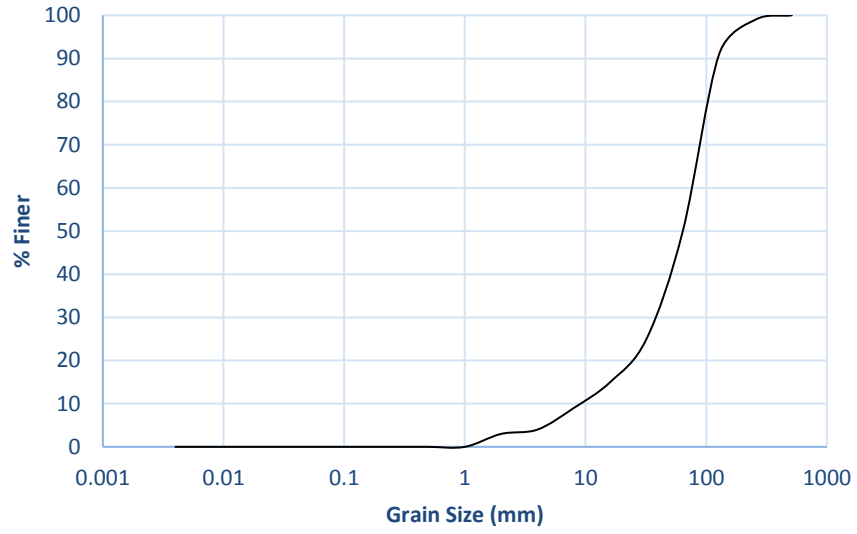


Figure 39: Cross Section 12 Sediment % Finer

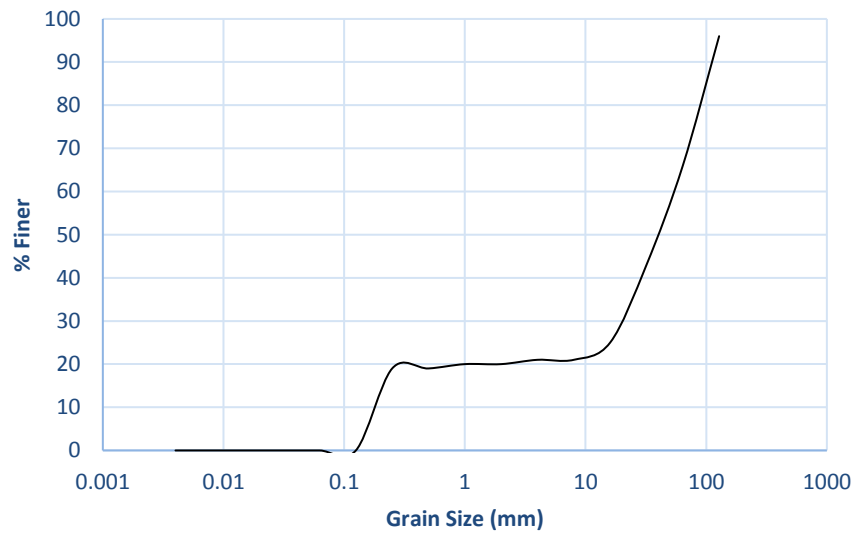


Figure 40: Cross Section 13 Sediment % Finer

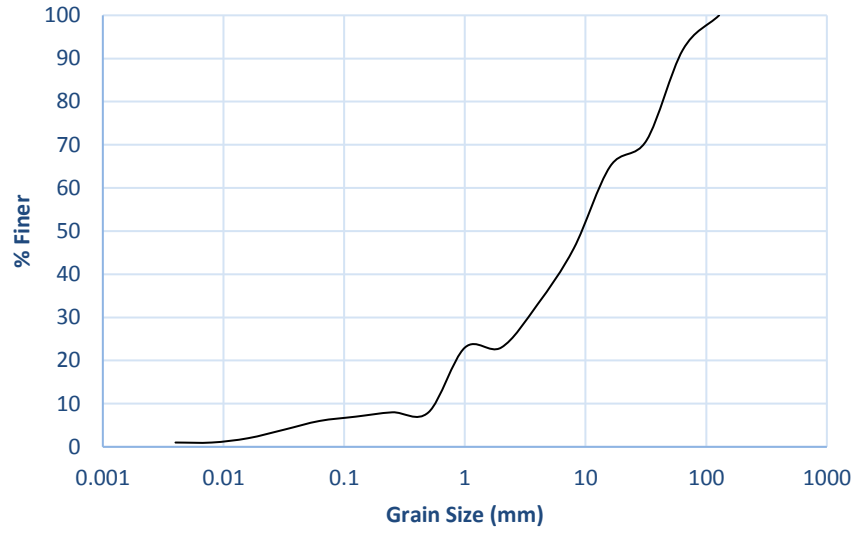


Figure 41: Cross Section 14 Sediment % Finer

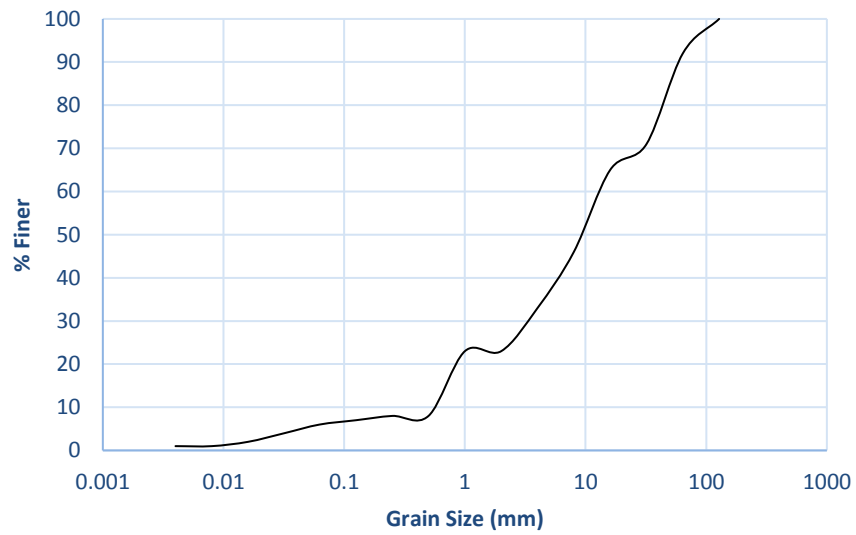


Figure 42: Cross Section 15 Sediment % Finer

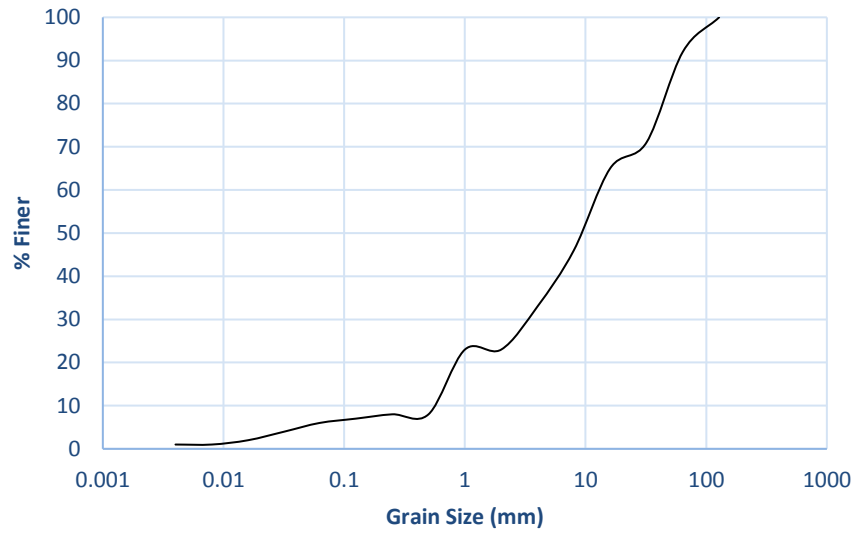


Figure 43: Cross Section 16 Sediment % Finer

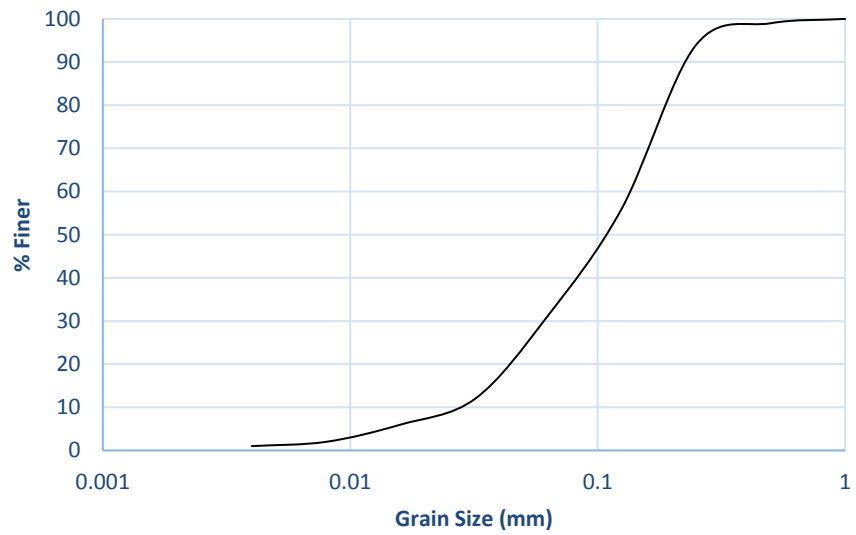


Figure 44: Cross Section 17 Sediment % Finer

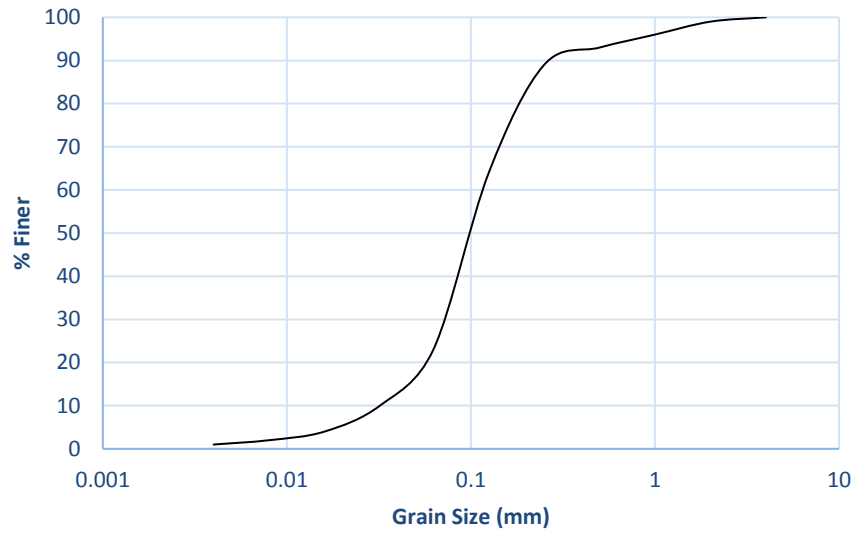


Figure 45: Cross Section 18 Sediment % Finer

Appendix C: Pictures of Spencer Creek



Figure 46: Spencer Creek downstream showing bank erosion



Figure 47: Spencer Creek Cross Section 18



Figure 48: Spencer Creek showing dead ash trees and bank erosion downstream



Figure 49: Spencer Creek Cross Section 2



Figure 50: Spencer Creek Bank Stabilization Structure



Figure 51: Spencer Creek Exposed Tree Roots



Figure 52: Spencer Creek Exposed Banks

Appendix D: Lag Time Showing Hysteresis Conditions

Table 8: Complete Time to Peak and Lag Time Showing Hysteresis Conditions for the Existing Channel

XS	Event 2			Event 3			Event 4		
	t _r (hr)	t _s (hr)	t _i (hr)	t _r (hr)	t _s (hr)	t _i (hr)	t _r (hr)	t _s (hr)	t _i (hr)
2	11	23	-12	8	20	-12	16	4	12
3	11	10	1	8	8	0	16	17	-1
4	11	10	1	8	8	0	16	16	0
5	11	10	1	8	8	0	16	16	0
6	11	11	0	8	8	0	16	16	0
7	11	11	0	8	8	0	16	16	0
8	11	11	0	8	9	-1	16	17	-1
9	11	11	0	8	9	-1	16	17	-1
10	11	19	-8	8	10	-2	16	16	0
11	11	19	-8	8	8	0	16	16	0
12	11	19	-8	8	15	-7	16	16	0
13	11	4	7	8	4	4	16	16	0
14	11	19	-8	8	8	0	16	14	2
15	11	19	-8	8	15	-7	16	15	1
16	11	19	-8	8	15	-7	16	4	12
17	11	19	-8	8	15	-7	16	4	12
18	11	19	-8	8	15	-7	16	4	12

Table 9: Complete Time to Peak and Lag Time Showing Hysteresis Conditions for Modification 1

XS	Event 2			Event 3			Event 4		
	t _r (hr)	t _s (hr)	t _l (hr)	t _r (hr)	t _s (hr)	t _l (hr)	t _r (hr)	t _s (hr)	t _l (hr)
2	11	23	-12	8	20	-12	16	4	12
3	11	10	1	8	8	0	16	17	-1
4	11	10	1	8	8	0	16	16	0
5	11	10	1	8	8	0	16	16	0
6	11	11	0	8	8	0	16	16	0
7	11	11	0	8	8	0	16	16	0
8	11	11	0	8	9	-1	16	17	-1
9	11	11	0	8	9	-1	16	17	-1
10	11	19	-8	8	10	-2	16	16	0
11	11	19	-8	8	8	0	16	16	0
12	11	19	-8	8	15	-7	16	16	0
13	11	4	7	8	4	4	16	16	0
14	11	19	-8	8	8	0	16	14	2
15	11	19	-8	8	15	-7	16	16	0
16	11	19	-8	8	15	-7	16	4	12
17	11	19	-8	8	15	-7	16	4	12
18	11	19	-8	8	15	-7	16	4	12

Table 10: Complete Time to Peak and Lag Time Showing Hysteresis Conditions for Modification 2

XS	Event 2			Event 3			Event 4		
	t _r (hr)	t _s (hr)	t _l (hr)	t _r (hr)	t _s (hr)	t _l (hr)	t _r (hr)	t _s (hr)	t _l (hr)
2	11	23	-12	8	20	-12	16	4	12
3	11	10	1	8	8	0	16	17	-1
4	11	10	1	8	8	0	16	16	0
5	11	10	1	8	8	0	16	16	0
6	11	11	0	8	8	0	16	16	0
7	11	11	0	8	8	0	16	16	0
8	11	11	0	8	9	-1	16	17	-1
9	11	11	0	8	9	-1	16	17	-1
10	11	19	-8	8	10	-2	16	16	0
11	11	19	-8	8	8	0	16	16	0
12	11	19	-8	8	15	-7	16	16	0
13	11	4	7	8	4	4	16	16	0
14	11	19	-8	8	8	0	16	14	2
15	11	21	-10	8	15	-7	16	16	0
16	11	21	-10	8	15	-7	16	4	12
17	11	21	-10	8	15	-7	16	4	12
18	11	21	-10	8	15	-7	16	4	12

Appendix E: Cross Sectional Profiles of Spencer Creek

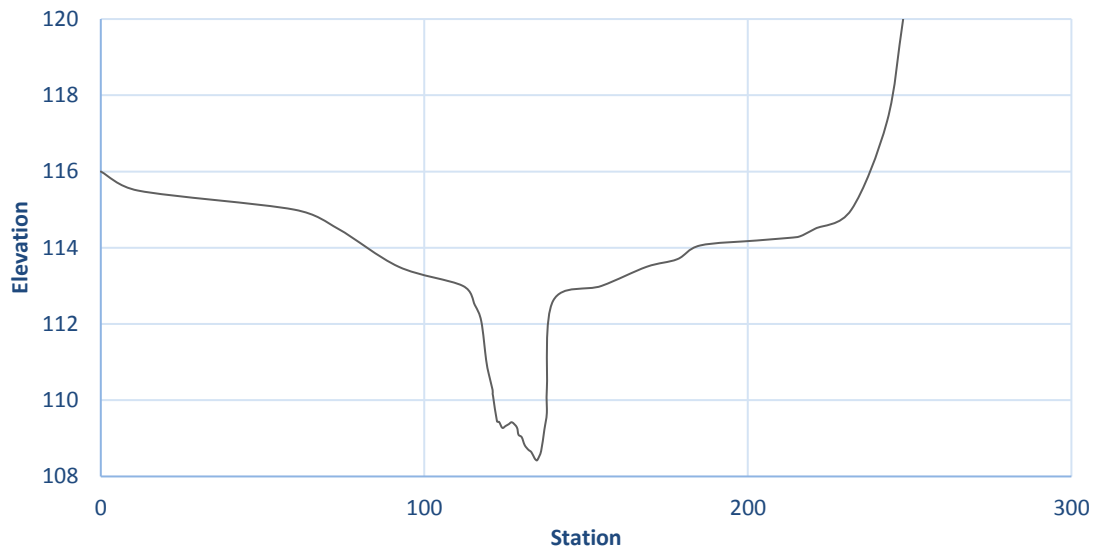


Figure 53: XS 2 Bed Profile

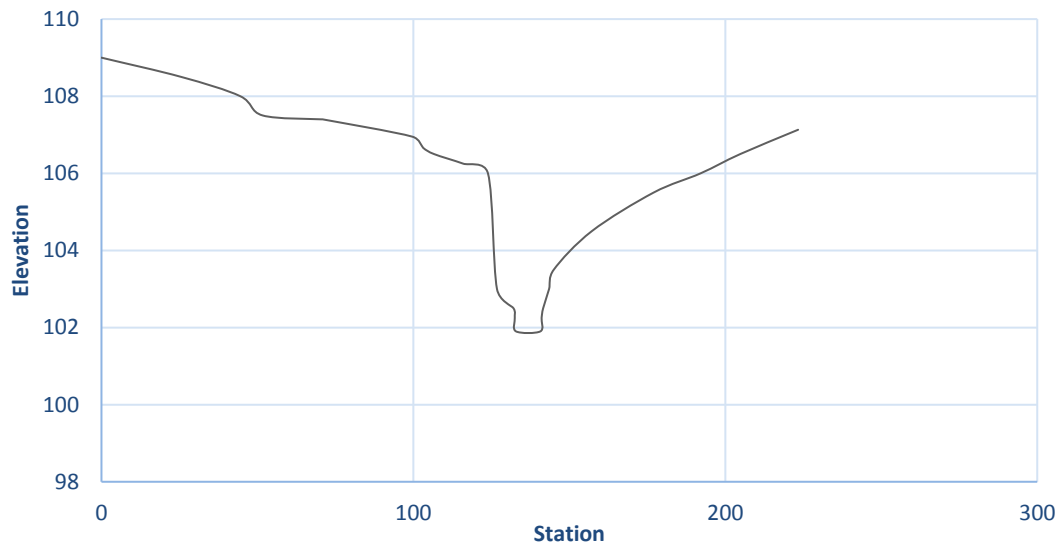


Figure 54: XS 3 Bed Profile

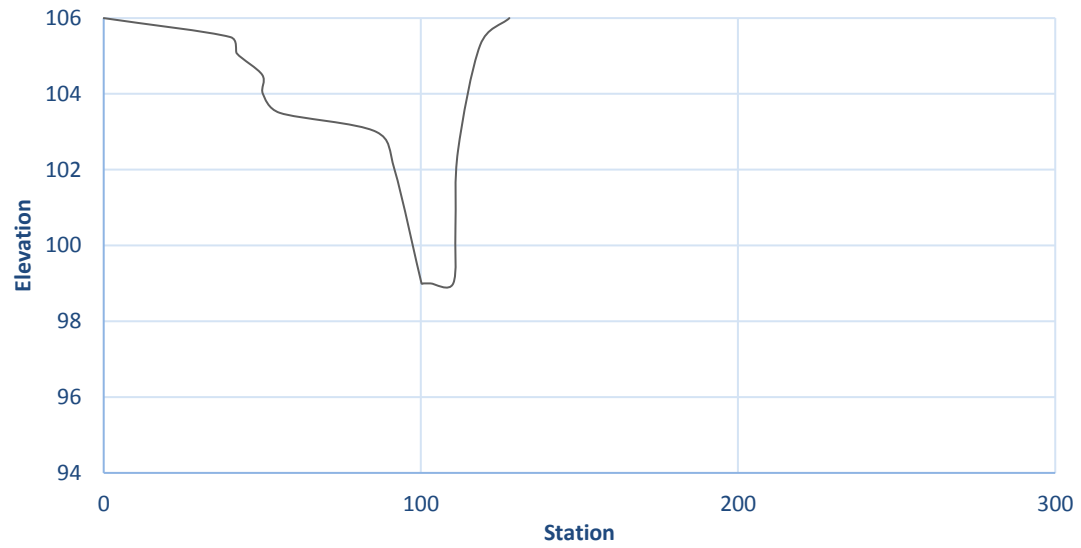


Figure 55: XS 4 Bed Profile

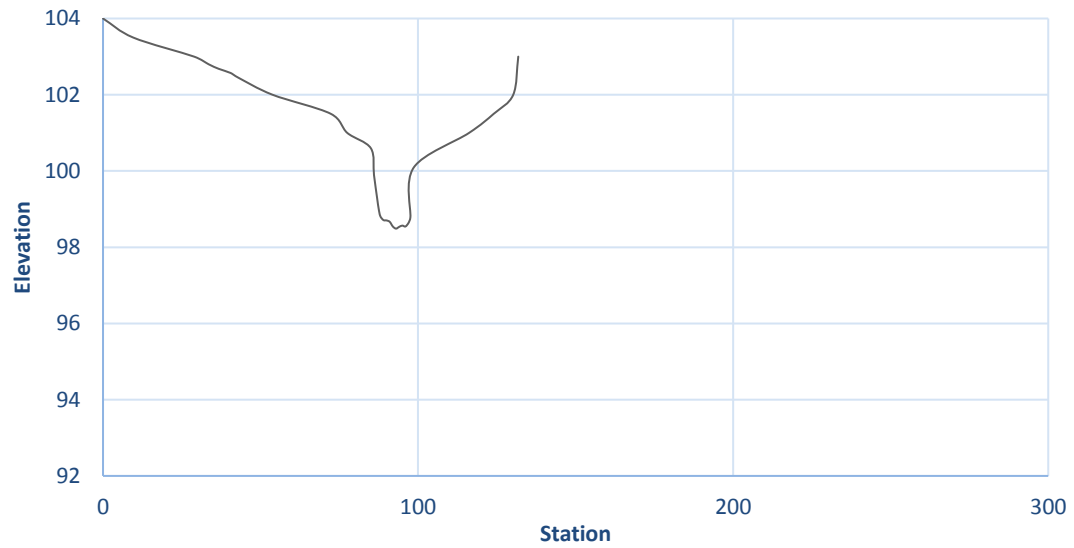


Figure 56: XS 5 Bed Profile

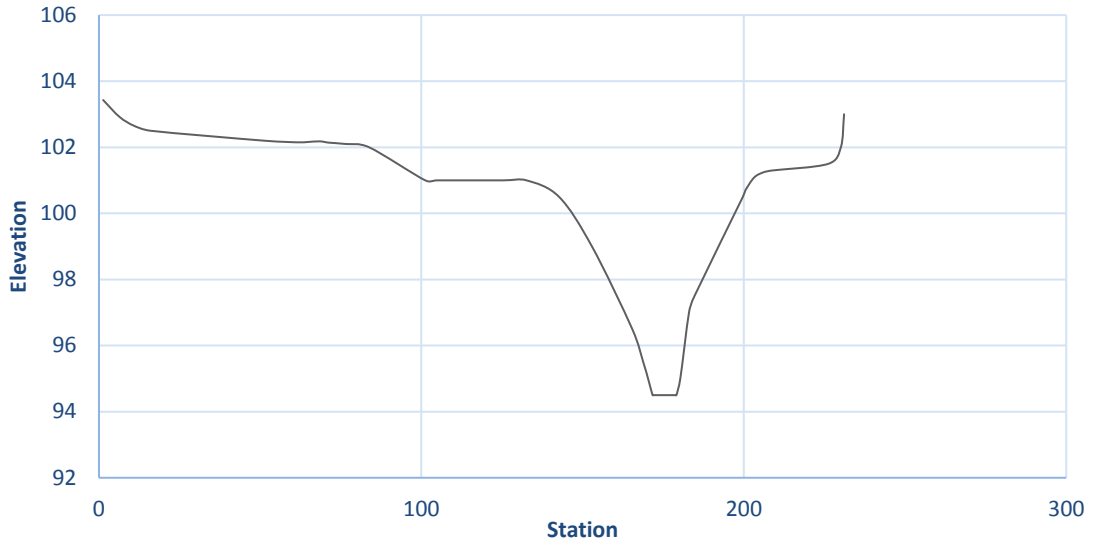


Figure 57: XS 6 Bed Profile

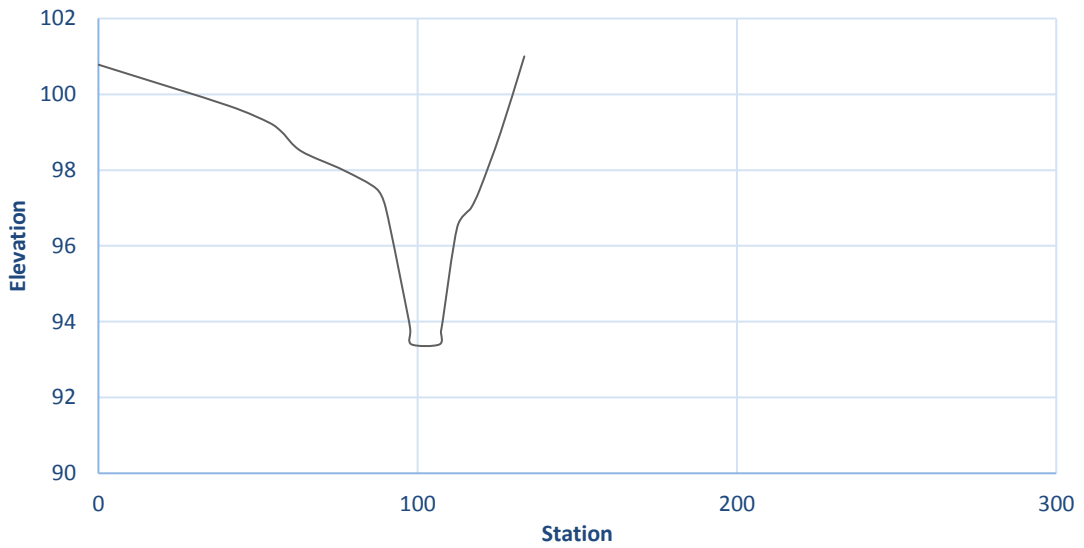


Figure 58: XS 7 Bed Profile

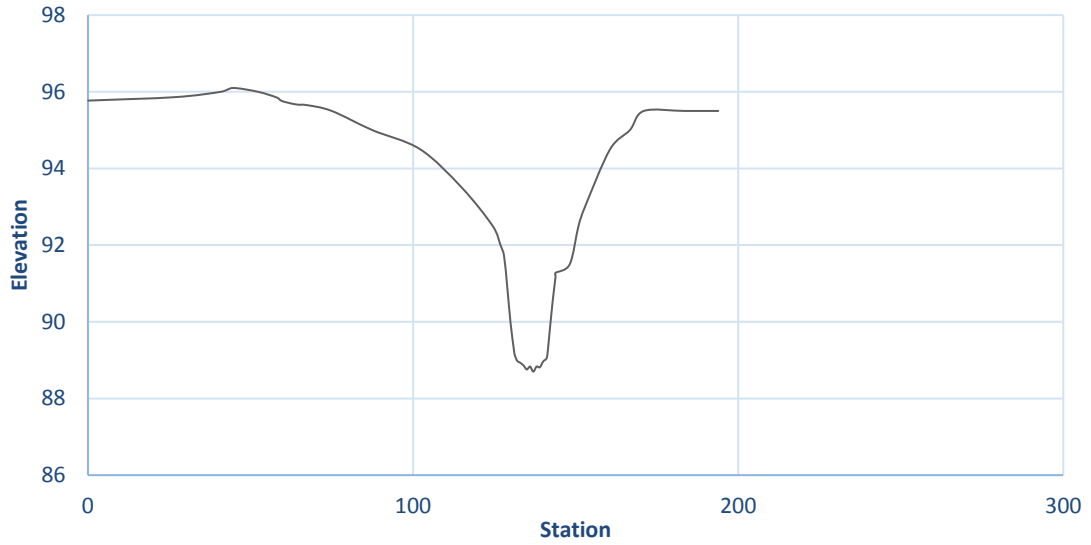


Figure 59: XS 8 Bed Profile

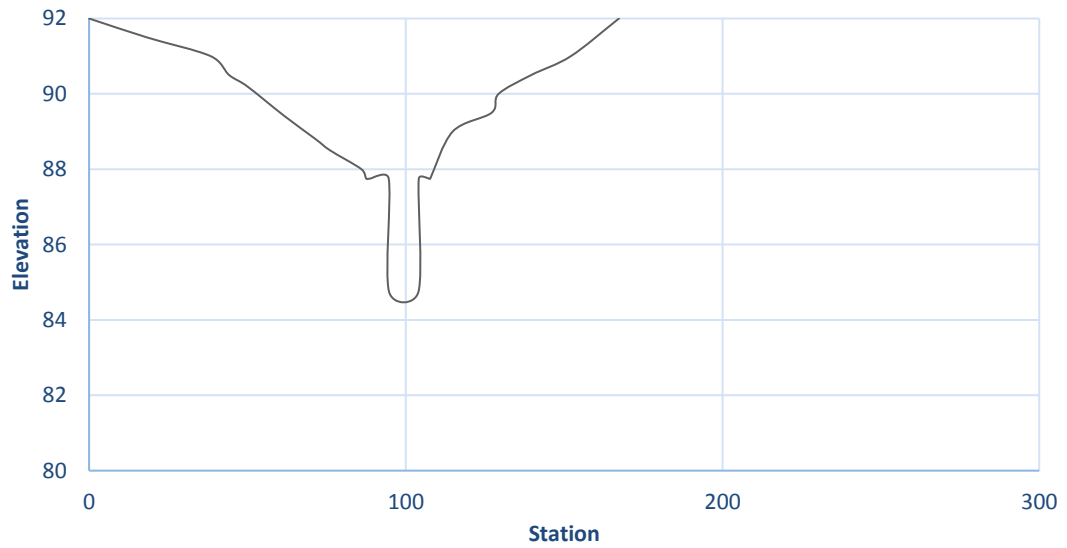


Figure 60: XS 9 Bed Profile

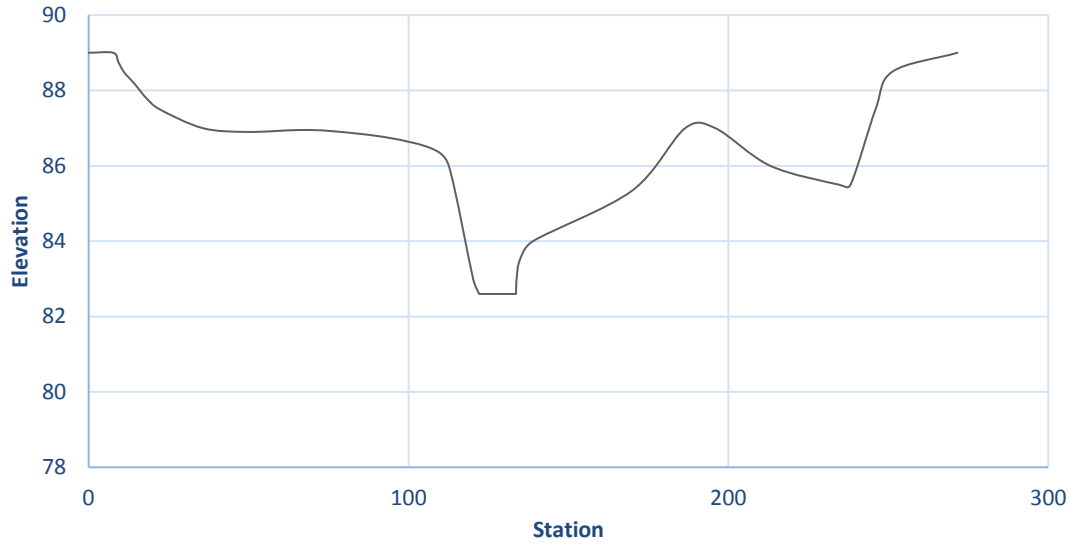


Figure 61: XS 10 Bed Profile

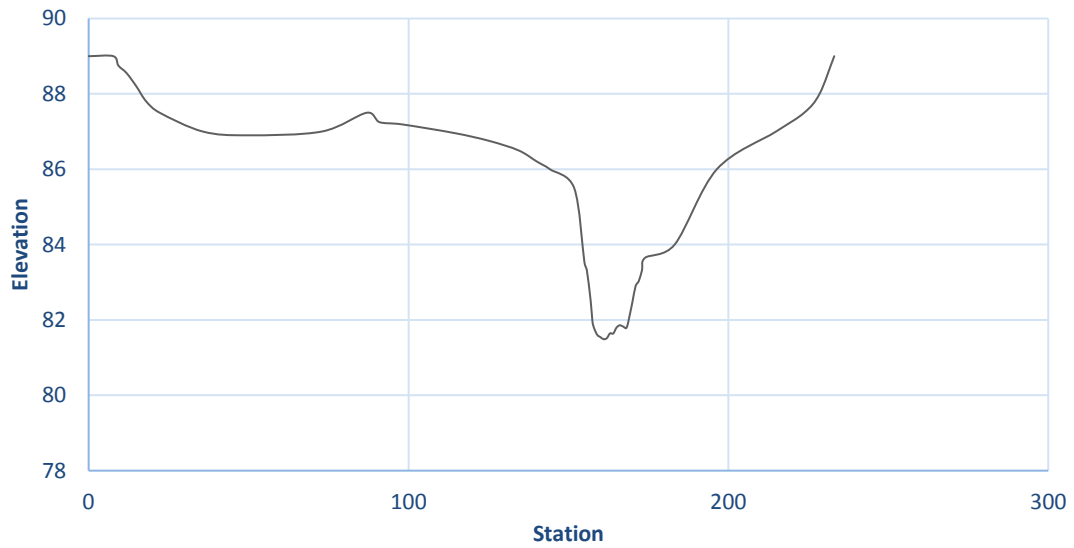


Figure 62: XS 11 Bed Profile

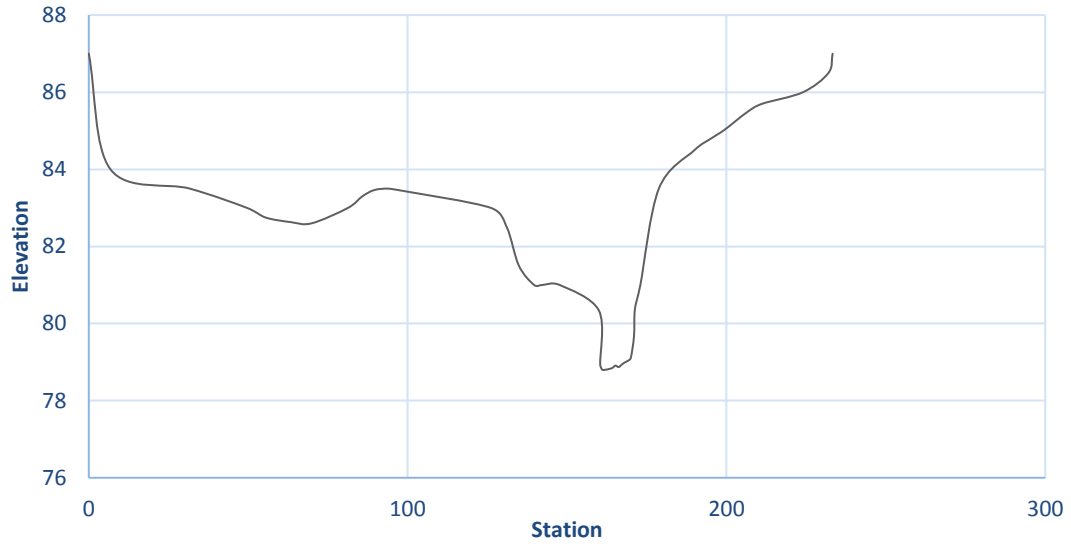


Figure 63: XS 12 Bed Profile

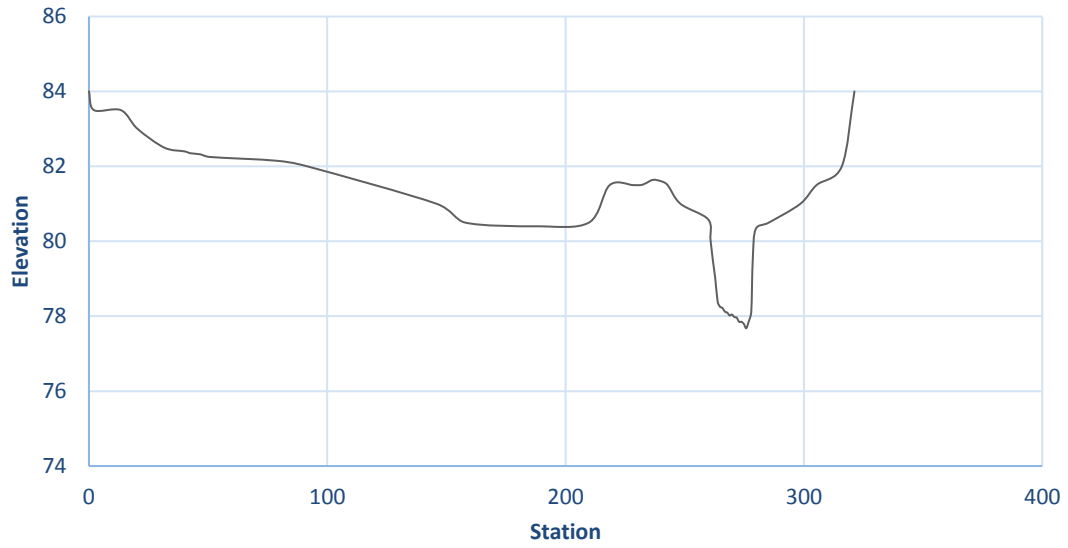


Figure 64: XS 13 Bed Profile

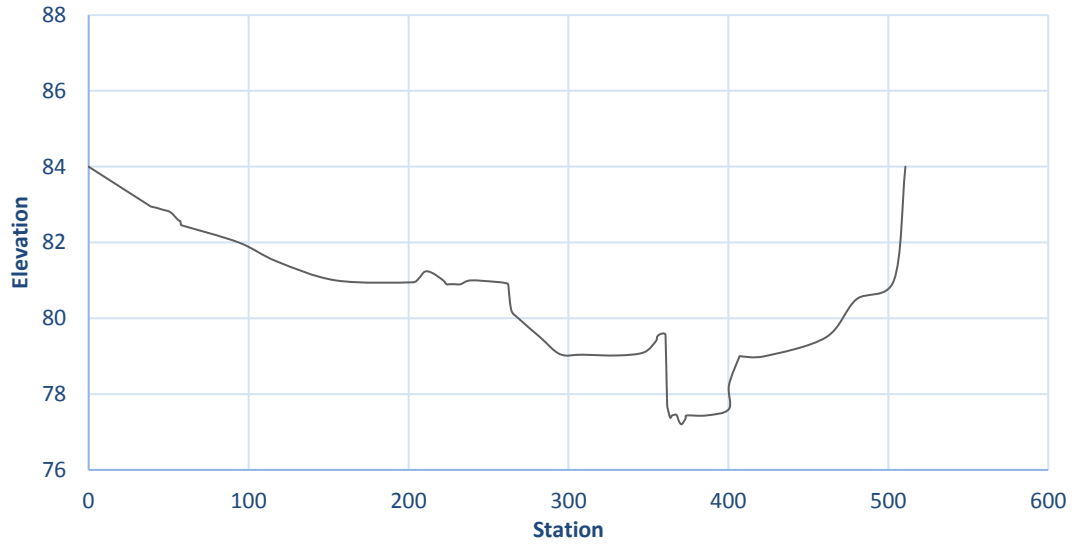


Figure 65: XS 14 Bed Profile

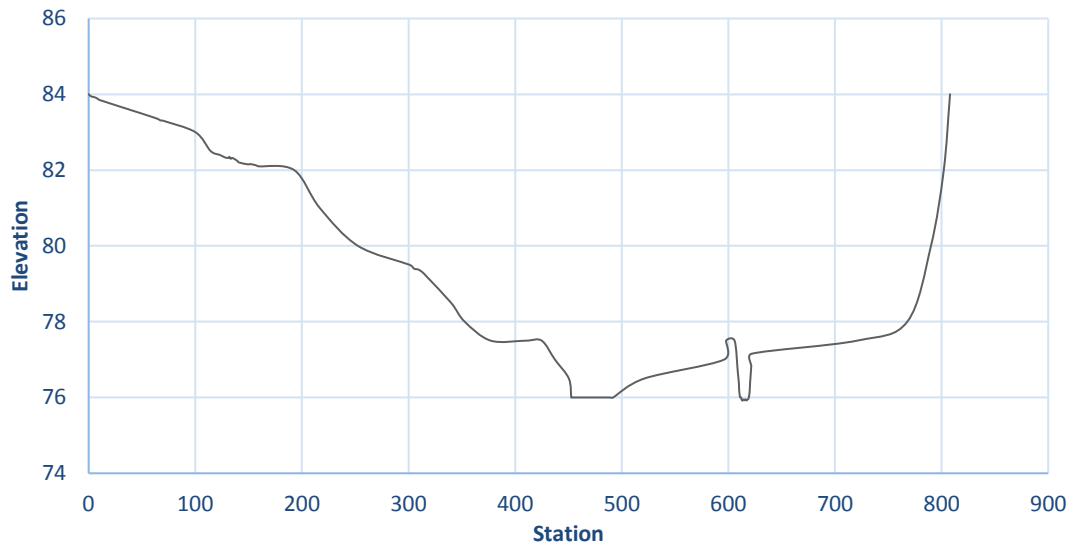


Figure 66: XS 15 Bed Profile

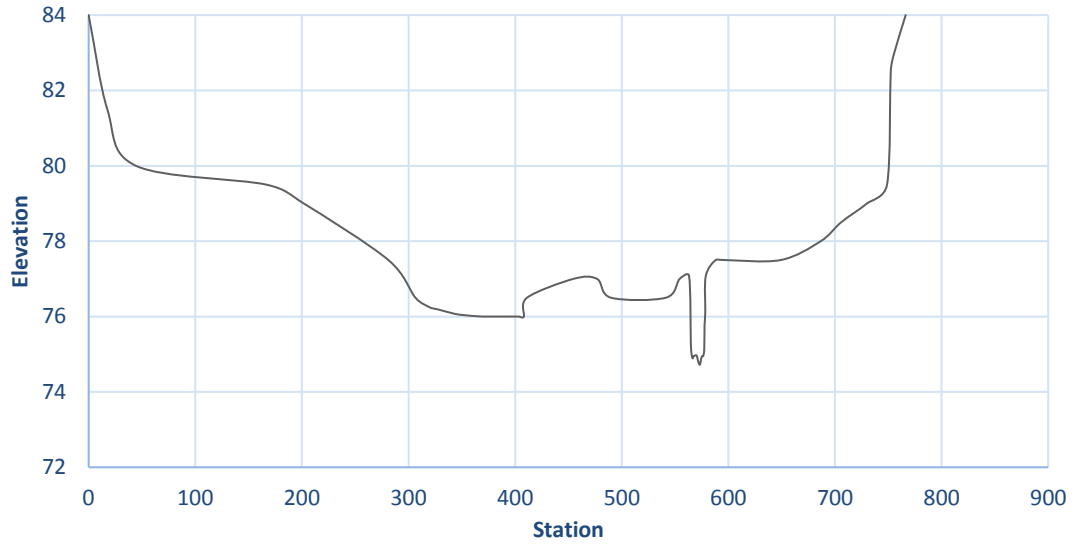


Figure 67: XS 16 Bed Profile

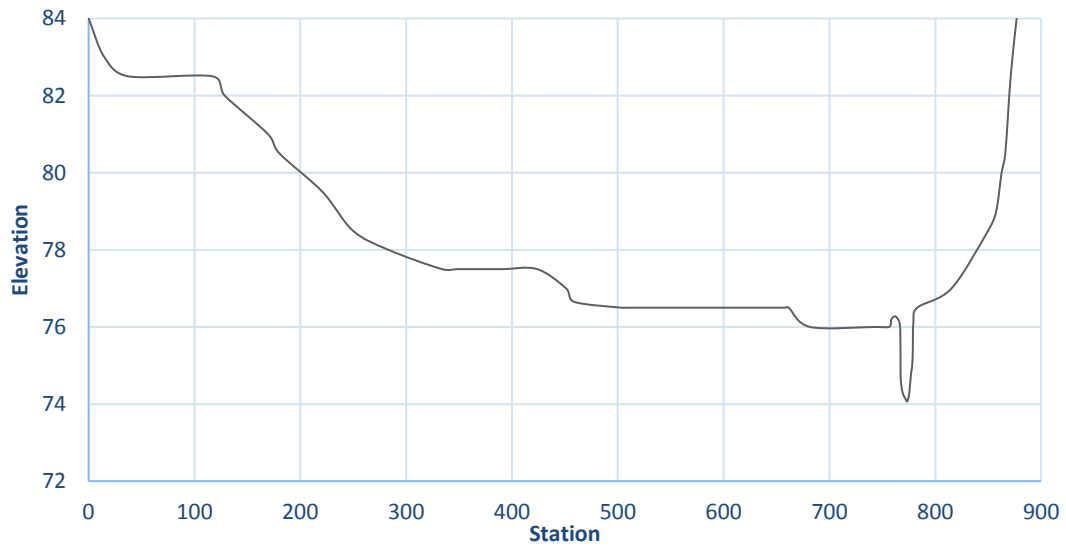


Figure 68: XS 17 Bed Profile

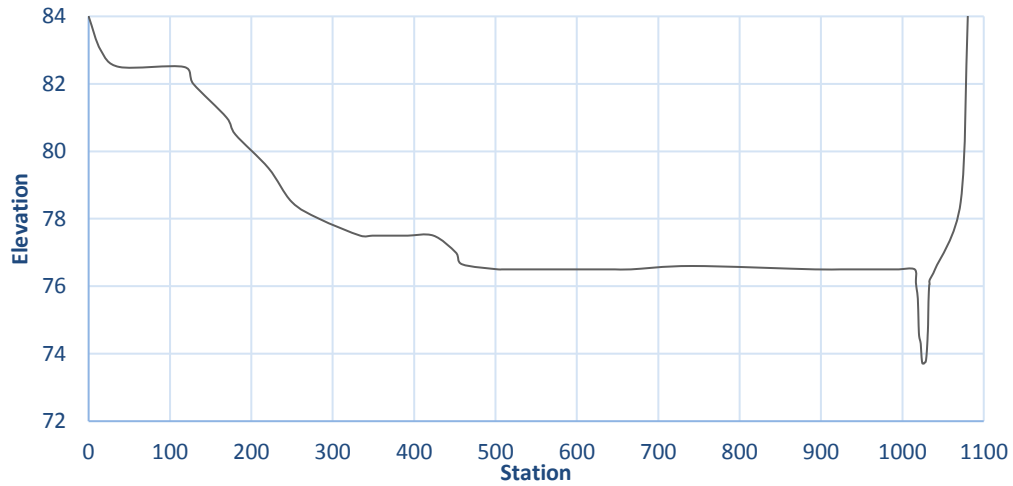


Figure 69: XS 18 Bed Profile

Table 11: Width and Length at Each Cross Section

XS	Width (m)	New Width (m)	Length (m)	New Length (m)
2	19.0	19.0	-	-
3	18.0	18.0	95	95
4	20.0	20.0	145	145
5	13.6	13.6	280	280
6	15.0	15.0	362	362
7	26.0	26.0	140	140
8	15.8	15.8	275	275
9	9.4	9.4	322	322
10	13.6	13.6	128	128
11	18.0	18.0	84	84
12	11.3	11.3	300	300
13	20.0	20.0	135	135
14	19.0	19.0	200	200
15	16.0	18.4	177	177
16	8.3	9.5	388	427
17	12.9	15.0	279	307
18	17	19.5	417	459

Appendix F: Simulation Summary Tables

Table 12: Summary of Results for Simulation 1 (Existing Channel; Event 1)

XS	Event Duration (hours)	Flow		Sediment		Velocity	
		Q _p (m ³ /s)	t _r (hr)	S _p (mg/l)	t _s (hr)	V _{mean} (m/s)	V _{max} (m/s)
2	24	1.248	n/a	2072	24	1.37	1.37
3	24	1.248	n/a	272	24	0.037	0.04
4	24	1.248	n/a	292	6	0.77	0.77
5	24	1.248	n/a	323	17	0.93	0.96
6	24	1.248	n/a	414	12	0.9	0.93
7	24	1.248	n/a	410	12	1.11	1.11
8	24	1.248	n/a	359	12	0.56	0.56
9	24	1.248	n/a	361	12	0.29	0.29
10	24	1.248	n/a	538	17	1.00	1.01
11	24	1.248	n/a	541	17	1.25	1.25
12	24	1.248	n/a	491	21	0.92	0.92
13	24	1.248	n/a	488	21	0.96	0.97
14	24	1.248	n/a	388	21	0.75	0.76
15	24	1.248	n/a	376	21	0.063	0.063
16	24	1.248	n/a	369	21	0.040	0.040
17	24	1.248	n/a	367	21	0.038	0.038
18	24	1.248	n/a	364	21	0.037	0.037

Table 13: Summary of Results for Simulation 2 (Existing Channel; Event 2)

XS	Event Duration (hours)	Flow		Sediment		Velocity	
		Q _p (m ³ /s)	t _r (hr)	S _p (mg/l)	t _s (hr)	V _{mean} (m/s)	V _{max} (m/s)
2	12	6.313	11	2079	23	1.63	2.00
3	12	6.313	11	853	10	0.072	0.13
4	12	6.313	11	452	10	1.02	1.40
5	12	6.313	11	514	10	1.24	1.84
6	12	6.313	11	490	11	1.19	1.61
7	12	6.313	11	493	11	1.41	1.86
8	12	6.313	11	389	11	0.78	1.14
9	12	6.313	11	387	11	0.52	0.91
10	12	6.313	11	534	19	1.28	1.69
11	12	6.313	11	540	19	1.43	1.78
12	12	6.313	11	544	19	1.17	1.56
13	12	6.313	11	555	14	1.17	1.61
14	12	6.313	11	467	19	1.01	1.49
15	12	6.313	11	453	19	0.13	0.26
16	12	6.313	11	446	19	0.087	0.18
17	12	6.313	11	444	19	0.083	0.17
18	12	6.313	11	442	19	0.082	0.17

Table 14: Summary of Results for Simulation 3 (Existing Channel; Event 3)

XS	Event Duration (hours)	Flow		Sediment		Velocity	
		Q _p (m ³ /s)	t _r (hr)	S _p (mg/l)	t _s (hr)	V _{mean} (m/s)	V _{max} (m/s)
2	6	9.361	8	2081	20	1.55	2.16
3	6	9.361	8	938	8	0.063	0.16
4	6	9.361	8	560	8	0.94	1.63
5	6	9.361	8	655	8	1.14	2.08
6	6	9.361	8	596	8	1.11	1.88
7	6	9.361	8	600	8	1.32	2.10
8	6	9.361	8	456	9	0.72	1.37
9	6	9.361	8	452	9	0.46	1.18
10	6	9.361	8	581	10	1.20	1.91
11	6	9.361	8	585	8	1.39	2.00
12	6	9.361	8	553	21	1.12	1.79
13	6	9.361	8	627	13	1.10	1.88
14	6	9.361	8	536	8	0.94	1.66
15	6	9.361	8	452	15	0.12	0.35
16	6	9.361	8	445	15	0.077	0.25
17	6	9.361	8	435	20	0.073	0.24
18	6	9.361	8	440	15	0.072	0.24

Table 15: Summary of Results for Simulation 4 (Existing Channel; Event 4)

XS	Event Duration (hours)	Flow		Sediment		Velocity	
		Q _p (m ³ /s)	t _r (hr)	S _p (mg/l)	t _s (hr)	V _{mean} (m/s)	V _{max} (m/s)
2	24	12.23	17	2047	22	1.84	2.18
3	24	12.23	17	1083	17	0.14	0.21
4	24	12.23	17	729	16	1.38	1.80
5	24	12.23	17	808	16	1.69	2.26
6	24	12.23	17	801	16	1.60	2.05
7	24	12.23	17	816	16	1.82	2.27
8	24	12.23	17	686	17	1.13	1.54
9	24	12.23	17	689	17	0.94	1.44
10	24	12.23	17	844	16	1.66	2.08
11	24	12.23	17	880	16	1.77	2.17
12	24	12.23	17	840	16	1.60	2.09
13	24	12.23	17	883	16	1.55	2.01
14	24	12.23	17	765	14	1.41	1.82
15	24	12.23	17	516	15	0.25	0.39
16	24	12.23	17	429	4	0.19	0.32
17	24	12.23	17	426	4	0.18	0.30
18	24	12.23	17	423	4	0.18	0.30

Table 16: Summary of Results for Simulation 5 (Modification 1; Event 1)

XS	Event Duration (hours)	Flow		Sediment		Velocity	
		Q _p (m ³ /s)	t _r (hr)	S _p (mg/l)	t _s (hr)	V _{mean} (m/s)	V _{max} (m/s)
2	24	1.248	n/a	2072	24	1.37	1.37
3	24	1.248	n/a	272	24	0.037	0.040
4	24	1.248	n/a	292	6	0.77	0.77
5	24	1.248	n/a	323	17	0.93	0.96
6	24	1.248	n/a	413	12	0.90	0.93
7	24	1.248	n/a	410	12	1.11	1.11
8	24	1.248	n/a	359	12	0.56	0.56
9	24	1.248	n/a	361	12	0.29	0.29
10	24	1.248	n/a	538	17	1.01	1.01
11	24	1.248	n/a	541	17	1.25	1.25
12	24	1.248	n/a	491	21	0.92	0.92
13	24	1.248	n/a	488	21	0.96	0.97
14	24	1.248	n/a	388	21	0.75	0.76
15	24	1.248	n/a	375	21	0.043	0.043
16	24	1.248	n/a	367	21	0.035	0.035
17	24	1.248	n/a	364	21	0.034	0.034
18	24	1.248	n/a	361	21	0.022	0.022

Table 17: Summary of Results for Simulation 6 (Modification 1; Event 2)

XS	Event Duration (hours)	Flow		Sediment		Velocity	
		Q _p (m ³ /s)	t _r (hr)	S _p (mg/l)	t _s (hr)	V _{mean} (m/s)	V _{max} (m/s)
2	12	6.313	11	2080	23	1.63	2
3	12	6.313	11	853	10	0.072	0.13
4	12	6.313	11	452	10	1.02	1.40
5	12	6.313	11	514	10	1.24	1.84
6	12	6.313	11	490	11	1.19	1.61
7	12	6.313	11	493	11	1.41	1.86
8	12	6.313	11	389	11	0.78	1.14
9	12	6.313	11	387	11	0.52	0.91
10	12	6.313	11	535	19	1.28	1.69
11	12	6.313	11	540	19	1.43	1.78
12	12	6.313	11	544	19	1.17	1.56
13	12	6.313	11	555.	14	1.17	1.61
14	12	6.313	11	467	19	1.01	1.50
15	12	6.313	11	452	19	0.094	0.19
16	12	6.313	11	445	19	0.076	0.157
17	12	6.313	11	443	19	0.076	0.157
18	12	6.313	11	440	19	0.051	0.11

Table 18: Summary of Results for Simulation 7 (Modification 1; Event 3)

XS	Event Duration (hours)	Flow		Sediment		Velocity	
		Q_p (m³/s)	t_r (hr)	S_p (mg/l)	t_s (hr)	V_{mean} (m/s)	V_{max} (m/s)
2	6	9.361	8	2081	20	1.55	2.16
3	6	9.361	8	938	8	0.063	0.16
4	6	9.361	8	560	8	0.94	1.63
5	6	9.361	8	656	8	1.14	2.08
6	6	9.361	8	596	8	1.11	1.87
7	6	9.361	8	600	8	1.32	2.10
8	6	9.361	8	450	8	0.72	1.37
9	6	9.361	8	452	9	0.46	1.18
10	6	9.361	8	581	10	1.20	1.91
11	6	9.361	8	555	10	1.39	2.00
12	6	9.361	8	552	21	1.12	1.79
13	6	9.361	8	636	11	1.10	1.88
14	6	9.361	8	536	8	0.94	1.68
15	6	9.361	8	451	15	0.083	0.27
16	6	9.361	8	443	15	0.067	0.22
17	6	9.361	8	440	15	0.067	0.22
18	6	9.361	8	438	15	0.045	0.16

Table 19: Summary of Results for Simulation 8 (Modification 1; Event 4)

XS	Event Duration (hours)	Flow		Sediment		Velocity	
		Q _p (m ³ /s)	t _r (hr)	S _p (mg/l)	t _s (hr)	V _{mean} (m/s)	V _{max} (m/s)
2	24	12.23	16	2163	4	1.84	2.18
3	24	12.23	16	1082	17	0.13	0.21
4	24	12.23	16	729	16	1.38	1.80
5	24	12.23	16	808	16	1.69	2.26
6	24	12.23	16	800	16	1.60	2.05
7	24	12.23	16	816	16	1.82	2.27
8	24	12.23	16	686	16	1.13	1.54
9	24	12.23	16	689	17	0.94	1.44
10	24	12.23	16	844	16	1.66	2.08
11	24	12.23	16	880	16	1.77	2.17
12	24	12.23	16	840	16	1.60	2.09
13	24	12.23	16	883	16	1.55	2.01
14	24	12.23	16	752	16	1.41	1.82
15	24	12.23	16	492	16	0.20	0.33
16	24	12.23	16	426	4	0.17	0.28
17	24	12.23	16	424	4	0.17	0.28
18	24	12.23	16	421	4	0.12	0.20

Table 20: Summary of Results for Simulation 8 (Modification 2; Event 1)

XS	Event Duration (hours)	Flow		Sediment		Velocity	
		Q _p (m ³ /s)	t _r (hr)	S _p (mg/l)	t _s (hr)	V _{mean} (m/s)	V _{max} (m/s)
2	24	1.248	n/a	2072	24	1.36	1.38
3	24	1.248	n/a	272	24	0.045	0.059
4	24	1.248	n/a	292	6	0.79	0.82
5	24	1.248	n/a	323	17	0.90	0.96
6	24	1.248	n/a	413	12	0.87	0.92
7	24	1.248	n/a	410	12	1.11	1.11
8	24	1.248	n/a	359	12	0.56	0.56
9	24	1.248	n/a	361	12	0.29	0.29
10	24	1.248	n/a	538	17	1.01	1.01
11	24	1.248	n/a	541	17	1.25	1.25
12	24	1.248	n/a	491	21	0.19	0.92
13	24	1.248	n/a	488	21	0.96	0.97
14	24	1.248	n/a	388	21	0.75	0.76
15	24	1.248	n/a	376	21	0.062	0.062
16	24	1.248	n/a	368	21	0.040	0.040
17	24	1.248	n/a	365	21	0.038	0.038
18	24	1.248	n/a	360	21	0.037	0.037

Table 21: Summary of Results for Simulation 10 (Modification 2; Event 2)

XS	Event Duration (hours)	Flow		Sediment		Velocity	
		Q _p (m ³ /s)	t _r (hr)	S _p (mg/l)	t _s (hr)	V _{mean} (m/s)	V _{max} (m/s)
2	12	6.313	11	2080	23	1.63	2
3	12	6.313	11	853	10	0.072	0.13
4	12	6.313	11	452	10	1.02	1.40
5	12	6.313	11	514	10	1.24	1.84
6	12	6.313	11	490	11	1.19	1.61
7	12	6.313	11	493	11	1.41	1.86
8	12	6.313	11	389	11	0.78	1.14
9	12	6.313	11	387	11	0.52	0.91
10	12	6.313	11	535	19	1.28	1.69
11	12	6.313	11	540	19	1.43	1.78
12	12	6.313	11	544	19	1.17	1.56
13	12	6.313	11	555.	14	1.17	1.61
14	12	6.313	11	467	19	1.01	1.50
15	12	6.313	11	463	21	0.13	0.26
16	12	6.313	11	454	21	0.087	0.18
17	12	6.313	11	451	21	0.082	0.17
18	12	6.313	11	447	21	0.082	0.17

Table 22: Summary of Results for Simulation 11 (Modification 2; Event 3)

XS	Event Duration (hours)	Flow		Sediment		Velocity	
		Q_p (m³/s)	t_r (hr)	S_p (mg/l)	t_s (hr)	V_{mean} (m/s)	V_{max} (m/s)
2	6	9.361	8	2081	20	1.55	2.16
3	6	9.361	8	938	8	0.063	0.16
4	6	9.361	8	560	8	0.94	1.63
5	6	9.361	8	656	8	1.14	2.08
6	6	9.361	8	596	8	1.11	1.88
7	6	9.361	8	600	8	1.32	2.20
8	6	9.361	8	450	8	0.72	1.37
9	6	9.361	8	452	9	0.46	1.18
10	6	9.361	8	581	10	1.20	1.91
11	6	9.361	8	555	10	1.39	2.00
12	6	9.361	8	555	21	1.12	1.79
13	6	9.361	8	636	11	1.10	1.88
14	6	9.361	8	536	8	0.94	1.68
15	6	9.361	8	454	15	0.12	0.35
16	6	9.361	8	446	15	0.077	0.25
17	6	9.361	8	443	15	0.073	0.24
18	6	9.361	8	438	15	0.072	0.24

Table 23: Summary of Results for Simulation 12 (Modification 2; Event 4)

XS	Event Duration (hours)	Flow		Sediment		Velocity	
		Q _p (m ³ /s)	t _r (hr)	S _p (mg/l)	t _s (hr)	V _{mean} (m/s)	V _{max} (m/s)
2	24	12.23	16	2163	4	1.84	2.18
3	24	12.23	16	1083	17	0.13	0.21
4	24	12.23	16	729	16	1.38	1.80
5	24	12.23	16	808	16	1.69	2.26
6	24	12.23	16	801	16	1.60	2.05
7	24	12.23	16	816	16	1.82	2.27
8	24	12.23	16	686	17	1.13	1.54
9	24	12.23	16	689	17	0.94	1.44
10	24	12.23	16	844	16	1.66	2.08
11	24	12.23	16	880	16	1.77	2.17
12	24	12.23	16	840	16	1.60	2.09
13	24	12.23	16	883	16	1.55	2.01
14	24	12.23	16	752	16	1.41	1.82
15	24	12.23	16	483	16	0.27	0.41
16	24	12.23	16	429	4	0.19	0.31
17	24	12.23	16	426	4	0.18	0.30
18	24	12.23	16	421	4	0.18	0.30

Table 24: % Difference Between Velocity and Sediment Concentration for Each Event (Existing Channel)

Cross Section	Velocity (m/s)			Sediment Concentration (mg/l)		
	Event 1 to Event 2	Event 1 to Event 3	Event 1 to Event 4	Event 1 to Event 2	Event 1 to Event 3	Event 1 to Event 4
2	37%	44%	45%	0.35%	0.42%	1%
3	104%	121%	135%	103%	110%	120%
4	58%	71%	80%	39%	59%	82%
5	63%	74%	80%	23%	47%	66%
6	54%	67%	76%	17%	36%	63%
7	51%	61%	68%	18%	37%	66%
8	69%	84%	93%	8%	24%	62%
9	102%	120%	132%	7%	22%	62%
10	51%	62%	69%	-0.5%	7%	44%
11	35%	46%	54%	-0.25%	-7%	47%
12	51%	64%	76%	10%	12%	52%
13	50%	64%	70%	12%	25%	57%
14	66%	76%	82%	1%	15%	49%
15	112%	138%	145%	0.6%	0.4%	14%
16	127%	145%	155%	1%	0.7%	-3%
17	127%	145%	155%	0.42%	0%	-3%
18	128%	146%	156%	1%	1%	-3%

Table 25: % Difference Between Velocity and Sediment Concentration for Each Event (Modification 1)

Cross Section	Velocity (m/s)			Sediment Concentration (mg/l)		
	Event 1 to Event 2	Event 1 to Event 3	Event 1 to Event 4	Event 1 to Event 2	Event 1 to Event 3	Event 1 to Event 4
2	37%	44%	45%	0.35%	0.42%	1%
3	104%	121%	135%	103%	110%	120%
4	58%	71%	80%	39%	59%	82%
5	63%	74%	80%	23%	47%	66%
6	54%	67%	76%	17%	36%	63%
7	51%	61%	68%	18%	37%	66%
8	69%	84%	93%	8%	24%	62%
9	102%	120%	132%	7%	22%	62%
10	51%	62%	69%	-0.5%	7%	44%
11	35%	46%	54%	-0.25%	-7%	47%
12	51%	64%	76%	10%	12%	52%
13	50%	64%	70%	12%	25%	57%
14	66%	76%	82%	1%	15%	49%
15	127%	144%	153%	0.5%	0.4%	9%
16	127%	146%	156%	1%	0.8%	-3%
17	129%	147%	157%	1%	0.9%	-3%
18	132%	150%	160%	2%	1%	-3%

Table 26: % Difference Between Velocity and Sediment Concentrations for Each Event (Modification 2)

Cross Section	Velocity (m/s)			Sediment Concentration (mg/l)		
	Event 1 to Event 2	Event 1 to Event 3	Event 1 to Event 4	Event 1 to Event 2	Event 1 to Event 3	Event 1 to Event 4
2	37%	44%	45%	0.35%	0.42%	1%
3	104%	121%	135%	103%	110%	120%
4	58%	71%	80%	39%	59%	82%
5	63%	74%	80%	23%	47%	66%
6	54%	67%	76%	17%	36%	63%
7	51%	61%	68%	18%	37%	66%
8	69%	84%	93%	8%	24%	62%
9	102%	120%	132%	7%	22%	62%
10	51%	62%	69%	-0.5%	7%	44%
11	35%	46%	54%	-0.25%	-7%	47%
12	51%	64%	76%	10%	12%	52%
13	50%	64%	70%	12%	25%	57%
14	66%	76%	82%	1%	15%	49%
15	124%	139%	148%	4%	3%	9%
16	127%	145%	155%	3%	1%	-3%
17	127%	145%	155%	3%	0.8%	-3%
18	128%	146%	156%	3%	1%	-3%

Appendix G: Event 2 and 3 Comparison Graphs

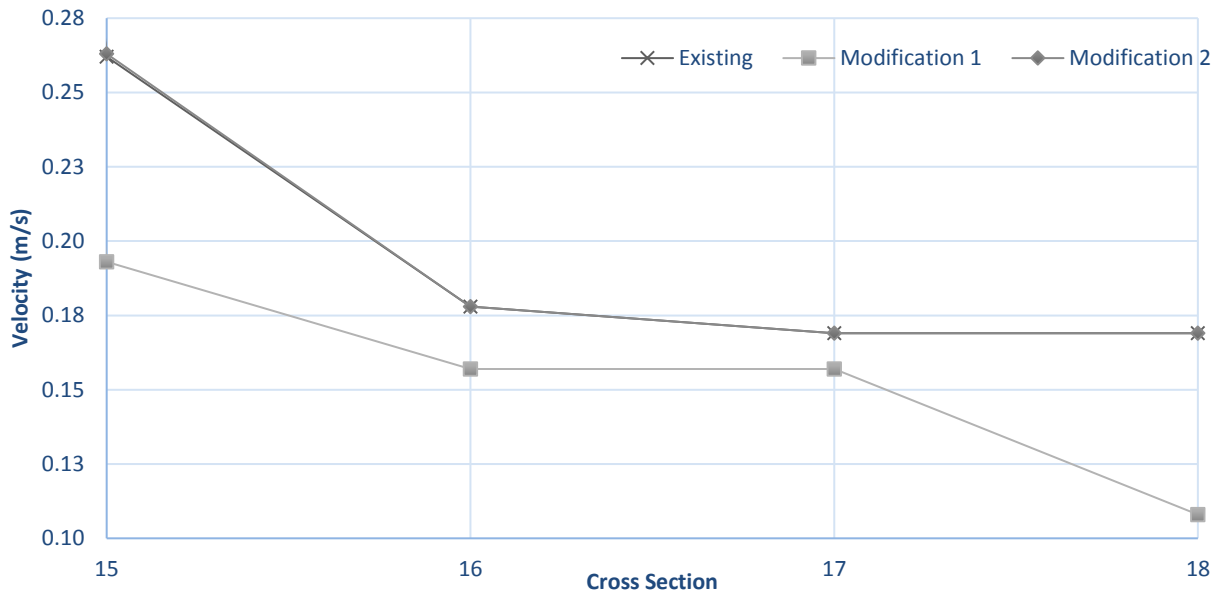


Figure 70: Maximum Velocity for All Channel Configurations for Event 2

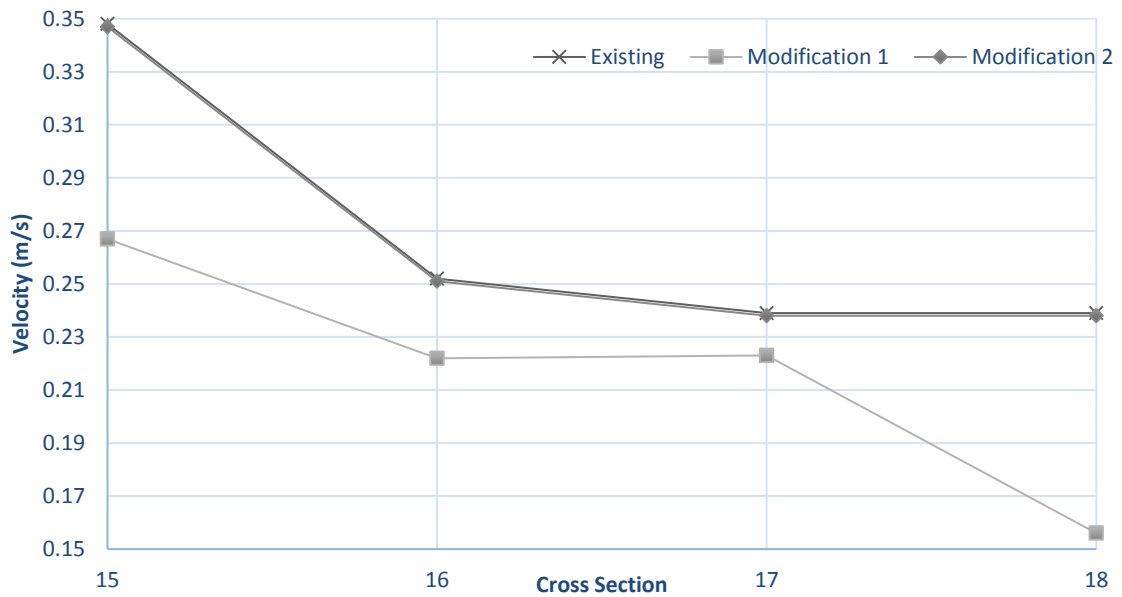


Figure 71: Maximum Velocity for All Channel Configurations for Event 3

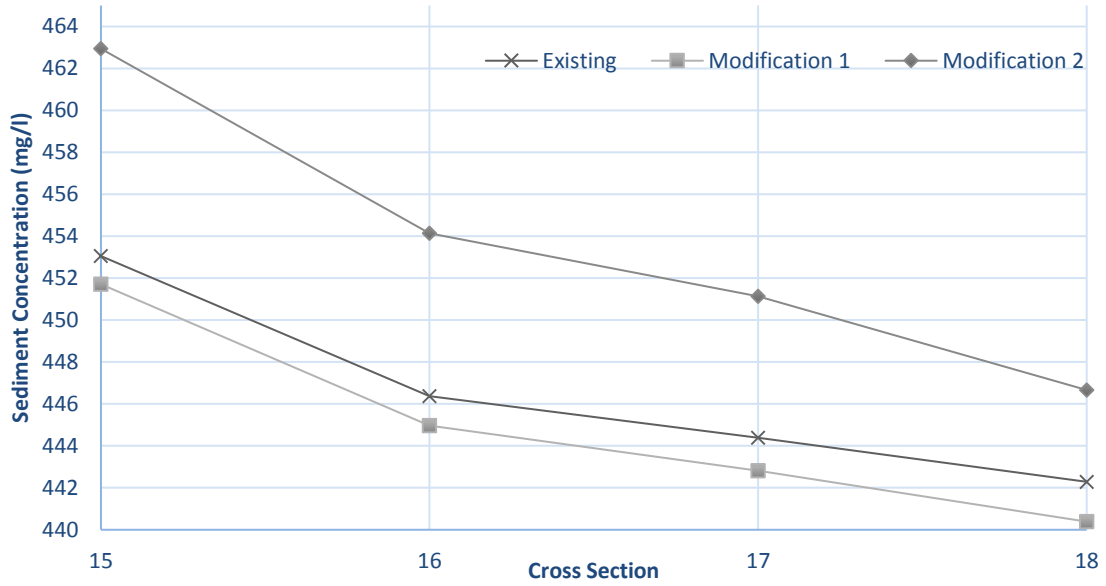


Figure 72: Peak Sediment Concentration for all Channel Configurations for Event 2

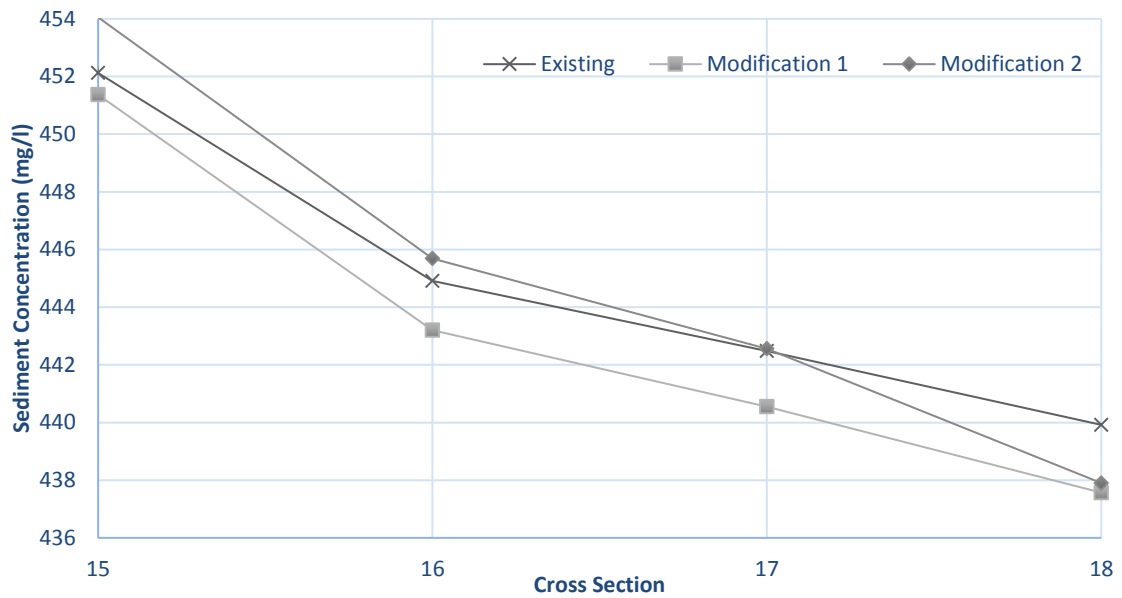


Figure 73: Peak Sediment Concentration for all Channel Configurations for Event 3

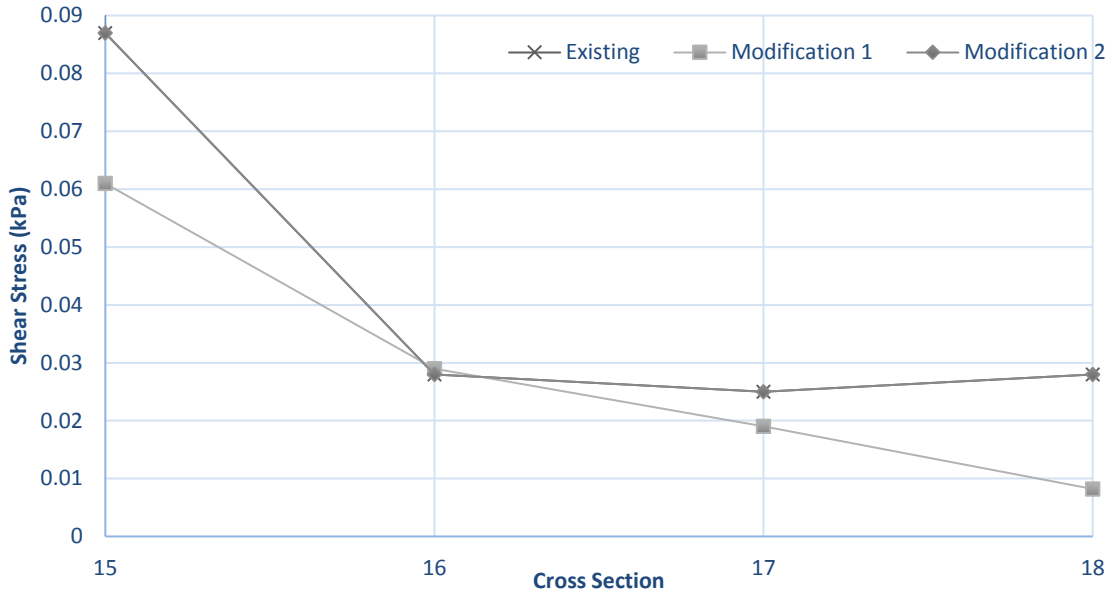


Figure 74: Maximum Shear Stress Comparison for Event 2

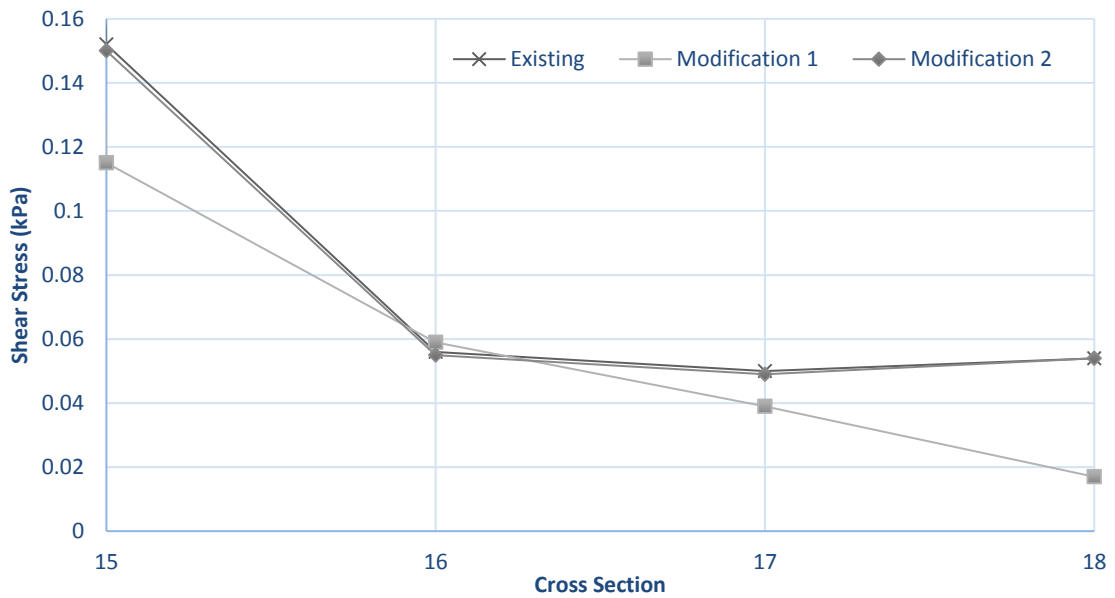


Figure 75: Maximum Shear Stress Comparison for Event 3

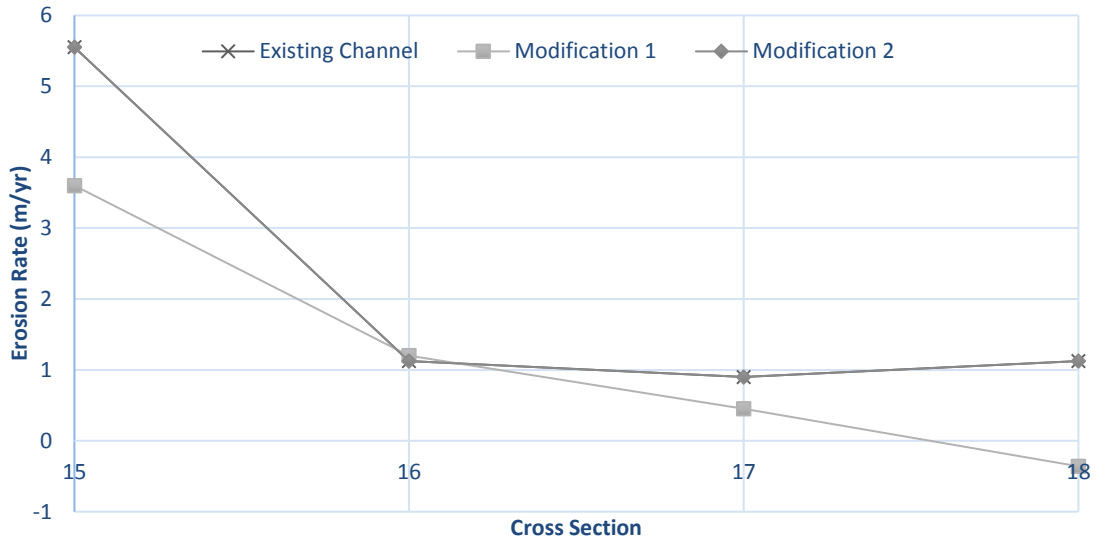


Figure 76: Erosion Rates for Event 2

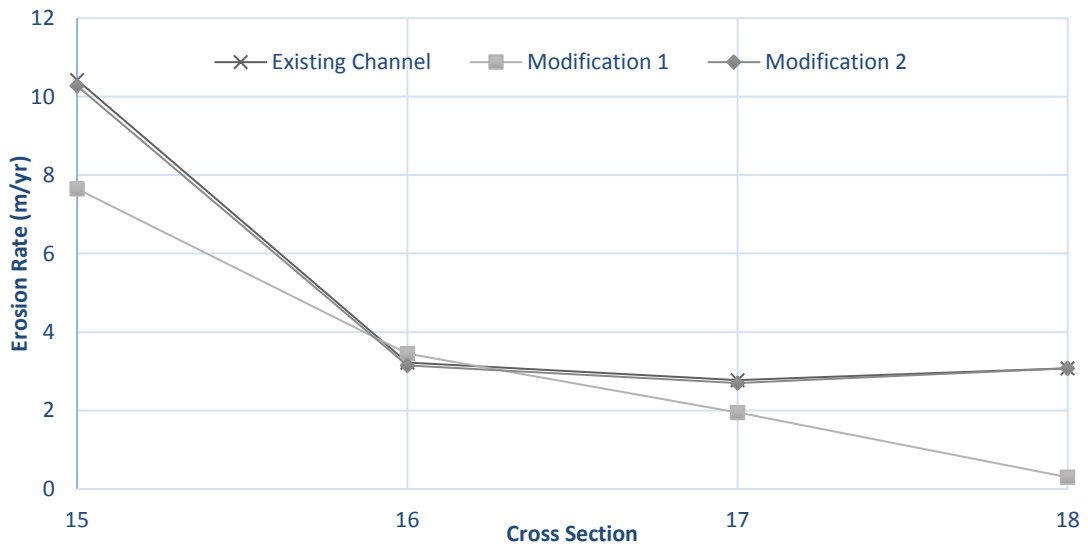


Figure 77: Erosion Rates for Event 3

Appendix H: HEC-RAS Equations

Meyer-Peter and Müller (1948)

The Meyer-Peter and Müller formula was developed in 1948 to deal with well-sorted, fine gravel in an open channel. This equation is widely used in laboratory and field studies, and in numerical simulations of bedload transport (Meyer-Peter and Müller, 1948).

$$q_b = \rho_s 8 \sqrt{g(s-1)D_{50}^3} \left(\left(\frac{n'}{n} \right)^{\frac{3}{2}} \theta - 0.047 \right)^{\frac{3}{2}} \quad (27)$$

Where:

q_b = bedload transport (m²/s)

D_{50} = median grain size (m)

s = sediment density ratio

n' = particle roughness (see Eq (28))

n = total roughness (see Eq (29))

θ = dimensionless shear stress (See Eq (30))

The particle roughness is calculated using Eq. (28).

$$n' = D_{90}^{1/6} / 26 \quad (28)$$

Where:

D_{90} = particle diameter representing 90% of sediment (m)

The total roughness is calculated using Eq. (29).

$$n = (s^{1/2}d^{2/3})/\bar{u} \quad (29)$$

Where:

s = water surface slope

d = water depth (m)

The dimensionless shear stress is calculated using Eq. (30).

$$\theta = \frac{dS}{D_{50}(s - 1)} \quad (30)$$

Engelund-Hansen (1972)

Engelund and Hansen (1972) developed an equation for sediment transport dealing with sediment under a current by applying Bagnold's stream power concept. This equation may be applied for particles greater than 0.15 mm (Engelund and Hansen, 1972).

$$G = K \frac{0.05WV^{0.5}h^{1.5}S^{1.5}}{(s - 1)^2D\sqrt{g}} \quad (31)$$

Where:

G = volumetric sediment transport rate

K = calibration coefficient

W = flow width

S = water surface slope

s = specific gravity of sediment

Yang (1979)

Yang (1979) presented Eq. (28), a unit stream power equation used in the computation and prediction of total sediment concentration. This equation focuses on sediment in the sand-sized range and can be applied to channels with varying flow and sediment conditions and flows with different bed forms.

$$\log C_t = I + J \log(VS/\omega) \quad (32)$$

Where

C_t = total sediment concentration (ppm)

VS = unit stream power

I, J = coefficients in the dimensionless unit stream power equation

The coefficient I is calculated using Eq. (33). The coefficient J is calculated using Eq. (34).

$$I = A_1 + A_2 \log(\omega d/v) + A_3 \log(U_*/\omega) \quad (33)$$

$$J = B_1 + B_2 \log(\omega d/v) + B_3 \log(U_*/\omega) \quad (34)$$

Where

$A_1, A_2, A_3, B_1, B_2, B_3$ = coefficients

d = median sieve diameter of sediment

Flow conditions at incipient motion can be calculated using Eq. (35) or Eq. (36).

$$V_{cr}/\omega = 2.5 [\log(U_*d/v) - 0.06]^{-1} + 0.66, \quad 1.2 < U_*d/v < 70 \quad (35)$$

$$V_{cr}/\omega = 2.05, \quad 70 \leq U_*d/v \quad (36)$$

Where

V_{cr} = average flow velocity at incipient motion (m/s)

Wilcock-Crowe (2003)

Wilcock and Crowe (2003) presented a sediment transport formula that incorporates many grain sizes, ranging from sand to gravel. Due to the incorporation of multiple grain sizes, this equation is more complicated than other sediment transport equations presented above. This equation considers the critical shear stress for each grain size, fraction of for each grain size in the total sediment supply, and incorporates a hiding function (Wilcock and Crowe, 2003).

$$W_i^* = f(\tau/\tau_{ri}) \quad (37)$$

Where:

τ = bed shear stress (Pa)

τ_{ri} = reference value of τ

W_i^* = dimensionless transport rate of size fraction i (see Eq. (38))

W_i^* is calculated using Eq. (38).

$$W_i^* = \frac{(s-1)gq_{bi}}{F_i u_*^3} \quad (38)$$

Where:

q_{bi} = volumetric transport rate per unit width of size i (m^2/s)

F_i = proportion of size i on the bed surface

u_* is calculated using Eq. (39).

$$u_* = [\tau/\rho]^{0.5} \quad (39)$$

Appendix I: Maps

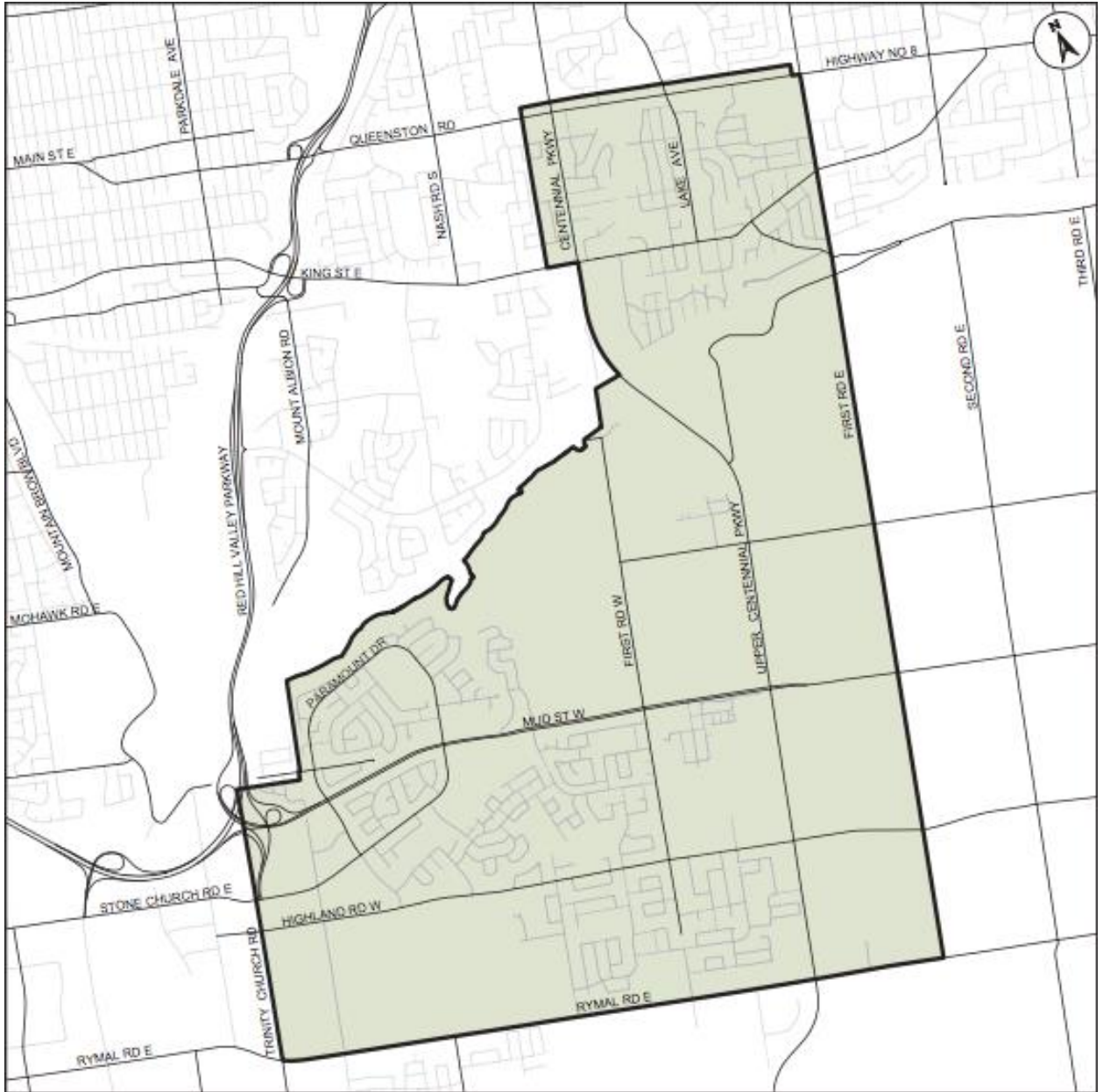


Figure 78: Ward 9 of Hamilton (City of Hamilton, 2015)

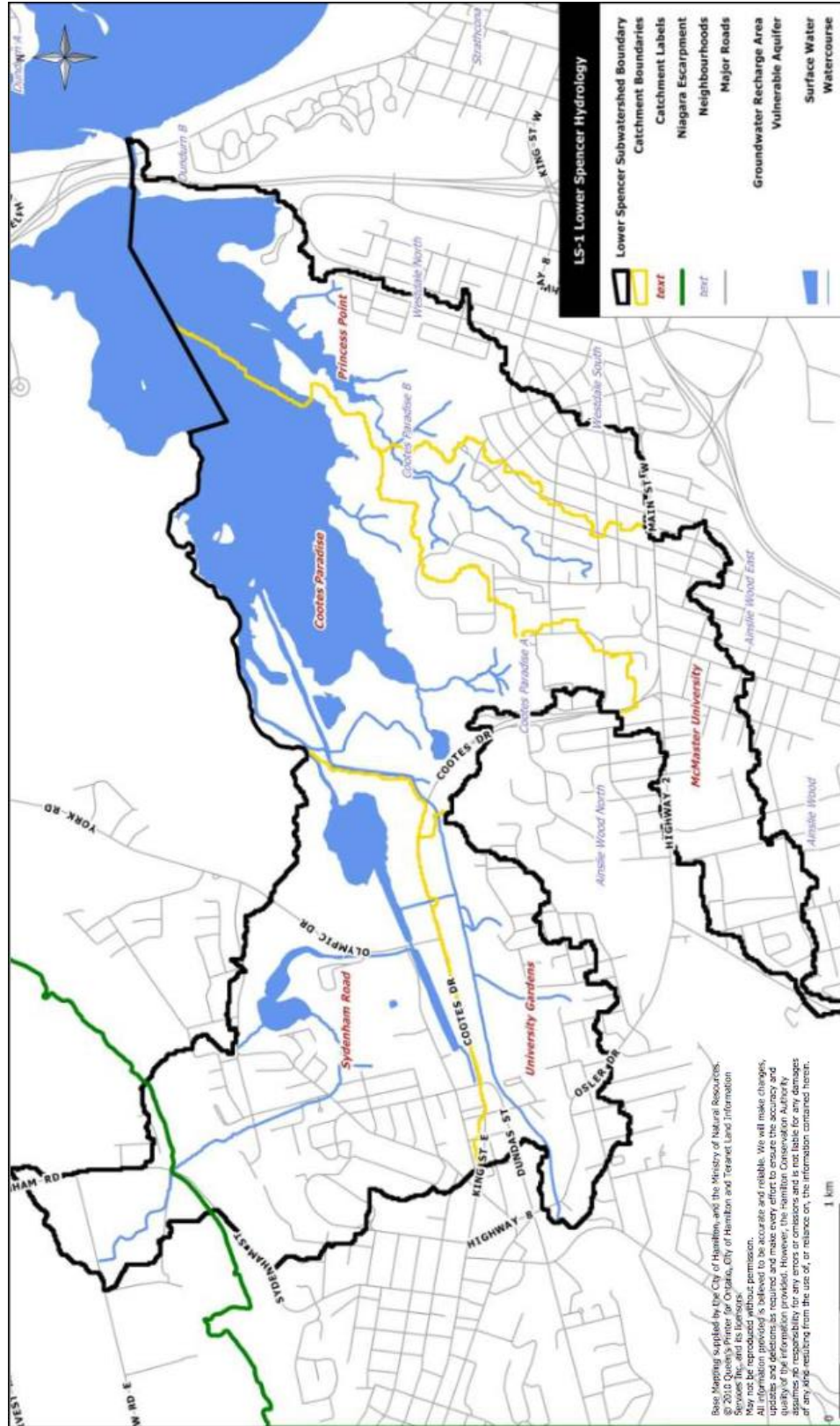


Figure 79: Lower Spencer Subwatershed (HCA, 2010)

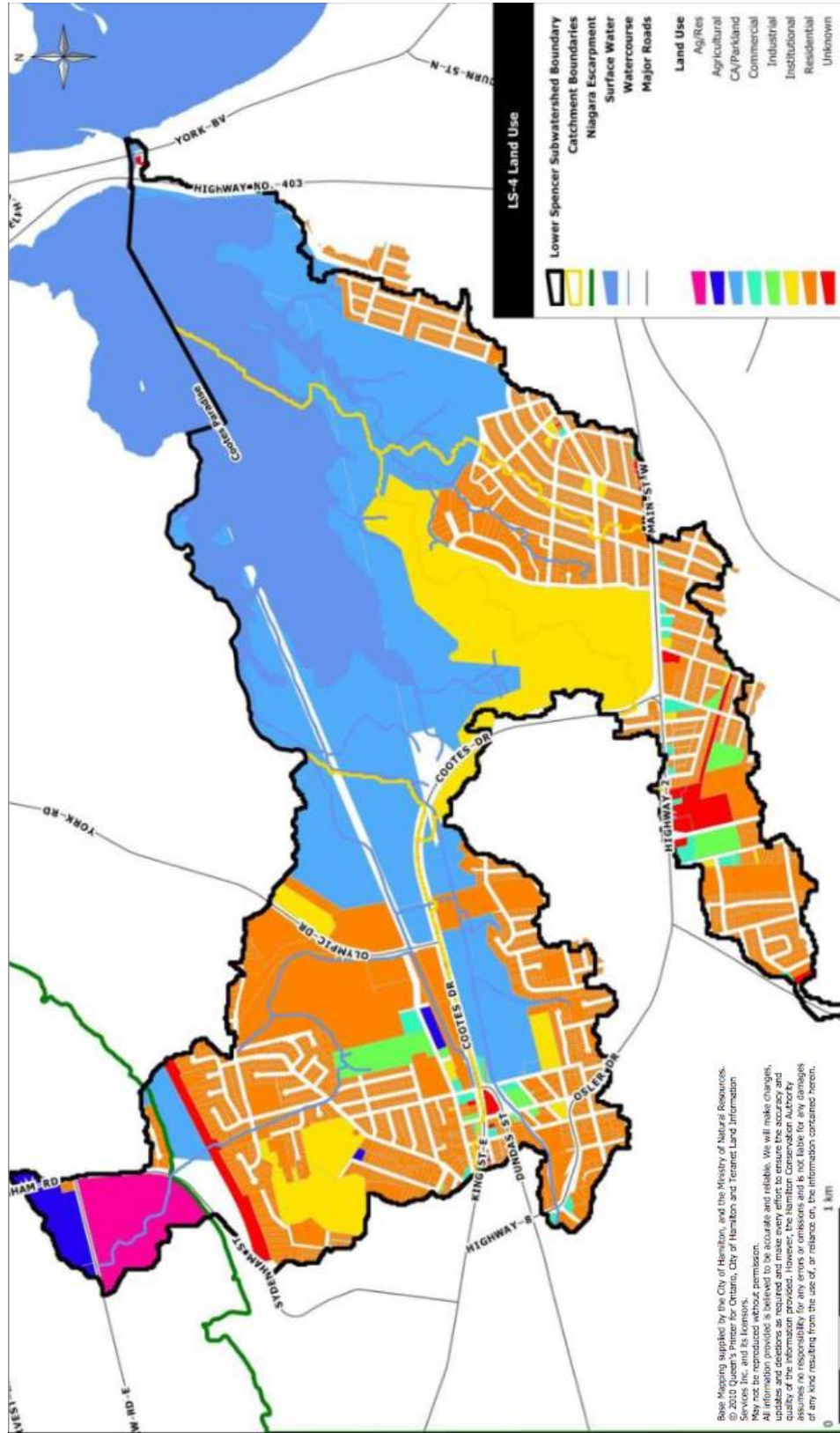


Figure 80: Lower Spencer Subwatershed Land Use (HCA, 2010)

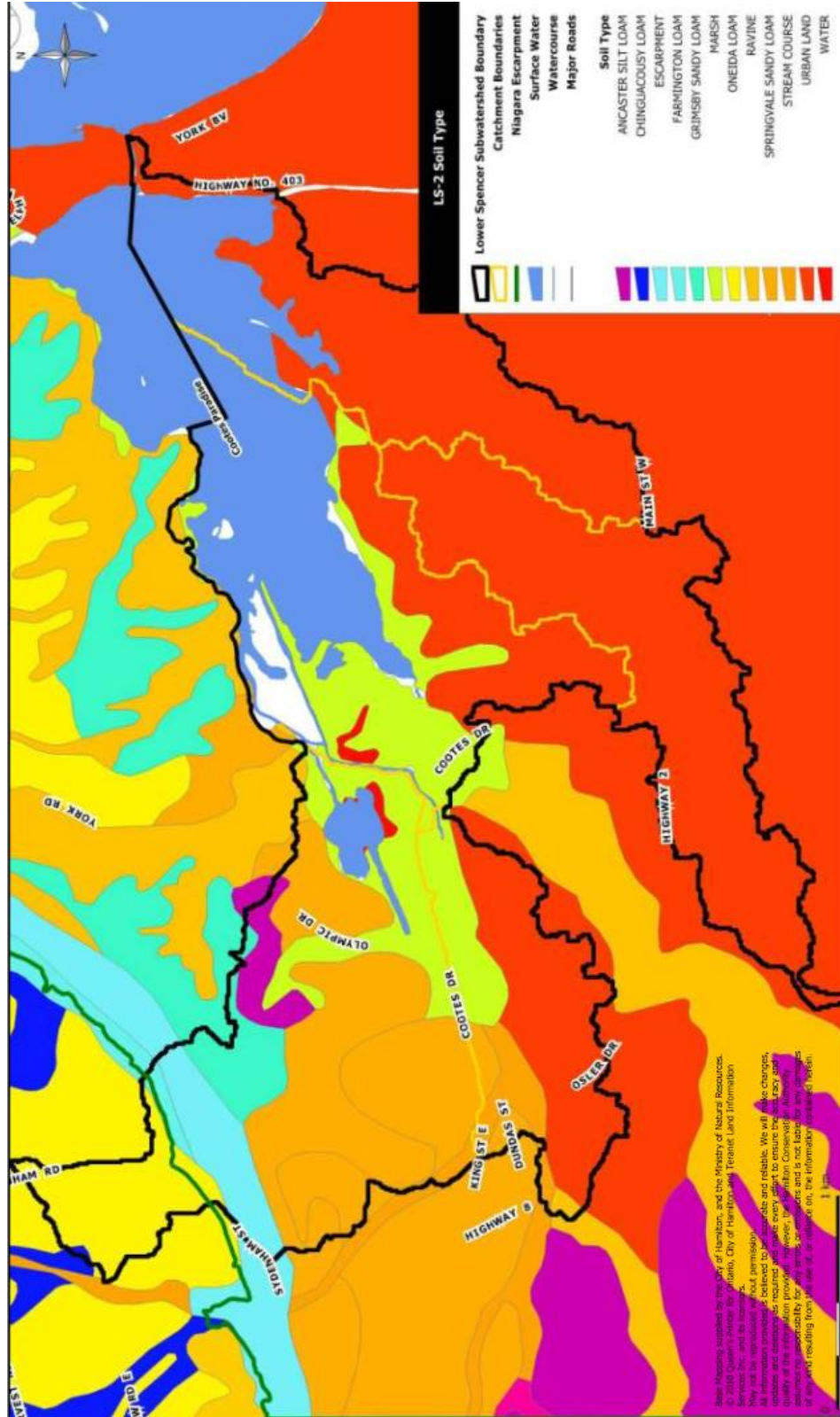


Figure 81: Lower Spencer Subwatershed Soil Distribution (HCA, 2010)

Curriculum Vitae

Name: Emily Martin

Post-Secondary Education and Degrees: University of New Brunswick
Fredericton, NB, Canada
2010 – 2014 B.Sc. Eng. Civil

University of Western Ontario
London, ON, Canada
2014 – Expected 2017 M. E. Sc.

Honours and Awards: Rudy and Theresa Esterbauer Research Fund - 2014

George Cedric Ferguson Memorial Engineering Bursary - 2011

Related Work Experience: Laboratory Research Assistant
University of New Brunswick
2012-2014

Teaching Assistant
University of New Brunswick
2014

Research Assistant
University of New Brunswick
2014

Teaching Assistant
University of Western Ontario
2014-2016

Technical Workshops: Hydraulic Modeling with HEC-RAS
2016